

DYNAMIC MODELING AND SUPERVISORY  
CONTROLLER DESIGN FOR A SMALL ISOLATED  
HYBRID SYSTEM WITH PUMPED HYDRO STORAGE

MD. RAHIMUL HASAN ASIF







**DYNAMIC MODELING AND SUPERVISORY CONTROLLER DESIGN FOR A  
SMALL ISOLATED HYBRID SYSTEM WITH PUMPED HYDRO STORAGE**

by

© Md. Rahimul Hasan Asif

A Thesis submitted to the

School of Graduate Studies

in partial fulfillment of the requirements for the degree of

**Masters in Engineering**

**Faculty of Engineering and Applied Science**

Memorial University of Newfoundland

**October 2013**

St. John's

Newfoundland

*Dedicated to my*

*Mother who has always been there for me when I needed her, even when I couldn't admit  
that I needed her*

## **ABSTRACT**

In this research dynamic modeling of a remote hybrid power system and feasibility of a pumped hydro storage system is presented. Existing hybrid system in Ramea, Newfoundland has an electrolyzer, hydrogen storage and generator system. This research proposes a pumped hydro storage as a replacement to the hydrogen system. Detailed MATLAB-Simulink modeling has been done for every component of the Ramea hybrid power system. Incorporation of a pumped hydro system and some lead acid batteries will eliminate the low turn around efficiency of the electrolyzer and hydrogen generator system. The system dynamic model and simulations presented here is fast, accurate and includes dynamic and supervisory controllers. The proposed real time supervisory controller algorithm observes the available surplus/lacking power in the system and regulates pump/turbine and charging/discharging of the battery bank to maintain a stable system frequency. This thesis presents dynamic model, supervisory controller design and algorithm, six case studies and detailed simulation results. This thesis also presents different operational modes of diesel engine generator to estimate the fuel consumption, no of switching and system frequency deviation.

## **ACKNOWLEDGEMENTS**

The author would like to convey his profound, heartfelt and sincere gratitude and respect to his supervisor Dr. Tariq Iqbal as during the course of his research work at Memorial University of Newfoundland Dr. Iqbal provides a proficient supervision and persistent support and encouragement. The author is grateful to him for sharing his vast experience and knowledge over past two years. Without his help this thesis work might not have been completed successfully.

The author is grateful to his friends and family members, especially his mother, younger brother, uncles and aunts for their unconditional love, affections and mental supports to the author. Finally the author also wants to thank The Wind Energy Strategic Network (WESNet) which is a Canada wide research network, funded by industry and the Natural Sciences and Engineering Research Council of Canada (NSERC); School of Graduate Studies and Faculty of Engineering and Applied Science for funding this research and provide necessary help when needed.

## Table of Contents

ABSTRACT.....	iii
ACKNOWLEDGEMENTS.....	iv
Table of Contents.....	v
List of Tables.....	xi
List of Figures.....	xii
List of Symbols.....	xix
List of Abbreviations.....	xx
List of Appendices.....	xxii
1 Introduction.....	1
1.1 Overview.....	1
1.2 Motivation.....	3
1.2.1 Improvement of overall performance with a suitable energy storage system	3
1.2.2 Meet the customer demand when needed.....	9
1.2.3 Reducing the diesel consumption, high cost of energy and environmental impact.....	9
1.2.4 Intelligent supervisory controller.....	12
1.3 Methodology.....	14
1.4 Organization of the Thesis.....	18

1.5	References .....	20
2	Literature Review.....	24
2.1	Hybrid power system with PHS .....	24
2.1.1	Site selection and reservoir size analysis .....	24
2.1.2	Study on complete design of a pumped storage.....	25
2.1.3	Study on hybrid system with multiple renewable energy sources .....	27
2.1.4	Study on optimal scheduling, control, economic operation methodology...28	
2.1.5	Optimal sizing of pumped storage .....	32
2.1.6	Simple dynamic modeling method .....	33
2.2	Dynamic modeling of all subsystem .....	35
2.2.1	Diesel engine generator modeling .....	35
2.2.2	Centrifugal pump and penstock modeling .....	36
2.2.3	Turbine selection and design .....	39
2.3	High penetration Wind-diesel hybrid power system.....	42
2.4	References .....	44
3	A novel method to model a hybrid power system with pumped hydro storage for Ramea, Newfoundland.....	52
	Preface.....	52
	Abstract.....	52

3.1	Introduction .....	53
3.2	Model description.....	57
3.2.1	Wind speed and Load data .....	57
3.2.2	Wind turbine model .....	57
3.2.3	Diesel Engine Generator model .....	58
3.2.4	Induction motor and Centrifugal Pump model .....	60
3.2.5	Penstock model .....	61
3.2.6	Water reservoir model.....	62
3.2.7	Turbine model.....	62
3.2.8	Battery bank model .....	63
3.3	Simulation and Result .....	65
3.4	Conclusion.....	68
3.5	Acknowledgment .....	69
3.6	References .....	69
4	Dynamic Modeling and Analysis of a Remote Hybrid Power System with Pumped Hydro Storage .....	72
	Preface.....	72
	Abstract .....	72
4.1	Introduction .....	73

4.2	Dynamic Modeling.....	77
4.2.1	Wind Speed Data .....	77
4.2.2	Load Data.....	77
4.2.3	Wind Turbine Model.....	77
4.2.4	Diesel Engine Generator Model.....	79
4.2.5	Induction Motor and Centrifugal Pump Model .....	80
4.2.6	Penstock Model.....	81
4.2.7	Water Reservoir Model.....	82
4.2.8	Turbine Model .....	82
4.2.9	Battery Bank Model.....	83
4.2.10	Dump Load Model.....	85
4.2.11	Model of the Electrical System.....	86
4.3	Supervisory Controller .....	86
4.4	Results: Six Case Studies .....	87
4.4.1	Case 1: Low Load and Low Wind .....	88
4.4.2	Case 2: Low Load and High Wind .....	95
4.4.3	Case 3: High Load and Low Wind.....	100
4.4.4	Case 4: High Load and High Wind.....	105

4.4.5	Case 5: Abrupt Change of Load While Wind Speed is Steady in the Midrange .....	110
4.4.6	Case 6: Load is Steady in the Midrange and Wind Speed is Changed Abruptly .....	115
4.5	Conclusions .....	121
4.6	Acknowledgment .....	122
4.7	References .....	122
5	Diesel Consumption in a High Penetration Remote Hybrid Power System with a Pumped Hydro and Battery Storage .....	125
	Preface .....	125
	Abstract .....	125
5.1	Nomenclature .....	126
5.2	Introduction .....	127
5.3	Dynamic Model Description .....	129
5.3.1	Inputs: Wind Speed and Load Data .....	129
5.3.2	Subsystem Blocks .....	130
5.3.3	Outputs .....	132
5.4	Study of diesel consumption .....	132
5.4.1	Mode 1: DEG always ON .....	133
5.4.2	Mode 2: DEG is operating independently without time constraint .....	136

5.4.3	Mode 3: DEG is operating with 10 minutes time constraint.....	142
5.5	Conclusion.....	145
5.6	Acknowledgment .....	146
5.7	References .....	146
5.8	Biographies.....	148
6	Conclusion, Contribution and Future Work.....	150
6.1	Conclusion.....	150
6.1.1	Faster simulation with simpler but detailed dynamic model and intelligent supervisory controller is possible.....	150
6.1.2	Analyses for all extreme cases could be done.....	151
6.1.3	Modified control of DEG is required for high penetration of wind energy .....	152
6.2	Contribution .....	153
6.2.1	Novel method for dynamic modeling .....	153
6.2.2	Compatibility and flexibility.....	153
6.2.3	Supervisory controller design and simulation.....	154
6.3	Future Work .....	155
Appendix A	.....	A-1
Appendix B	.....	B-1

## **List of Tables**

Table 1.1. List of Pumped Hydro Storage systems under construction and new projects...	6
Table 1.2. Rates for diesel powered electricity .....	12
Table 2.1. Typical start-up time for different operation of a PHS plant .....	26
Table 2.2. Penetration level of wind-diesel system and their operating characteristics ....	43
Table 4.1. Six different cases of load and wind speed .....	88
Table 5.1. Study of Diesel consumption for different modes .....	145
Table 6.1. Maximum system frequency deviation for all six cases .....	151

## List of Figures

Figure 1.1. Typical model of a Wind - Pumped Hydro Storage system .....	4
Figure 1.2. Suitability of different energy storage technologies .....	5
Figure 1.3. Remote diesel plants in Newfoundland and Labrador .....	11
Figure 1.4. An example of Wind Turbine Overview screen of the supervisory controller in a Wind-Diesel system at Selawik, Alaska .....	13
Figure 1.5. 3*100kW Northern power 100 wind turbines in Ramea island .....	15
Figure 1.6. 6*65kW Windmatics 15s wind turbines in Ramea island .....	16
Figure 1.7. Top of 'Man of War' hill at Ramea Island .....	17
Figure 1.8. Block diagram of Ramea Wind-Diesel hybrid power system with a proposed pumped hydro storage system, battery bank and controllable dump load .....	17
Figure 2.1. Operating regions of different water turbines.....	40
Figure 3.1. A block diagram of Ramea hybrid power system with proposed pumped hydro storage system .....	55
Figure 3.2. 1s Wind speed data .....	58
Figure 3.3. Load demand data.....	59
Figure 3.4. Wind turbine power curve and conditions.....	59
Figure 3.5. Simulink - MATLAB embedded function blocks based dynamic model of Ramea hybrid power system with pumped hydro storage and battery bank .....	60
Figure 3.6. Part flow efficiency of a Pelton Wheel Turbine .....	62
Figure 3.7. Varying DEG output to cover load demand in between 300kW to 925kW ....	66
Figure 3.8. Pump and Turbine operation .....	67

Figure 3.9. Battery discharge and charging operation .....	67
Figure 3.10. Comparison between two scenarios where bottom curve is representing the grid power with pumped hydro and battery system .....	68
Figure 4.1. Block diagram of Ramea hybrid power system with a proposed pumped hydro storage system, battery bank and dump load .....	75
Figure 4.2. Wind turbine power curve and limiting conditions .....	77
Figure 4.3. Simulink - MATLAB embedded function blocks based dynamic model of Ramea hybrid power system with pumped hydro storage, battery bank and dump load ..	78
Figure 4.4. Part flow efficiency of a Pelton wheel turbine .....	83
Figure 4.5. Simple flowchart of the algorithm used as supervisory controller .....	89
Figure 4.6. Load demand (kW) and wind speed (m/s) data for the case 1 .....	90
Figure 4.7. In top figure, the grid available power (kW) and DEG varying output (kW) (with a minimum 300kW value) is shown and in the lower figure dump power (kW) is shown for the case 1 .....	91
Figure 4.8. Pump power consumption (kW), pump water flow ( $m^3/s$ ), the upper reservoir water volume ( $m^3$ ), turbine water flow rate ( $m^3/s$ ) and the turbine generated power (kW) for the case 1 .....	92
Figure 4.9. Charging current (kA), charging power (kW), percentage of state of charge, discharging current (kA) and the power to the grid (kW) due to the discharging of the battery are shown for the case 1 .....	93
Figure 4.10. Grid surplus power (kW) with and without pumped storage, battery and dump load and the resultant frequency deviation for the case 1 .....	94

Figure 4.11. Simulation result has been zoomed from 57700s to 57800s to show the transients. In top figure, the grid available power (kW) and DEG varying output (kW) is shown and in the lower figure the resultant frequency deviation is shown for the case 1.95

Figure 4.12. Load demand (kW) and wind speed (m/s) data for case 2 .....96

Figure 4.13. In the top part, grid available power (kW) and DEG output (kW) (with flat 300kW value) are shown and in the lower part dump power (kW) is shown for the case 2 .....97

Figure 4.14. Pumping power (kW), pumping water flow rate (m<sup>3</sup>/s), upper reservoir water volume (m<sup>3</sup>), turbine water flow (m<sup>3</sup>/s) and turbine generated power (kW) for the case 2 .....98

Figure 4.15. Charging current (kA), charging power (kW), percentage of state of charge, discharging current (kA) and the power injected to the grid (kW) due to the discharging of the battery are shown above for the case 2 .....99

Figure 4.16. Grid surplus power (kW) with and without pumped storage, battery and dump load and the resultant frequency deviation are shown above for the case 2 ..... 100

Figure 4.17. Load demand (kW) and wind speed (m/s) data for the case 3 ..... 101

Figure 4.18. In top figure, grid available power (kW) and DEG varying output (kW) (from 400kW to 925kW) are shown and in the bottom part dump power (kW) is shown for the case 3 ..... 102

Figure 4.19. Pumping power (kW), pumping water flow (m<sup>3</sup>/s), upper reservoir water volume (m<sup>3</sup>), turbine water flow (m<sup>3</sup>/s) and turbine generated power (kW) are shown for the case 3 ..... 103

Figure 4.20. Charging current (kA), charging power (kW), percentage of state of charge, discharging current (kA) and injected power to the grid (kW) due to the discharging of the battery are for the case 3 .....	104
Figure 4.21. Grid surplus power (kW) with and without pumped storage, battery and dump load and the resultant system frequency deviation for the case 3 .....	105
Figure 4.22. Load demand (kW) and wind speed (m/s) data for the case 4 .....	106
Figure 4.23. In top figure grid available power (kW) and DEG output (kW) (flat 300kW value) are shown and in the lower part dump power (kW) is shown for the case 4 .....	107
Figure 4.24. Pumping power (kW), pumping water flow (m <sup>3</sup> /s), upper reservoir water volume (m <sup>3</sup> ), turbine water flow (m <sup>3</sup> /s) and turbine generated power (kW) for the case 4 are shown above.....	108
Figure 4.25. Charging current (kA), charging power (kW), percentage of state of charge, discharging current (kA) and the power injected to the grid (kW) due to the discharging of the battery are shown above for the case 4 .....	109
Figure 4.26. Grid surplus power (kW) with and without pumped storage, battery and dump load are shown above. The resultant frequency deviation is also plotted for the case 4.....	110
Figure 4.27. Load demand (kW) and wind speed (m/s) data for the case 5 .....	111
Figure 4.28. In top part, grid available power (kW) and DEG varying output (kW) (that changes from 300kW to 500kW) are shown. In the lower part dump load power (kW) is plotted for the case 5 .....	112

Figure 4.29. Pumping power (kW), pumping water flow (m <sup>3</sup> /s), upper reservoir water volume (m <sup>3</sup> ), turbine water flow (m <sup>3</sup> /s) and turbine generated power (kW) are plotted above for the case 5.....	113
Figure 4.30. Charging current (kA), charging power (kW), percentage of state of charge, discharging current (kA) and injecting power to the grid (kW) due to the discharging of the battery are plotted above for the case 5.....	114
Figure 4.31. The grid surplus power (kW) with and without pumped storage, battery and dump load and the resultant frequency deviation for the case 5.....	115
Figure 4.32. Load demand (kW) and wind speed (m/s) data for the case 6 .....	116
Figure 4.33. In the top part, grid available power (kW) and DEG varying output (kW) (with a flat 300kW) and in bottom part dump power (kW) is shown for the case 6 .....	117
Figure 4.34. Pumping power (kW), pumping water flow (m <sup>3</sup> /s), upper reservoir water volume (m <sup>3</sup> ), turbine water flow (m <sup>3</sup> /s) and turbine generated power (kW) are shown above for the case 6.....	118
Figure 4.35. Charging current (kA), charging power (kW), percentage of state of charge, discharging current (kA) and injected power to the grid (kW) due to the discharging of the battery are plotted above for the case 6.....	119
Figure 4.36. Grid surplus power (kW) with and without pumped storage, battery and dump resistance and the resultant frequency deviation are shown above for the case 6 .	120
Figure 5.1. Simulink - MATLAB embedded function block based dynamic model of Ramea hybrid power system with PHS, BB and DL .....	129
Figure 5.2. Load demand data and Wind speed data for one day (86400s).....	130

Figure 5.3. In top figure, the grid available power (kW) and DEG output (kW) (with a minimum 300kW value) is shown and in the lower figure dump power (kW) is shown for mode 1 .....	133
Figure 5.4. Pump power consumption (kW), pump water flow (m <sup>3</sup> /s), the upper reservoir water volume (m <sup>3</sup> ), turbine water flow rate (m <sup>3</sup> /s) and the turbine generated power (kW) for the Mode 1 .....	134
Figure 5.5. BB charging current (kA), charging power (kW), percentage of state of charge, discharging current (kA) and the power to the grid (kW) due to the discharging of the battery are shown for the mode 1 .....	135
Figure 5.6. Grid surplus power (kW) with and without pumped storage, battery and dump load and the resultant frequency deviation for the mode 1 .....	136
Figure 5.7. In the top part, grid available power (kW) and DEG output (kW) (with flat 300kW value) are shown and in the lower part dump power (kW) is shown for the mode 2 .....	137
Figure 5.8. Pumping power (kW), pumping water flow rate (m <sup>3</sup> /s), upper reservoir water volume (m <sup>3</sup> ), turbine water flow (m <sup>3</sup> /s) and turbine generated power (kW) for the mode 2 .....	138
Figure 5.9. BB charging current (kA), charging power (kW), percentage of state of charge, discharging current (kA) and the power injected to the grid (kW) due to the discharging of the battery are shown above for the mode 2 .....	139
Figure 5.10. Grid surplus power (kW) with and without pumped storage, battery and dump load and the resultant frequency deviation are shown above for the mode 2 .....	140

Figure 5.11. In the top part, grid available power (kW) and DEG output (kW) are shown and in the lower part the resultant frequency deviation (Hz) are shown for 14800s to 16000s in mode 2 .....	141
Figure 5.12. In the top part, grid available power (kW) and DEG output (kW) are shown and in the lower part the resultant frequency deviation (Hz) are shown for the continuous control of DEG in Mode 2 .....	141
Figure 5.13. In the top part, grid available power (kW) and DEG output (kW) (with flat 300kW value) are shown and in the lower part dump power (kW) is shown for the mode 3 .....	142
Figure 5.14. Pumping power (kW), pumping water flow rate (m <sup>3</sup> /s), upper reservoir water volume (m <sup>3</sup> ), turbine water flow (m <sup>3</sup> /s) and turbine generated power (kW) for the mode 3 .....	143
Figure 5.15. BB charging current (kA), charging power (kW), percentage of state of charge, discharging current (kA) and the power injected to the grid (kW) due to the discharging of the battery are shown above for the mode 3 .....	144
Figure 5.16. Grid surplus power (kW) with and without pumped storage, battery and dump load and the resultant frequency deviation are shown above for the mode 3 .....	145

## List of Symbols

$h_f$  - head loss due to friction (SI units: m)

$L$  - length of the pipe (m)

$D$  - hydraulic diameter of the pipe (m)

$V$  - average velocity of the fluid flow (m/s)

$g$  - local acceleration due to gravity ( $\text{m/s}^2$ )

$f_D$  - a dimensionless coefficient called the Darcy friction factor

$Q$  - volumetric flow rate ( $\text{m}^3/\text{s}$ )

$A_w$  - cross-sectional wetted area ( $\text{m}^2$ ).

$\xi$  - minor loss coefficient

$h_{\text{minor\_loss}}$  - minor head loss (m)

## **List of Abbreviations**

RAPS - Remote Area Power Supply

HPS - Hybrid Power System

PHS - Pumped Hydro Storage

WT - Wind Turbine

DEG - Diesel Engine Generator

HES - Hydrogen Electrolyzer and Storage

HPG - Hydrogen Powered Generator

BB - Battery Bank

SOC - State of Charge

IM - Induction Motor

CP - Centrifugal Pump

DL - Dump Load

PWT - Pelton Wheel Turbine

TF - Transfer Functions

TC - Time Constant

PID - Proportional-Integral-Derivative

MOI - Moment of inertia

DTM - Digital Terrain Model

SCC - Survey Control Centre

TIN - Triangulated Irregular Network

NWPP - Northwest Power Pool

CT - Conventional Turbines

HRES - Hybrid Renewable Energy System

GUI - Graphical User Interface

NREL - National Renewable Energy Laboratory

FESS - Flywheel Energy Storage System

## List of Appendices

Figure A.1. Power curve for Windmatic 15s wind turbine .....	A-1
Figure A.2. Technical specification of Windmatic 15s wind turbine .....	A-1
Figure A.3. Power curve of Northern Power 100 wind turbine .....	A-2
Figure A.4. Technical specification of Northern Power 100 wind turbine.....	A-2
Figure A.5. Datasheet of 1000kW Diesel Engine Generator, fuel consumption data has been taken from here.....	A-3
Figure A.6. Datasheet of 816kW Diesel Engine Generator, inertia data has been taken from here .....	A-4
Figure A.7. Centrifugal pump with induction motor coupled .....	A-5
Figure A.8. Multi-jet Pelton wheel turbine .....	A-5
Figure B.1. Wind data input window .....	B-1
Figure B.2. Load data input window .....	B-1
Figure B.3. Simulink built in interactive PID tuner .....	B-2
Figure B.4. Simulink function block for diesel engine frequency droop.....	B-2
Figure B.5. Simulink function block for measurement of diesel consumption .....	B-2
Figure B.6. Simulink function block for upper water reservoir .....	B-3
Figure B.7. Simulink function block for dynamic losses inside the pipe .....	B-3
Figure B.8. Simulink function block for battery bank .....	B-4
Figure B.9. Part of the code in supervisory controller .....	B-4

## 1 Introduction

### 1.1 Overview

Hybrid power systems are designed for the generation of electrical power from a number of power generation devices such as wind turbines, photovoltaic panels, geothermal, micro combined heat and power, micro-hydro and/or fossil fuel generators. Generally hybrid power systems are independent of large centralized electricity distribution system and used in remote areas. Often they are known as stand-alone power system (SAPS or SPS) or remote area power supply (RAPS). Storage can be used in RAPS e.g. battery bank, hydrogen storage, compressed air, pumped hydro storage etc. Hybrid power systems range from small systems designed for one or several homes to very large ones for remote island grids or large communities. RAPS are considered as a solution to provide electricity to many isolated communities where the large scale electrical grid expansion is prohibitive and the transportation of diesel is costly too. RAPS system diminishes fuel cost, permits green energy generation and improves the standard of living for the people in remote areas. [1]

Abundant power of the Sun is the ultimate source of all renewable energy. From the very ancient time when our ancestors made fire they used the power of photosynthesis, an indirect form of solar energy. Solar energy which can be harnessed directly as thermal energy or electric energy caused by the solar radiation or indirectly as biofuel, water or wind energy. Continuous improvement with the technologies to harness all kind of

renewable energies had been observed right up to the industrial revolution and then high energy concentrated fossil fuels replaced most part of these renewable energy uses in the homes, transport system and industries. Now coal, oil and natural gas are providing 75% of the total energy this world needs. After 1970s several profound reasons made people to think seriously about renewable energy e.g. oil price hike, possibility of 'fossil fuels' running out, air pollution, mining accidents etc. Emergence of nuclear energy after World War II it seemed like the world got a cheap, clean and plentiful alternative sources for fossil fuels but due to increased concern about safety, waste disposal, price etc. development and installation of the nuclear energy has slowed down. In recent decades these concerns about the fossil and nuclear fuels reintroduced the attention on renewable energy and searching for sustainable energy sources. This kind of energy source will not be exhausted over time, has no environmental effect and risk of human life. Renewable or alternative energy sources are more sustainable than other fuels. The form of energy can be kinetic, gravitational, electrical and nuclear [2]. In Ramea Island, Newfoundland, Canada fossil fuel consumption of the isolated diesel power system has been reduced by installing wind turbines which use kinetic energy of the wind and converts into electrical energy. For more wind penetration a Hydrogen Electrolyzer and Storage (HES) system and 4 Hydrogen Powered Generators (HPG) capable of producing 250kW power altogether have been installed. In this research a pumped hydro storage (PHS) system has been proposed to store the excess renewable energy instead of the HEG and HPG system. Here energy stored in the form of gravitational or potential energy. This can be used later when energy is needed and potential energy stored in the water will convert into kinetic

energy and that will produce mechanical hence electrical energy by means of a water turbine. A storage battery bank has also been considered in this research which will store electrical energy for later use.

## **1.2 Motivation**

In this research a new method of dynamic modeling has been developed and a supervisory controller has been introduced to ensure stable system operation with reduced diesel consumption and high wind penetration. In the following sections a brief description of the methods as well as motivations of this research are described.

### **1.2.1 Improvement of overall performance with a suitable energy storage system**

Wind-Diesel hybrid power system is one the most popular and widely implemented RAPS (Remote Area Power Supply) in the world. There are many remote communities which have this kind of RAPS e.g. islands of Alaska, Canada, Australia, Chile etc. [3]. For stable operation and high penetration of renewable energy in such system, some kind of energy storage system is used e.g. sealed lead acid battery, compressed air, flywheel, pumped hydro storage etc. Due to its tremendous range of uses and configurations, energy storages may assist renewable energy integration in any number of ways. As shown in Figure 1.2, compared to other energy storage systems pumped hydro storage has the highest discharge time at rated power but the system module size is the largest. Pumped hydro storage (PHS) can supply steady amount of power for a long period of

time and that is the reason for choosing this system when problem arises with enormous amount of energy storing options [5].

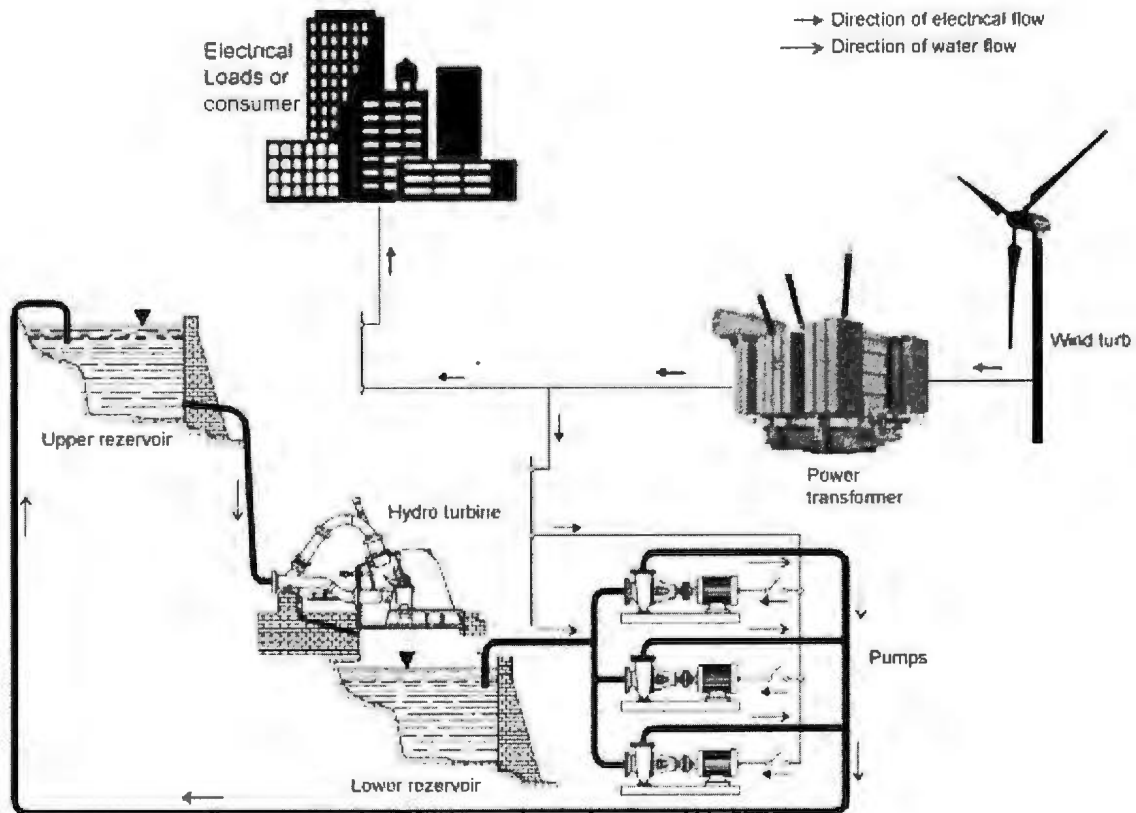
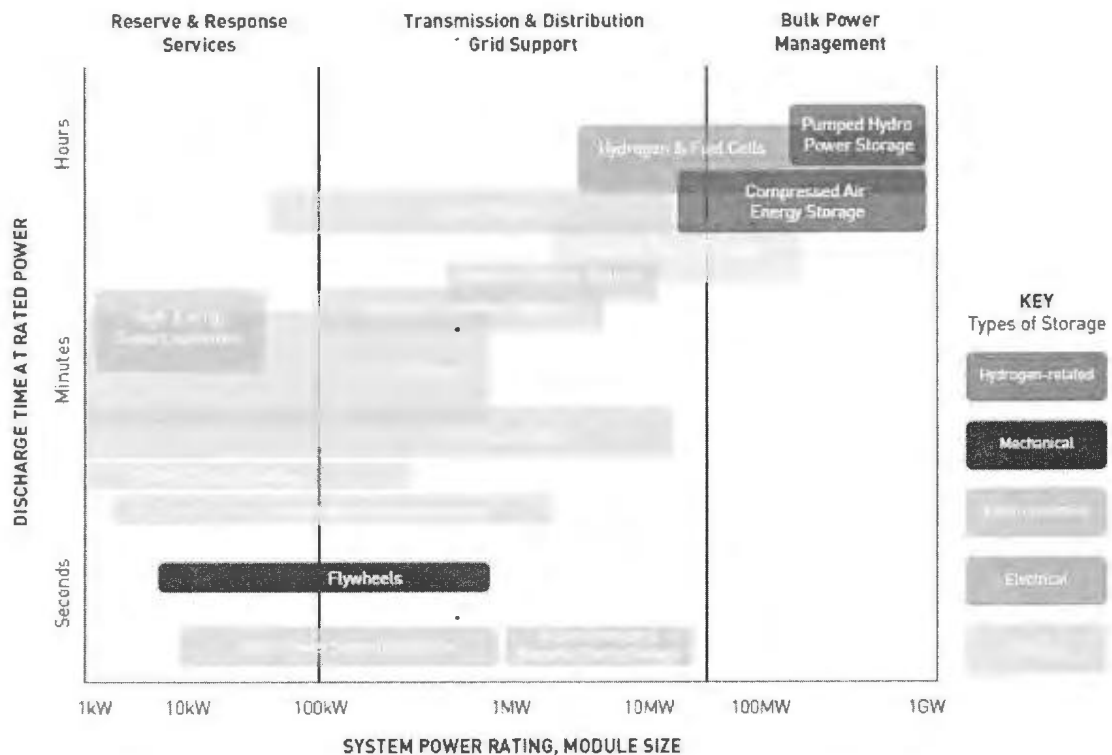


Figure 1.1. Typical model of a Wind - Pumped Hydro Storage system [Redrawn from [4]]

Water and gravity work together to capture off-peak power and discharge it at times of high demand. PHS systems use two reservoirs at different heights and take the advantage of natural topography. The vertical height from the lower reservoir to upper reservoir is considered as the 'head' of that particular PHS. Higher the head of a PHS system, greater the water pressure which results more hydropower potential. Considering bulk energy storage in a short period of time PHS systems are most widely used technique in the

world. In Table 1.1 few PHS systems under construction and recent projects already commissioned have been listed. According to the EPRI (Electric Power Research Institute) - the research arm of America's power utilities and Germany's Fraunhofer Institute; more than 99% of current installed energy storage capacity worldwide is PHS which is around 127GW in total [6].



**Figure 1.2. Suitability of different energy storage technologies [Regenerated from [5]]**

PHS is capable to accommodate sudden load swings within seconds that would otherwise lead to inefficient dispatch of gas, coal-fired and conventional hydropower units which reduce fuel costs and emissions. PHS can stabilize and provide flexibility to the grid. For

example, Dinorwig Pumped Storage Station in Wales, United Kingdom has peak capacity of 1,700 MW, is used to stabilize the entire 60 GW U.K. National Grid. This station can either consume energy when pumping or produce electricity when generating so a power “swing” of about 3.4 GW can be achieved by this single plant only. In a single day, the Dinorwig plant switches between consuming and producing electricity an average of more than 100 times. This plant has a surprising ability to ramp up and down to accommodate the needs of the grid which is more than 100 MW/s to over a range of more than 1 GW [7].

**Table 1.1. List of Pumped Hydro Storage systems under construction and new projects [8]**

<b>Under construction</b>					
<b>Name of the project</b>	<b>Location</b>	<b>Capacity</b>	<b>Details</b>	<b>Companies</b>	<b>Investment</b>
Baixo Sabor	Sabor River in northern Portugal	171MW	Two dams, two powerhouses one containing two 70 MW pump-turbine units and the other containing two reversible 15.5 MW units. Build by. Construction began in June 2008, and scheduled to begin operating in early 2013.	Consortium of Andritz Hydro and Ensulmeci (supplying generating equipment) and a consortium of Bento Pedroso Construcoes SA and LENA Engenharia e Construcoes SA (building the project)	€354 million (US\$484 million).
Feldsee	Carinthia, Austria	75MW	Second 75 MW unit at the existing 140 MW Feldsee project operating since September 2009, two reservoirs, owned by Karntner Elektrizitats-Aktiengesellschaft (Kelag).	ABB (which supplied the control system), Alstom Hydro Austria GmbH (which supplied the motor-generator, excitation and auxiliary systems), and Andritz VA Tech Hydro (supplier of the pump-turbine, digital governor, and shut-off and globe valves).	€50 million (\$63.3 million)

Limberg 2	Austria	480MW	Two reservoirs and the underground powerhouse will contain two pump-turbine units.	Verbund Austrian Hydro Power AG, ABB AG, Andritz VA Tech Hydro, Hans Kunz GmbH of Austria, Jakko Poyry Group Oyj, Siemens AG Osterreich, Voith Hydro, WPK Werkstoff-Planung-Kontroll GmbH of Austria, and YIT Austria GmbH.	
Limmern	Linthal Valley in eastern Switzerland	1GW	Four 250 MW reversible vertical Francis pump-turbines and four 280 MVA vertical asynchronous motor-generator units. Expected to begin operating in 2015.	Kraftwerke Linth-Limmern AG, ABB Ltd, Alstom Hydro, Nexans, Poyry	CHF1.8 billion (\$1.77 billion)
Nant de Drance	southwest Switzerland	600MW	Four 157 MW vertical Francis reversible pump-turbines and four 170 MVA vertical asynchronous motor-generators. Expected to begin operating fully in 2017.	Nant de Drance SA, Alpiq, federal railway group SBB, and Forces Motrices Valaisannes, AF Colenco and Alstom Hydro SA Switzerland	CHF990 million (\$950 million)
Qingyuan	Guangdong Province, China	1.28GW	Four 320 MW units consisting of pump-turbines, motor-generators. Expected to be commissioned in October 2014.	CSG Power Generation Company and Toshiba Corporation	
Reisseck 2	Reisseck/Kr euzeck complex in Upper Carinthia, Austria	430MW	Expected commissioning in 2014	Verbund Austrian Hydro Power AG and Poyry	€335 million (\$412 million)
<b>New Projects online</b>					
Avce	Soca River in Slovenia	185MW	One variable speed reversible vertical Francis pump-turbine. Began producing electricity in April 2010.	Soske Elektrarne Nova Gorica d.o.o., Gorenje d.d.; HSE Invest; a consortium of Melco, Rudis, and Simitomo, Mikomi d.o.o.; Mitsubishi; Montavar metalna nova d.o.o.; and a consortium of Primorje d.d. and SCT d.d.	€122 million (\$164 million)

Dnister	Dnister River in Ukraine	2268 MW	In total, the plant contains seven identical units. Began operating in January 2010	UkrHydro Open Joint Stock Company	UAH5.8 billion (\$720 million)
Jixi	Anhui Province, China	1.8GW	Two reservoirs, total storage volume of 21.85 million m <sup>3</sup> Began operating in July 2010	State Grid, East China Grid, Jiangsu Electric Power, Shanghai Electric Power, Xuangcheng municipal government, and the local government	CNY8.2 billion (\$1.2 billion)

PHS systems are cost effective in long run, environment friendly as they do not produce any hazardous gases or chemicals, long functional life, have low operational maintenance etc. And unlike different kind of storage batteries system efficiency of a pumped hydro storage doesn't decline that much over time. There are some issues with PHS systems e.g. high initial capital, a clean water source nearby at lower level as the lower reservoir and suitable large flat area with an appropriate natural height to build the higher reservoir.

All of the factors above motivate to implement a PHS system at Ramea Island where a suitable place is already there and hydrogen system is not giving an accepted efficiency. Moreover H<sub>2</sub> gas is hazardous and takes large volume for storage. Proposed PHS could store 685kWh energy in the upper reservoir. For high penetration of wind energy in Ramea Wind-Diesel hybrid system and reduced diesel consumption, PHS is the best option.

### **1.2.2 Meet the customer demand when needed**

Objectives of this thesis are to develop and study dynamic model, supervisory and dynamic controllers for a remote hybrid power system and integrate an optimum sized pumped hydro storage in it. This pumped storage system should flatten the intermittent generation and try to follow the demand curve by pumping when energy is surplus and generating electricity when generation is less and demand is high. Optimal sizing refers to the size of system components including reservoir, penstock, reversible machines and associated electrical control. Size of the system depends on the demand variation, maximum demand, wind speed availability and trend, suitable site, available energy sources etc. Dynamic controller is required to operate a pumped hydro storage system for optimum power output, efficiency and economic benefits. Key purpose of this control is to meet the customers demand whatever the actual generation is.

### **1.2.3 Reducing the diesel consumption, high cost of energy and environmental impact**

As shown in Figure 1.3, Newfoundland and Labrador Hydro (NLH) has 21 isolated diesel generating stations serving approximately 4,400 customers with 31MW of net capacity [9]. Amongst these 15 are in Labrador and 6 are on the island part of the province. Boats and aircrafts are the only means to access 12 of these plants. The rest of the places are connected with public highway system. Except Ramea which has daily truck deliveries, only marine tankers are used to deliver fuel to all of these plants which is costly, time consuming and involves environmental hazards. Due to the high cost of service for these

remote communities Newfoundland government subsidize the cost of utility which is in fact affecting the economy. From below comparison we can see that consumer of diesel plants are paying a little more than what domestic grid connected customers are paying but generation cost is much higher for diesel plants [10] and moreover government is giving rebates to the consumers.

Newfoundland and Labrador Board of Commissioners of Public Utilities (the Public Utilities Board or PUB) regulates all utilities in Newfoundland and Labrador by the Electrical Power Control Act 1994 (EPCA) . As part of its Northern Strategic Plan the Provincial Government of Labrador announced an electricity rebate to reduce the cost of basic electricity consumption for Hydro residential customers in Labrador's coastal rural isolated diesel and the Labrador Straits communities (approximately 2,600 customers) in July 2007. This rebate is not included in the PUB-approved rates. The average monthly electricity rebate is approximately \$45-\$65 depending on usage [11].

Newfoundland Power and NL Hydro electricity rate for Domestic Services [12] [13]

**Basic Customer Charge:**

Not Exceeding 200 Amp Service .....\$15.68 per month

Exceeding 200 Amp Service .....\$20.68 per month

**Energy Charge:**

All kilowatt-hours .....@10.945¢ per kWh



Figure 1.3. Remote diesel plants in Newfoundland and Labrador [10]

NL Hydro power electricity rate for Domestic Diesel [13]

**Basic Customer Charge:** ..... \$15.68 per month

Exceeding 200 Amp Service: ..... \$20.68 per month

**Energy Charge:**

First Block (See Table Below) kilowatt-hours per month ..... @ 10.945 ¢ per kWh

Second Block (See Table Below) kilowatt-hours per month ..... @ 12.373 ¢ per kWh

All kWh over 1000 kilowatt-hours per month ..... @ 16.776 ¢ per kWh

Table 1.2. Rates for diesel powered electricity [13]

	Jan.	Feb.	Mar.	Apr.	May	Jun.	Jul.	Aug.	Sept.	Oct.	Nov.	Dec.
<b>First Block</b>	1000	1000	900	900	800	800	700	700	700	800	900	1000
<b>Second Block</b>	0	0	100	100	200	200	300	300	300	200	100	0

Exhausts of these diesel generators are polluting the environment. On site large volume fuel storage is another issue. Because of the short shipping season, in the communities of Northern Labrador a minimum storage of 9 months' supply is maintained and in Newfoundland it is at least one month supply. On the other hand, Nain, Cartwright and Ramea, these larger plants are full scaled automated for varying load management. Rest of the plants have semi-automated system where each units have automatic system with run-up and synchronizing etc. a plant operator is required for the total load management. [10]

#### 1.2.4 Intelligent supervisory controller

Industrially available supervisory controllers can control several diesel and/or gas generators, wind turbines and photovoltaic inverters. It also monitor/control multiple secondary loads (thermal loads, water pumping, desalination, ice-making), charge/discharge management of the battery bank/flywheel, load feeders, load shading, dispatch optimal combination of generators to meet load with highest fuel efficiency, seamless transition between diesel-on and diesel-off modes of operation etc. An industrial

supervisory controller also has an operator interface, fault detection and annunciation system, performance data logging system, remote access via Ethernet/wired communication system etc. An industrial-type panel mount computer with color touch screen monitor as shown in Figure 1.4 is the heart of a supervisory controller. It offers powerful operator interfaces and variety of options for dispatch and remote connectivity. The operator interface provides great flexibility to change the operating strategy through a variety of user-settable parameters [14].

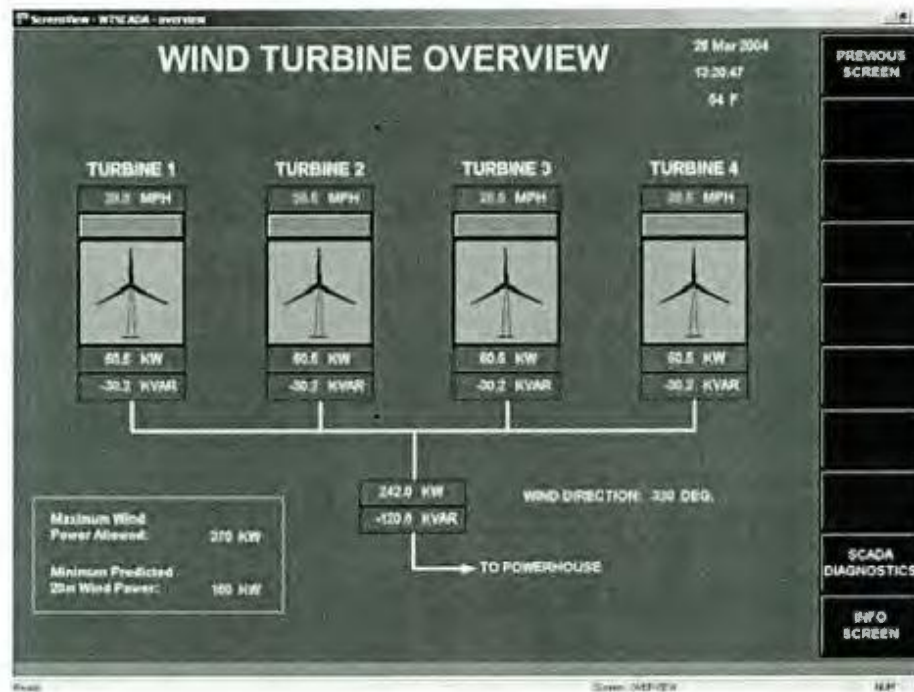


Figure 1.4. An example of Wind Turbine Overview screen of the supervisory controller in a Wind-Diesel system at Selawik, Alaska [Regenerated from [15]]

In dynamic modeling of Ramea an intelligent supervisory controller has been designed which can be used to manage all components, their outputs and operating mode and priority sequences.

### **1.3 Methodology**

Ramea is a small island located off the south coast of Newfoundland, Canada. This island was selected by the Newfoundland and Labrador Hydro as the first pilot project site in 2004 for a hybrid power system which is a pioneer project in the world to integrate wind, hydrogen and diesel generation in an isolate power system. The primary goal was to demonstrate substantial enhancement of energy efficiency and reliability after integrating Wind-Diesel Integrated Control System (WDICS) in the island's grid which can reduce the use of fossil fuel by hosting renewable wind energy in remote and isolated location. Here wind energy has been used to supplement the diesel requirements of the remote community which will reduce the required storage of fuel, cost and pollution [16]. Every year this wind-diesel pilot system is generating almost  $10^6$  kWh of electricity and offsetting nearly 750 tons of greenhouse gas emissions per annum [17] [18]. Presently transmission and distribution system for a total of 29.2MW of diesel generation in Newfoundland is operated and maintained by Transmission and Rural Operations (TRO) of Newfoundland [19].



**Figure 1.5. 3\*100kW Northern power 100 wind turbines in Ramea island**

Ramea Wind-Diesel-Hydrogen energy system has three 100kW NorthernPower100 [Figure 1.5] and six 65kW Windmatic 15s [Figure 1.6] wind turbines (WT). Three diesel engine generators (DEG) with a capacity of 925kW each are used as the main power sources. As storage, a Hydrogen Electrolyzer and Storage (HES) and a 250kW Hydrogen Powered Generator (HPG) have been installed. When generated wind energy surpasses the load demand the electrolyzer produces hydrogen from water electrolysis which is stored in the storage tanks. And when harnessed wind power is inadequate to supply the total load the stored hydrogen is fed into a HPG as a fuel which delivers electricity to the grid and maintains the stability [18]. This HES system produces hydrogen at 70% efficiency and HPG generates electricity at less than 35% efficiency. Overall it gives a

poor turn around conversion efficiency that is less than 25% [20]. Due to its complexity Ramea system has many operational issues that's why so far, it never operated as designed.



**Figure 1.6. 6\*65kW Windmatics 15s wind turbines in Ramea island**

Detailed information, analysis and dynamic simulation for the optimal size and site selection of a pumped hydro storage (PHS) system replacing the HES and HPG have been presented in Reference [21]. It has been shown that almost 37% renewable energy fraction can be attained using a 150kW PHS system with a 3932m<sup>3</sup> water reservoir at 63m height on top of 'Man of War' hill as shown in Figure 1.7. Topographical map of that hill shows that it has 2000m<sup>2</sup> of area to build a 2m high hydro storage reservoir.



Figure 1.7. Top of 'Man of War' hill at Ramea Island

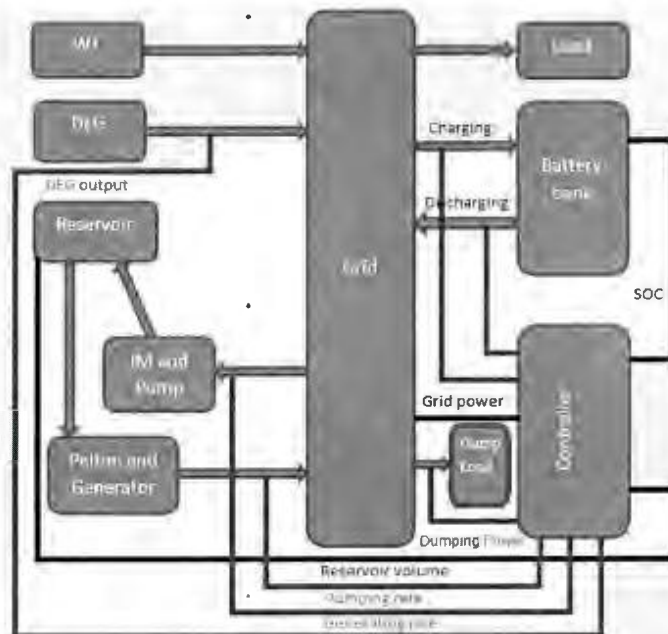


Figure 1.8. Block diagram of Ramea Wind-Diesel hybrid power system with a proposed pumped hydro storage system, battery bank and controllable dump load

In Reference [21] only 24s of dynamic simulation had been presented as it took days of computer time to simulate 1 minute of system operation which didn't even converge in the time period of 11s to 16s. Simple first order modeling of every system component can significantly reduce the simulation time, make the analysis easier and gives fairly accurate solutions.

A simple, fast and novel method has been introduced in this research work to simulate the system dynamics of Ramea hybrid power system with a proposed pumped hydro storage (PHS) system. As the block diagram in Figure 1.8, a Battery bank (BB) has been used to supply or store the intermittent power as induction motor (IM) and centrifugal pump (CP) or turbine and generator require some time to reach a certain operating point and have larger time constant than a BB. A PWM controlled dump load (DL) has also been used to dump the excess power. PID controllers have been used with all of the subsystems. Characteristic data and parameters of the aforementioned WTs and DEG used in Ramea hybrid system are taken from the respective manufacturers. All other subsystem models e.g. CP, Pelton Wheel Turbine (PWT), BB have been created using first principle and practical model.

#### **1.4 Organization of the Thesis**

Detailed literature study has been included in the next chapter. Following three chapters contain three manuscripts of the author.

In the first part of this study a novel method of dynamic modeling of the hybrid system with 1<sup>st</sup> order transfer functions (TF) are considered with proportional controller with all the subsystems. Simulink function blocks have been used here with characteristics and dynamic equations of the corresponding components implemented in MATLAB code. Simulation has been done for average wind and load data of Ramea and for 10000s. This model calculates only active power flow. DEG has been regulated from 30% to 100% rated and no dump load. A simple supervisory controller has been used here. Details of this study are provided in Chapter 3. This chapter has been accepted, published in the conference proceedings and presented in the *IEEE Newfoundland Electrical and Computer Engineering Conference 2012, St. John's, Newfoundland and Labrador, Canada*.

In the second part of this study PID controllers have been used as dynamic controller with an intelligent and complicated supervisory controller. Hybrid system configuration has been modified by adding a controllable dump load to mitigate the frequency swelling. More complex dynamic control of DEG has been introduced here to reduce fuel consumption and increase system frequency stability. Simulations have been done for one day (86400s). Six extreme cases are considered to observe the operation of supervisory controller. Simulation results and details can be found in Chapter 4. This chapter has been accepted for publishing in the *International Journal of Energy Science*.

Finally, in the last part diesel consumptions as well as the system operations have been studied and discussed for the different operational modes of the DEG i.e. Diesel always ON, Diesel ON-OFF, continuous control and time constrained ON-OFF operation. Simulations have been done for whole one day (86400s). This modified supervisory controller permits to implement a high penetration hybrid system in Ramea with diesel on-off and continuous control. Simulation results and details can be found in Chapter 5. This chapter has been accepted for presentation and publishing in the conference *IEEE Electrical Power and Energy Conference 2013, Halifax, Nova Scotia, Canada*.

Summary of the research work, major findings, research contribution, limitations and future work have been included in the last chapter of this thesis.

## 1.5 References

- [1] Center for Energy Efficiency and Renewable Energy,  
[http://www.ceere.org/rerl/projects/software/hybrid2/hybrid\\_power\\_systems.html](http://www.ceere.org/rerl/projects/software/hybrid2/hybrid_power_systems.html)  
[Online], Accessed June 10 2013
- [2] Boyle, G. (2012). Renewable energy: Power for a sustainable future. (pp. 2-4)  
OUP Oxford
- [3] Baring-Gould, E. Ian et al, Worldwide Status Of Wind-Diesel Applications,  
[http://www.windpoweringamerica.gov/winddiesel/pdfs/2004\\_wind\\_diesel/101\\_status.pdf](http://www.windpoweringamerica.gov/winddiesel/pdfs/2004_wind_diesel/101_status.pdf)  
[Online], Accessed June 2 2013

- [4] Dursun B. and Alboyaci. B., “The contribution of wind-hydro pumped storage systems in meeting Turkey’s electric energy demand”, *Renewable and Sustainable Energy Reviews* 14 (2010) 1979–1988, 2010, page 7, DOI: 10.1016/j.rser.2010.03.030
- [5] Peter Taylor, Ronan Bolton, Dave Stone, Xiao-Ping Zhang, Chris Martin, Paul Upham, Yongliang Li, Richard Porter, Eduardo Pereira Bonvallet, *Pathways for energy storage IN THE UK*. 2012, Pub: The Centre for Low Carbon Futures 2012, pp 22, <http://www.lowcarbonfutures.org/sites/default/files/Pathways%20for%20Energy%20Storage%20in%20the%20UK.pdf>
- [6] Pumped-storage key to energy storage, November 2012, International Electro-technical Commission, [http://www.iec.ch/etech/2012/etech\\_1112/tech-1.htm](http://www.iec.ch/etech/2012/etech_1112/tech-1.htm) [Online], Accessed June 1 2013
- [7] Summary Report of the 2010 Technology Summit Meeting on Pumped Storage Hydropower, Oak Ridge National Laboratory, the National Hydropower Association, and the Hydropower Research Foundation, Washington, DC, September 20-21, 2010, <http://www.esd.ornl.gov/WindWaterPower/PSHSummit.pdf> [Online], Accessed June 12 2013
- [8] Elizabeth A. Ingram, *Worldwide Pumped Storage Activity*, October 05, 2010, <http://www.renewableenergyworld.com/rea/news/article/2010/10/worldwide-pumped-storage-activity> [Online], Accessed June 10 2013
- [9] 2013 CAPITAL BUDGET APPLICATION Volume: 1&2, AN APPLICATION TO THE BOARD OF COMMISSIONERS OF PUBLIC UTILITIES, page 7

- [10] Canadian Off-Grid Utilities Association, [http://www.cogua.ca/history/nlh\\_systems.html](http://www.cogua.ca/history/nlh_systems.html) [Online], Accessed October 22 2012
- [11] Electricity, Department of Natural Resources, Newfoundland and Labrador, <http://www.nr.gov.nl.ca/nr/energy/electricity/> [Online], Accessed June 10 2013
- [12] Schedule of rates, rules and regulations, Newfoundland power Inc., <https://secure.newfoundlandpower.com/AboutUs/PDF/ratebook.pdf> [Online], Accessed July 5 2013, page 21
- [13] The hydro rate manual, Newfoundland and Labrador hydro, [http://www.nlh.nl.ca/hydroweb/nlhydroweb.nsf/SubContent/22DB93D546D178A4A32575BE004D9031/\\$File/Complete%20Set%20of%20Rates%20effective%20July%2013.pdf](http://www.nlh.nl.ca/hydroweb/nlhydroweb.nsf/SubContent/22DB93D546D178A4A32575BE004D9031/$File/Complete%20Set%20of%20Rates%20effective%20July%2013.pdf) [Online], Accessed July 5 2013, page 41, 49
- [14] Hybrid System Supervisory Controller Product profile, Sustainable Power Systems, <http://www.sustainablepowersystems.com/wp-content/uploads/2012/09/Hybrid-System-Controller-Rev-4.pdf> [Online], Accessed June 15 2013, page 2
- [15] System Integration and Advanced Controls for Wind Hybrid Village Power and Distributed Generation, Sustainable Automation, [http://www.windpoweringamerica.gov/winddiesel/pdfs/2004\\_wind\\_diesel/company/sustainable\\_automation.pdf](http://www.windpoweringamerica.gov/winddiesel/pdfs/2004_wind_diesel/company/sustainable_automation.pdf) [Online], Accessed June 20 2013, page 4
- [16] Newfoundland and Labrador Hydro: Transmission and Rural Operations, <http://www.nlh.nl.ca/hydroweb/nlhydroweb.nsf/TopSubContent/Operations-Transmission%20and%20Rural%20Operations?OpenDocument> [Online], Accessed October 22 2012

- [17] Govt. of Ramea, "Ramea Island," [Online]. Available: <http://www.ramea.ca/>. [Accessed 05 10 2012].
- [18] CANMET Energy, "Natural Resource Canada," Natural Resource Canada,07-07-2007.[Online].Available: <http://canmetenergy.nrcan.gc.ca/renewables/wind/464>. [Accessed 05 10 2012].
- [19] Transmission and Rural Operations, Newfoundland and Labrador Hydro, <http://www.nlh.nl.ca/hydroweb/nlhhydroweb.nsf/TopSubContent/Operations-Transmission%20and%20Rural%20Operations?OpenDocument> [Online], Accessed October 22 2012
- [20] M. Oprisan, " Introduction of Hydrogen Technologies to Ramea Island", IEA Wind – KWEA Joint Workshop, 01-04-2007. [Online].Available: [http://www.ieawind.org/wnd\\_info/KWEA\\_pdf/Oprisan\\_KWEA\\_.pdf](http://www.ieawind.org/wnd_info/KWEA_pdf/Oprisan_KWEA_.pdf). [Accessed 30 01 2013]. Page 21
- [21] T. Iqbal, "Feasibility Study of Pumped Hydro Energy Storage for Ramea Wind-Diesel Hybrid Power System," The Harris Centre, St. John's, 2009

## 2 Literature Review

### 2.1 Hybrid power system with PHS

#### 2.1.1 Site selection and reservoir size analysis

Site selection is a very crucial decision as it is involved lot of money and time. In article [1] authors developed a computer program to evaluate the terrain and propose a most economic and highest capacity possible PSH system. The authors discussed the methodology where they used Digital Terrain Model (DTM) data file for 800Km<sup>2</sup> area of South West Ireland which was imported into Atlas Computer's Limited's Survey Control Centre (SCC) software and processed to form a Delaunay Triangulated Irregular Network (TIN) model. An algorithm was developed to find suitable site for PSH from SCC. This algorithm searched for adjacent polygonal area with a minimum acceptable vertical separation which can be used for the upper and lower reservoirs after flattening the area by moving earth. They used series of analyses to determine the result and concluded that flat areas with large head are difficult to find without transferring huge amount of earth. The authors expected to add more features in their future work like lower processing time, avoiding residential and protected areas from the searching, adding financial calculation and more effective utilization of terrain data. They also have some rooms to work on the required adjustments of the grid and power plant operation after the installation of PHS system.

In article [2] authors described a methodology to determine the required size of the reservoir in a PHS system. They also studied the uncertainty in demands and supply capability with a Monte Carlo simulation method. This method examines the required reservoir size considering the system reliability and daily to weekly basis operation. The developed model consists of thermal and nuclear model, hydroelectric and PHS model and demand model. With actual data different states of thermal and nuclear model are simulated as a stochastic process. Water level variations are analyzed to determine the supply capability of the PHS model. And in the demand model consistency is made for weekly and daily basis by adding a device in the weekly model. Here seasonal impact on the reservoir size is also explained like smallest size in summer and largest in fall. This paper didn't cover the assessment of static, dynamic and economic advantages of PHS.

### **2.1.2 Study on complete design of a pumped storage**

In article [3], [4], [5] and [6] authors examined the impact of PHS units together with large renewable penetration. All of the authors primarily focused on the reduction of the operating cost and maximization of the usage of renewable energy based on unit commitments and dispatches. Relatively few studies [7], [8], [9] and [10] have described on the dynamic response of a PHS system. To study the dynamic interactions between the systems and the rest of the grid, including different renewable energy sources, dynamic models for pumped storage systems become obligatory [11]. In Table 2.1 typical start-up time of a PHS plant for different operational mode has been shown from the literature.

**Table 2.1. Typical start-up time for different operation of a PHS plant [11]**

<b>Mode</b>	<b>Condition</b>	<b>Response Time</b>
Generating	Shutdown to on-line	60 - 90 seconds
	On-line to full load	5 - 15 seconds
Pumping	Shutdown to rated	6 minutes
	Spinning-in-air to rated	60 seconds

In the paper [12] authors discussed about a case study where fluctuations and intermittent of wind energy may cause stability problem in an isolated wind PHS system. They also discussed about the characteristics of pipes, characteristics of pumps and its control, water level control in reservoir etc. In the simulation result they talked about two simulation mode. First one is the conventional one and second one is the peak pitching hydroelectric plant. To ensure stability in an isolated system, wind energy's variation can be tracked through the speed control of several groups of pumps and efficiency of this type of wind-PHS plant depends on the efficiency of pump system, the wind energy transmitting system, hydroelectricity generator, rain fall and the reservoir's capacity as well. Authors need more research to increase the efficiency for wide range of different speeds of pump. Systematic analysis for the cost and performance of the system is needed to find the proper pump for a system and stable operation within the modulating capability to design system parameters and hence the performance and optimal operation of the system.

Authors of the article [13] discussed about the integration of renewable energy resources in the Pacific Northwest power grid. They also considered the possible future expansion

of wind energy and the most efficient technical solution for the future balancing requirements of Northwest Power Pool (NWPP). Different kind of technologies are included in this study e.g. conventional turbines (CT), sodium sulfur batteries, lithium ion batteries, pumped hydro energy storage (PH), and demand response (DR). Here requirements for estimated total balancing in NWPP of wind energy in the 2019 time horizon is based on an assumption that all balancing authorities are combined together in a large balancing area. Life cycle, cost and optimal size of the pumped storage reservoir depends on the operation mode. It can be single, two or multiple mode. Detailed analysis is required to get longer life cycle for a particular mode of operation.

### **2.1.3 Study on hybrid system with multiple renewable energy sources**

In article [14] authors introduced a design of a hybrid renewable energy system (HRES) consists of a PHS plant, a wind power plant and a solar power plant. PHS plant has two control loops: the water tank level control loop and the load-dependent frequency control loop. Switch logic architecture has been introduced here for efficient energy distribution and reliable power supply. Three types of power converter e.g. Buck converter, AC-DC and DC-AC converter are analyzed by parameterization, modeling and simulation and then a graphical user interface (GUI) is developed for data monitoring, control and supervision within the designed SCADA system. Optimum economic operation of HRES is yet to be done. Authors intended to work with more sophisticated and recent power converter solutions and different control strategies for the system.

#### **2.1.4 Study on optimal scheduling, control, economic operation methodology**

Authors of the article [15] introduced an algorithm which optimizes the energy and later the profit produced by the pumped assisted hydroelectric plants. They considered a model of hydroelectric facilities with or without pump-assist involving some parameters like deterministically variable power prices and water inflows. They also showed that operations for both optimal economy and energy are not very much different under some reasonable choices of facility parameters and for fairly constant power prices. A PHS can be retrofitted with an existing hydro-generation plant if the water flow is intermittent. A close and higher elevation reservoir is chosen to store the pumped water where a reversible machine pumps the water when produced energy is surplus.

Their algorithm has different control paths to optimize the energy operation in various water flow condition like no flow, small inflow rate, increasing inflow rate and very large water flow rate. Price is considered as constant. But pumping is not optimal with this consideration. For best turbine efficiency at low inflow rate reservoir should be filled first. This algorithm maximizes not only the total amount of electrical energy produced during a given period of time but also can maximize the profit from the generated energy. Profit optimization algorithm is affected by the changing electricity price but if the price is steady both control paths of optimization would be same. For profit maximization the key concept is to pump when price is low and release water when price is high. Authors considered various combination of conditions e.g. inflow rate, reservoir height, price change rate to control for the profit maximization. The authors conclude like for small

inflow rate, variable price affects control strategy to maximize the turbine efficiency. And for large inflow rate, control strategy is not affected by changing price and it tries to maximize the output power keeping high reservoir height. Authors intended to research more on incorporation of demand prediction along with deterministic price of power. And here authors used separate machinery for generating electricity and pumping but recent pumped hydro systems are designed with reversible machineries which have comparatively slightly lower efficiency. So study with reversible machine would be more practical and may give different output after analysis.

Study of a suitable operation policy and simulation for the hybrid power system of Ikaria Island, Aegean Sea, Greece on an annual basis considering their existing regulatory framework has been done in article [16]. The island has solar PV, Wind energy, Diesel engine and hydroelectric plant. The Ikaria Island also has two new reservoirs for PHS and they are hydraulically connected by two penstocks which permit independent operation of turbine and pumping. For prolonged low wind periods the reserves of the storage system can be exhausted. So, to ensure adequate energy in the period of peak demand a limited amount of “grid-pumping” is allowed at low demand period, using conventional energy from the grid. The authors introduced 6 step operating policy that includes power request of island system operator, energy and load declaration of hybrid power system, energy dispatch and pump by island system operator etc. The authors also mentioned about some internal management decisions regarding the change of seasons and power balancing. In

the simulation they found average capacity factor between 29% - 43% and full cycle efficiency less than 60%.

To ensure sound dynamic behavior of the system individual for this strategy described in this paper a control system is required in the operation of island power system. Dynamic response and regulation issues are not well discussed in this paper. And 'Grid- pumping' is not possible for an isolated small scale PHS e.g. Ramea. In this research reservoir storage is used only for generating electricity not for irrigation and water supply. More study can be done for the compatibility of the system if more wind energy is added to the system and demand increases.

A model to evaluate power supply reliability considering a large PV integration into the power system is described in article [17]. As reliability is affected with this high PV integration they proposed for a PHS to improve the reliability though it increases operational cost of the system. The authors introduced a new method for more economical and reliable scheduling and operating the PHS. They also described briefly about generation scheduling, Monte Carlo simulation along with optimal operation scheduling by Pareto optimal model.

In terms of reliability of power system operation authors develop a good algorithm here but drawback is it increases total fuel cost of thermal power plants with this large penetration of PV. Authors did not consider any alternate reserve capacity for optimal

scheduling of thermal power plants. So more research works are required to develop an optimized cooperative scheduling method for both the operation of PHS Plant and hot reserve capacity of thermal power plants.

Authors of article [18] used a dynamic algorithm in their paper to optimize the operation of a PHS where the algorithm works with these two control variables, average generated flow and the pumping time. The authors discussed about medium and long term optimal dispatching model for the upper reservoir in a hybrid PHS system. In three steps they describe this model. Firstly, on basis of the features of the system use of medium and long term optimization is determined. Secondly, for maximum generation medium and long term optimal dispatching model is built. Thirdly, dynamic algorithm and optimizing algorithm is used to deal respectively with the model and the optimal operation.

Authors expect in future PHS and thermal power can be used in combined to reduce impact of starting and cooling time of a thermal plant on the grid. More research can be done to add other renewable energy sources with the PHS system to reduce cost and increase system reliability.

In the paper [19] the authors proposed a complete PHS system for Canarian Archipelago which has no negative impact on the existing power system and can meet the variable demand of customers. They introduced an algorithm which controls all switching of wind turbines, conventional power generators, hydroelectric systems, pumps and loads. They

also used wind speed distribution curve, maximum power generation curve, hourly demand curve for the analysis and several observations are shown e.g. CO<sub>2</sub> emission curve, total injected power into the grid. Unit cost of the proposed system is almost same as before but externality costs are reduced a lot like costs for CO<sub>2</sub> emissions.

Authors modeled the proposed system with optimum annual economic performance and in high wind seasons upper reservoir remains full for all the seasons. But in those windy seasons a possible reduction of cost for conventional energy can be done by increasing electricity production from the hydro plant using upper reservoir's water and deducting excess generation from the fossil fueled conventional power plants.

### **2.1.5 Optimal sizing of pumped storage**

Optimal sizing of a system is very important before starting dynamic analysis of that system. In the article [20] the authors studied short term optimal operation of a hybrid power system with a PHS. To minimize the production cost a mixed integer linear programming model is developed for optimal hourly operation of thermal, hydro and pumping. Realistic data of an example system is used in the test model which is studied for different demand and wind speed scenarios.

Demand data and wind speed data have been taken respectively from the webpage of Spanish Market Operator (OMEL) and HOMER software package, developed at the US National Renewable Energy Laboratory (NREL). All data are analyzed for four different

scenarios. In this study authors did not consider fixed design parameters of a PHS plant. The methodology presented here could be a basis for economic feasibility studies.

In reference [21] optimal size of a PHS system is determined using HOMER software simulation tool. There is no option to simulate PHS model in HOMER so author analyzed it using equivalent size of rechargeable batteries. The optimal size of the battery bank refers to the optimal size of the reservoir. And charging power can be analogous to pumping and discharging as generating electricity. Detailed information, analysis and dynamic simulation for the optimal size and site selection of a pumped hydro storage (PHS) system replacing the HES and HPG have been presented in this report. Author proposed a water reservoir at 63m height on top of 'Man of War' hill near the substation. Topographical map shows that around 2000m<sup>2</sup> of area is available on top of the mentioned hill to build a 2m high hydro storage reservoir.

This research work shows an alternative way to determine optimal size of a PHS but in dynamic simulation presented here did not converge and only 24s of simulation took days in a high end computer.

#### **2.1.6 Simple dynamic modeling method**

In article [22] authors analyzed a self-governing hybrid power system with storage and isolated load and showed the system stability by time domain simulations. The system has flywheel and batteries as energy storage system. Authors investigated three mathematical

models for three different sets of operating points and disturbance conditions. But the presented mathematical subsystems are too primitive and nonlinear efficiencies, frictional losses and different response times are totally overlooked. And this dynamic model has no controller. Authors led a way out for simple dynamic modeling but real obstruction would be to model practical subsystems with simple first order models with all necessary efficiencies, dynamic frictions and different time constants depending on the subsystem parameters.

In article [23] authors modeled each subsystems, supervisory controller and power versatile power transfer strategies. Versatile power transfer provides grid- or user-friendly operation by multimode operations, including normal operation without use of battery, power dispatching and averaging. The modeled supervisory controller regulates all power generation and individual components. Authors modeled and simulated the system with Power System Computer Aided Design/Electromagnetic Transients Program for DC (PSCAD/EMTDC), power-system transient-analysis software. Local controllers have also been used.

In article [24] authors proposed a new methodology 'power smoothing method' for frequency control with the aid of a Flywheel Energy Storage System (FESS) and checked the validity of the proposed method has been evaluated by computer simulations. They modeled an isolated power system with first order delay transfer functions (TF). The reference output from the wind farm to the grid is evaluated by inputting the net output of

the wind farm into a first order delay TF and FESS supply the difference between the reference power and the net output power to follow the wind farm-to-grid output to the reference value. Authors also expressed confidence that proposed method can be applied to other types of energy storage system and can contribute to increase renewable energy utilization in the isolated power systems.

## **2.2 Dynamic modeling of all subsystem**

### **2.2.1 Diesel engine generator modeling**

According to the report [25] and calculations from the equation [Equation 4.2] in user manual [26] of PowerFactory it has been found that Diesel Engine Generator (DEG) needs few seconds to start up from the rest. When a prime mover (here the DEG) has a droop governor, the rotational speed of the prime mover decreases with the increment of the load applied. Value of the droop is the rate of frequency decrease to the load increase [27].

In article [28] authors studied a theoretical analysis and synthesis, development and implementation, mathematical modeling and simulation using modern methods and optimal control procedures to control a new 3rd GS generator (GS3G) successfully. Permanent magnet synchronous generator attached with the diesel engine provides voltage and frequency proportional to the rotational speed of the rotor shaft. Steady voltage and frequency are obtained by means of feedback controller. In this thesis work a

DEG has been modeled with all necessary droop characteristics, 1<sup>st</sup> order time lag for engine inertia and feedback controller to maintain stable frequency and voltage on the isolated grid.

### **2.2.2 Centrifugal pump and penstock modeling**

In article [29] authors explained about the design procedure and performance analysis of a single-stage end suction centrifugal pump. This machine has two main components the impeller and the casing. Similar to the rotor of an induction motor, impeller is the rotating component and the casing is the stationary one. The casing guides the liquid to the impeller. Water enters in a centrifugal pump axially through the impeller eye and exits radially with a high velocity that converts into pressure inside the volute.

Moment of inertia (MOI) is an important parameter of a centrifugal pump (CP) which can affect the magnitude of transients generated during a pump startup or shutdown. In Reference [30] few equations of CP are shown to calculate the startup and shutdown time based upon the MOI of the pump and the motor driving the pump. According to these equations it is possible to determine theoretical values of MOI but in real scenario water inertia incorporate with the rotor and impeller MOI. From the experience it has been evidenced that the starting torque-speed curves considered without the inertia of the liquid are conservative, so it's important to include it with the calculations [31]. The starting up and shutting down of a pump slows down due to the inertia effect of the liquid. A lower value of the starting torque can be calculated if inertia of the liquid is neglected. From

these literatures a 200hp CP has been modeled in this research to meet the requirement considering 3000lb-ft<sup>2</sup> MOI at 1800 rpm which takes 30s to operate in its steady state.

Considering the flow from the CP through the long 70m pipe is laminar so Reynolds number is taken as 2000. Water could be turbulent at the beginning of the journey but after few meters through the pipe flow turns into a laminar one. The Darcy-Weisbach formula is often used to calculate pipe friction due to the water flow [32]. This formula identifies the changes of friction inside the pipe with water velocity, pipe wall roughness, pipe diameter, wetted surface area, viscosity and density. The Darcy-Weisbach equation for Head loss is as in Equation 2.1 [33],

$$h_f = f_D \frac{L V^2}{D 2g} \quad 2.1$$

$$V^2 = \frac{Q^2}{A_w^2} \quad 2.2$$

$$A_w^2 = \left( \frac{\pi D^2}{4} \right)^2 = \frac{\pi^2 D^4}{16} \quad 2.3$$

$h_f$  - the head loss due to friction (SI units: m)

$L$  - the length of the pipe (m)

$D$  - the hydraulic diameter of the pipe (m)

$V$  - the average velocity of the fluid flow (m/s)

$g$  - the local acceleration due to gravity (m/s<sup>2</sup>)

$f_D$  - a dimensionless coefficient called the Darcy friction factor. It can be found from a Moody diagram or more precisely by solving the Modified Colebrook equation.

Equation 2.2 and 2.3 relates the  $V$  and  $A_w$  with other quantities where  $Q$  is the volumetric flow rate ( $\text{m}^3/\text{s}$ ) and  $A_w$  is the cross-sectional wetted area ( $\text{m}^2$ ). Substituting these values into the original Equation 2.1 yields the final equation for frictional head loss in a full-flowing circular pipe as Equation 2.4

$$h_f = \frac{8f_D L Q^2}{g \pi^2 D^5} \quad 2.4$$

This equation has been used in the model of pipe. A water meter has been used in the model which causes minor frictional loss. Minor head loss in pipe and tube systems can be expressed as Equation 2.5.

$$h_{\text{minor\_loss}} = \xi \frac{V^2}{2g} \quad 2.5$$

Where,

$h_{\text{minor\_loss}}$  = minor head loss (m)

$\xi$  = minor loss coefficient, here it's considered as 7 for a water meter [34]

In the developed system dynamic model both of the dynamic frictional losses from pipe and water meter have been added together.

Detailed studies on dynamic modeling of PHS plant are summarized in article [35]. Authors also described different penstock configurations with both rigid and elastic dynamic models. In the time of generation conventional hydro turbine modeling method is used. For the dynamic model of pumping head-flow curve and the gating effects are considered in the system. Water dynamics of separate tunnel-penstock and single tunnel multiple penstocks are discussed here. System dynamics of speed governor and excitation, different plant operating conditions are simulated for both transient and the long-term responses. The authors studied specially the dynamics of elastic water model with multiple penstocks connected with a common water tunnel. This paper showed that for transient dynamic analysis water elasticity effects are negligible with temporary disturbances. For long term dynamic studies and hydraulic system studies water elasticity effects are significant. Further study is required to specify about the detailed relation with these terms in other configurations e.g. separate tunnel-penstock.

### **2.2.3 Turbine selection and design**

Two main reasons led to select and model a Pelton wheel turbine (PWT) for this PHS system in Ramea. Firstly, after studying the operating region of different kind of water turbines it is obvious that for this designed 200HP PHS system having around 70m

dynamic head and  $0.35\text{m}^3/\text{s}$  water flow rate only Pelton and Turgo type turbine can provide the best performance as shown in Figure 2.1 [36].

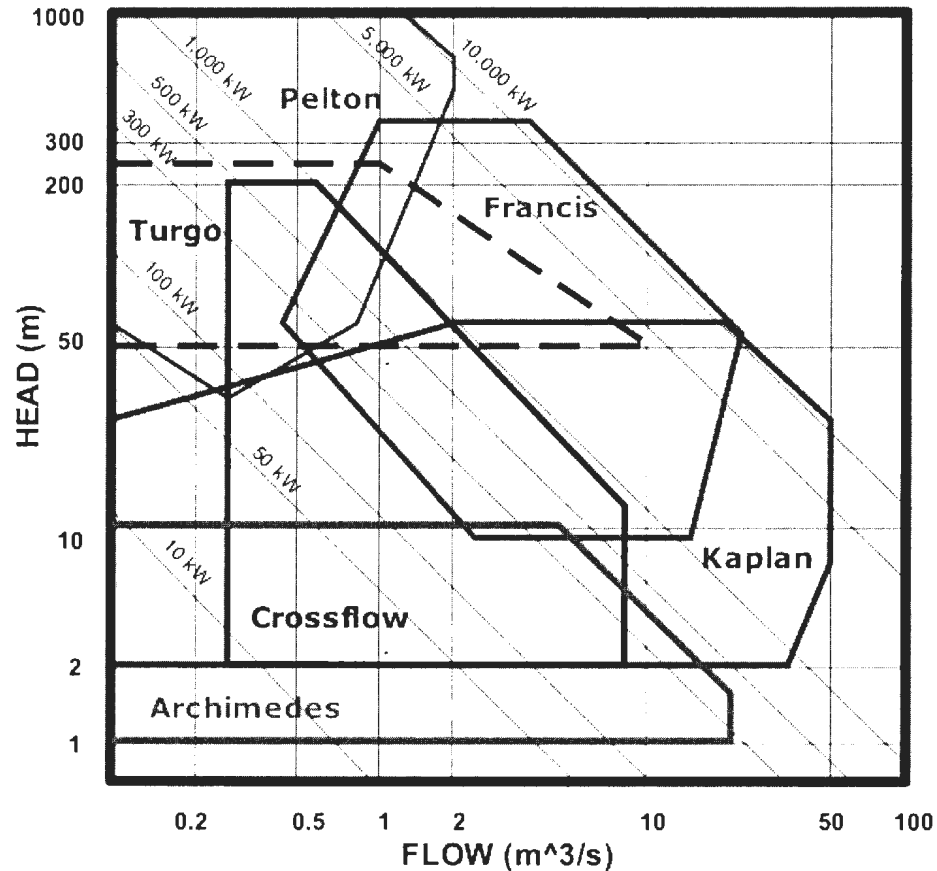


Figure 2.1. Operating regions of different water turbines [37]

Secondly, as this PHS system will be operated at variable load to meet the instantaneous demand, so very good partial flow efficiency is a must. PWT can provide up to 95% efficiency and in micro scale peak efficiency could be 90%. And this efficiency is almost constant from 40%-100% rated flow rate for single jet and from 20% -100% for twin

spear jet configuration. In Chapter 4 typical efficiency curve for a single (red curve) and twin spear-jet (blue curve) PWT is shown in Figure 4.4. With more spear-jets the PWT would operate at high efficiency over an even wider range of flow. PWT rotates at high speeds so it is possible to couple it with the generator directly. This reduces the cost and saves all of the losses in the belt-drive or gearbox which can be between 2% - 7% [37].

In article [38] and [39] authors performed analytical study of water flow through a PWT bucket and develop a mathematical model to justify the effect of blade friction on the performance of PWT. In the key components to design a PWT and its power capabilities are head, discharge, throat diameter and rotational speed of the runner. The power capability of the unit is limited due to the several types of losses e.g. frictional losses, inlet and bend losses and mechanical losses. In another article author developed a CFD model to characterize frictional losses in a PWT and determined issues which effects PWT efficiency. They tested their model for different rotating speed and different number, shape and size of buckets. They concluded that 30% improvement can be done with the overall efficiency [40]. Another author explains about the basic equations that can be applied to any turbine and has analyzed the performance of PWT in [41]. In article [42] author showed detailed processes of quantitative calculation for a PWT to estimate the hydraulic efficiencies and their dependency on both of the operating conditions and shape of the bucket.

### 2.3 High penetration Wind-diesel hybrid power system

High penetration in a hybrid power system can be achieved with integration of a storage system or diesel shut down operation in the time of high wind or both of them at the same time. High penetration of renewable energy may affect the stability of system frequency stability significantly in an isolated power system since wind and solar photovoltaic generation has neither inertia nor primary frequency regulation so any kind of storage is required [43]. In article [44] authors evaluate the ability of sustainable automation inverter to stabilize the power quality in a high penetration diesel-off mode hybrid power system using simulated components in a test bed facility. Amount of wind penetration is a factor for system design and measures the performance of the site.

$$\text{Instantaneous penetration} = \frac{\text{Wind power output, kW}}{\text{Primary electrical load, kW}} \quad 2.6$$

$$\text{Average penetration} = \frac{\text{Wind energy produced, kWh}}{\text{Primary energy demand, kWh}} \quad 2.7$$

Peak values are instantaneous; averages are long term. Maximum level of wind penetration for a particular site can be limited by many factors e.g. storage capacity, total generation, demand management. Penetration level and their operational features are pointed out below in Table 2.2.

Table 2.2. Penetration level of wind-diesel system and their operating characteristics [44] [45]

Penetration Level	Operating Features	Penetration, %	
		Peak Instantaneous	Annual Average
Low	<ul style="list-style-type: none"> <li>• Full-time diesel operation</li> <li>• Wind power diminishes net load on diesel</li> <li>• Primary load takes all wind energy</li> <li>• Does not need supervisory control system</li> </ul>	< 50	< 20
Medium	<ul style="list-style-type: none"> <li>• Full-time diesel operation</li> <li>• At high wind-power levels, secondary loads dispatched to ensure adequate diesel loading or wind generation are curtailed</li> <li>• Needs relatively simple control system</li> </ul>	50–100	20–50
High	<ul style="list-style-type: none"> <li>• During high wind availability diesel may be shut down</li> <li>• Secondary components required to adjust frequency and voltage</li> <li>• Needs sophisticated control system</li> </ul>	100–400	50–150

Various operational modes of a high penetration hybrid system of Wales, Alaska have been studied in technical report [46]. In operation without battery diesel is operated only when wind energy cannot meet the load and when diesel is ON, it controls system frequency and voltage. When diesel is OFF, dump load controls system frequency. In system with battery storage, when diesel is ON surplus diesel power is used to charge batteries. Any transient amount needed for load is drawn from the batteries which keeps

the diesel from being turned on. When diesel is OFF surplus wind power is used to charge the batteries first and further excess power is dissipated by the dump load and hence system frequency is kept constant. In Chapter 5 this kind of control has been established with an addition of pumped hydro storage in the hybrid system and energy has been drawn from this storage system for long term energy need. Transient energy needs has been met from the battery bank.

## 2.4 References

- [1] Connolly, D., MacLaughlin, S., & Leahy, M. (2010). Development of a computer program to locate potential sites for pumped hydroelectric energy storage. *Energy*, 35(1), 375. doi:<http://dx.doi.org/10.1016/j.energy.2009.10.004>
- [2] Nanahara, T., & Takimoto, A. (1994). A study on required reservoir size for pumped hydro storage. *Power Systems, IEEE Transactions on*, 9(1), 318-323. doi: 10.1109/59.317595
- [3] Garcia-Gonzalez, J., de la Muela, R., Santos, L., & Gonzalez, A. (May 2008). *IEEE Trans. Power Systems*, 23(2), 460-468.
- [4] Castronuovo, E. D., & Peas Lopes, J. A. (2004). On the optimization of the daily operation of a wind-hydro power plant. *Power Systems, IEEE Transactions on*, 19(3), 1599-1606. doi: 10.1109/TPWRS.2004.831707
- [5] Brown, P. D., Peas Lopes, J. A., & Matos, M. A. (2008). Optimization of pumped storage capacity in an isolated power system with large renewable penetration. *Power Systems, IEEE Transactions on*, 23(2), 523-531. doi: 10.1109/TPWRS.2008.919419

- [6] Tuohy, A., & O'Malley, M. (2009). Impact of pumped storage on power systems with increasing wind penetration. Paper presented at the *Power Energy Society General Meeting, 2009. PES '09. IEEE*, 1-8. doi: 10.1109/PES.2009.5275839
- [7] Taniguchi, H., Nagao, T., & Higasa, H. (1992). Development of a pumped-storage power station model for power system stability study. *Electrical Engineering in Japan*, 112(3), 50-62. doi: 10.1002/eej.4391120306
- [8] Hannett, L. N., Lam, B. P., Prabhakara, F. S., Qiu Guofu, Ding Mincheng, & Bian Beilei. (1998). Modeling of a pumped storage hydro plant for power system stability studies. Paper presented at the *Power System Technology, 1998. Proceedings. POWERCON '98. 1998 International Conference on*, 2 1300-1304 o.2. doi: 10.1109/ICPST.1998.729296
- [9] Mansoor, S. P., Jones, D. I., Bradley, D. A., Aris, F. C., & Jones, G. R. (1999). Stability of a pump storage hydro-power station connected to a power system. Paper presented at the *Power Engineering Society 1999 Winter Meeting, IEEE*, , 1 646-650 o.1. doi: 10.1109/PESW.1999.747531
- [10] Gao, H. M., & Wang, C. (2006). A detailed pumped storage station model for power system analysis. Paper presented at the *Power Engineering Society General Meeting, 2006. IEEE*, 5 pp. doi: 10.1109/PES.2006.1709259
- [11] Task Committee on Pumped Storage, Committee on Hydropower of the Energy Division of the American Society of Civil Engineers. (1995). *Hydroelectric pumped storage technology: International experience*. New York: American Society of Civil Engineers.

- [12] Qian, K., Jiang, Y., & Li, Z. (2011). Improve wind energy penetration in an isolated power system by a stand-alone wind pumped storage hydropower plant. Paper presented at the *Remote Sensing, Environment and Transportation Engineering (RSETE), 2011 International Conference on*, 406-411. doi: 10.1109/RSETE.2011.5964299
- [13] Kintner-Meyer, M., Chunlian Jin, Balducci, P., Elizondo, M., Xinxin Guo, Nguyen, T., Tuffner, F., Viswanathan, V. (2011). Energy storage for variable renewable energy resource integration #x2014; A regional assessment for the northwest power pool (NWPP). Paper presented at the *Power Systems Conference and Exposition (PSCE), 2011 IEEE/PES*, 1-7. doi: 10.1109/PSCE.2011.5772548
- [14] Delimustafic, D., Islambegovic, J., Aksamovic, A., & Masic, S. (2011). Model of a hybrid renewable energy system: Control, supervision and energy distribution. Paper presented at the *Industrial Electronics (ISIE), 2011 IEEE International Symposium on*, 1081-1086. doi: 10.1109/ISIE.2011.5984310
- [15] Zhao, G., & Davison, M. (2009). Optimal control of hydroelectric facility incorporating pump storage. *Renewable Energy*, 34(4), 1064. doi: <http://dx.doi.org/10.1016/j.renene.2008.07.005>
- [16] Papaefthymiou, S. V., Karamanou, E. G., Papathanassiou, S. A., & Papadopoulos, M. P. (2010). A wind-hydro-pumped storage station leading to high RES penetration in the autonomous island system of ikaria. *Sustainable Energy, IEEE Transactions on*, 1(3), 163-172. doi: 10.1109/TSTE.2010.2059053
- [17] Aihara, R., Yokoyama, A., Nomiya, F., & Kosugi, N. (2011). Optimal operation scheduling of pumped storage hydro power plant in power system with a large

- penetration of photovoltaic generation using genetic algorithm. Paper presented at the *PowerTech, 2011 IEEE Trondheim*, 1-8. doi: 10.1109/PTC.2011.6019279
- [18] Li, W., Huang, J., Li, G., & Wang, Z. (2011). Research on optimizing operation of the single reservoir of hybrid pumped storage power station. Paper presented at the *Electric Utility Deregulation and Restructuring and Power Technologies (DRPT), 2011 4th International Conference on*, 1389-1394. doi: 10.1109/DRPT.2011.5994113
- [19] Bueno, C., & Carta, J. A. (2006). Wind powered pumped hydro storage systems, a means of increasing the penetration of renewable energy in the Canary Islands. *Renewable and Sustainable Energy Reviews*, 10(4), 312. doi: <http://dx.doi.org/10.1016/j.rser.2004.09.005>
- [20] Pérez-Díaz, J. I., Perea, A., & Wilhelmi, J. R. (2010). Optimal short-term operation and sizing of pumped-storage power plants in systems with high penetration of wind energy. Paper presented at the *Energy Market (EEM), 2010 7th International Conference on the European*, 1-6. doi: 10.1109/EEM.2010.5558706
- [21] Iqbal, T. (2010). *Feasibility study of pumped hydro energy storage for ramea wind-diesel hybrid power system*. (Technical report). St. John's, NL, Canada
- [22] Lee, D., & Wang, L. (2008). Small-signal stability analysis of an autonomous hybrid renewable energy power Generation/Energy storage system part I: Time-domain simulations. *Energy Conversion, IEEE Transactions on*, 23(1), 311-320. doi: 10.1109/TEC.2007.914309
- [23] Kim, S., Jeon, J., Cho, C., Ahn, J., & Kwon, S. (2008). Dynamic modeling and control of a grid-connected hybrid generation system with versatile power

- transfer. *Industrial Electronics, IEEE Transactions on*, 55(4), 1677-1688. doi: 10.1109/TIE.2007.907662
- [24] Takahashi, R., & Tamura, J. (2008). Frequency control of isolated power system with wind farm by using flywheel energy storage system. Paper presented at the *Electrical Machines, 2008. ICEM 2008. 18th International Conference on*, 1-6. doi: 10.1109/ICELMACH.2008.4800025
- [25] Diesel engine starting fundamental. Retrieved October 10, 2012, from <http://www.cantecsystems.com/ccrdocs/Supercapacitor-Engine-Cranking-fundamentals.pdf>
- [26] Version 14.1 PowerFactory, *User's Manual*, 1st ed. Gomarigen, Germany: DIgSILENT, 2011, vol. 2.
- [27] Kundur, P., "Vice-president, Power Engineering," in *Power System Stability And Control*, Neal, J. and Mark, G., Eds. Palo Alto, California, USA: McGraw-Hill, 1994
- [28] ŘEŘUCHA, V., KRUPKA, Z., & LEUCHTER, J. (2003). The mechatronic approach to the optimal control of the vsfc genset. *Cybernetics Letters*, (2003-I)
- [29] Thin, K. C., Khaing, M. M., & Aye, K. M. (2008). *Design and performance analysis of centrifugal pump* World Academy of Science, Engineering and Technology.
- [30] *Moment of inertia and pump Startup/Failure*. (November 14 2003). (Stoner Software Knowledge Base). Advantica Ltd. Retrieved from [http://my.advanticagroup.com/support/allsecure/watersecure/releases\\_advisories/KBA\\_pump\\_moment\\_of\\_inertia.pdf](http://my.advanticagroup.com/support/allsecure/watersecure/releases_advisories/KBA_pump_moment_of_inertia.pdf)

- [31] Karassik, I., Messina, J., Cooper, P., & Heald, C. (2007). Centrifugal pumps: General performance characteristics. *Pump handbook* (3rd ed., pp. 2.363) McGraw-hill.
- [32] Manning, F. S., Thompson, R. E., & Thompson, R. E. (1995). *Oilfield processing of petroleum. vol. 1: Natural gas* (pp. 293) PennWell Corporation
- [33] Karassik, I., Messina, J., Cooper, P., & Heald, C. (2007). Pumping systems and system-head curves. *Pump handbook* (3rd ed., pp. 8.33-8.34) McGraw-hill.
- [34] The engineering toolbox - minor loss coefficient in pipes and tubes components. Retrieved January 30, 2013, from [http://www.engineeringtoolbox.com/minor-loss-coefficients-pipes-d\\_626.html](http://www.engineeringtoolbox.com/minor-loss-coefficients-pipes-d_626.html)
- [35] Jiaqi, L., & Harley, R. G. (2010). Pumped storage hydro-plant models for system transient and long-term dynamic studies. Paper presented at the *Power and Energy Society General Meeting, 2010 IEEE*, 1-8. doi: 10.1109/PES.2010.5589330
- [36] Nau, G. (2011). 3Helix power-turbine history. Retrieved June 1, 2013, from <http://www.3helixpower.com/hydropower/types-of-turbines/attachment/turbine-operating-regions-3/>
- [37] Renewable first - hydropower turbines - Pelton and Turgo turbines. Retrieved January 30, 2013, from <http://www.renewablesfirst.co.uk/hydro-learning-centre/pelton-turgo-turbines/>
- [38] Atthanayake, I., Sugathapala, T., & Fernando, R. (2011). Mathematical model for the effect of blade friction on the performance of Pelton turbine. *International Journal of Fluid Machinery and Systems*, 4(4), 396-406. doi: <http://dx.doi.org/10.5293/IJFMS.2011.4.4.396>

- [39] Atthanayake, I. (2009). Analytical study on flow through a pelton turbine bucket using boundary layer theory. *International Journal of Engineering & Technology (IJET)*, 9(9), 11-15.
- [40] Beucher, Y., Ksayer, E. V., & Clodic, D. (2010). Characterization of friction loss in Pelton turbine. *International Refrigeration and Air Conditioning Conference*, Purdue, IN, USA.
- [41] Daugherty, R. (1920). *Hydraulic turbines* (3rd ed.) Mc Graw Hill Book Company.
- [42] Zhang, Z. (2007). Flow interactions in Pelton turbines and the hydraulic efficiency of the turbine system. *Proceedings of the I MECH E Part A Journal of Power and Energy*, 221(3), 343-355. doi: 10.1243/09576509jpe294
- [43] Rouco, L., Azpiri, I., Gómez de Olea, I., & Taberero, J. (2011). Increasing penetration of renewals in isolated power systems using energy storage systems. *International Conference on Renewable Energies and Power Quality (Icrepq'11)*, Spain.
- [44] Muhando, B., Keith, K., & Holdmann, G. (2010). *Evaluation of the ability of inverters to stabilize high-penetration Wind-diesel systems in Diesel-off mode using simulated components in a test bed facility*. Alaska, USA: The Denali Commission under the Emerging Energy Technologies Grant Fund.
- [45] Baring-Gould, I., & Dabo, M. (May 2009). Technology, performance, and market report of wind-diesel applications for remote and island communities. *WINDPOWER 2009 Conference and Exhibition*, Chicago, Illinois, USA. (NREL/CP-500-45810)

- [46] Drouilhet, S., & Shirazi, M. (May 2002). *Wales, Alaska high-penetration wind-diesel hybrid power system - Theory of Operation*. (Technical report No. NREL/TP-500-31755). pp-13, National Renewable Energy Laboratory.

### **3 A novel method to model a hybrid power system with pumped hydro storage for Ramea, Newfoundland**

#### **Preface**

A version of this manuscript has been published in the conference proceedings of *IEEE Newfoundland Electrical and Computer Engineering Conference 2012, St. John's, Newfoundland and Labrador, Canada*. This paper has also been presented in that conference. The co-author Dr. Tariq Iqbal supervised the principle author Md. Rahimul Hasan Asif to develop the research on the entitled topic and helped him to conceptualize the techniques and theories available for this research. Md. Rahimul wrote the paper, developed the dynamic model, conducted simulation and associated analyses while Dr. Iqbal reviewed the manuscript and provided necessary suggestion.

#### **Abstract**

This work describes a novel method for modeling the hybrid power system of Ramea, Newfoundland and presents feasibility of a pumped hydro storage system instead of existing electrolyzer and hydrogen generator system. Detailed MATLAB modeling for every component has been done to simulate the Ramea hybrid power system. Incorporation of a pumped hydro system permits minimal use of lead acid batteries and eliminate the low turn around efficiency of electrolyzer and hydrogen generator system. This new modeling method is fast, accurate and any type of controllers can be implemented. The proposed real time control algorithm dynamically observes available

surplus/missing power in the system and operates pump/generation as required and also controls charging/discharging of the battery bank. The proposed controller of two energy storage systems flattens the total generation curve and follows the changing demand curve to reduce the system transients. This research presents system model, controller design and detailed simulation results.

**Index Terms:** System modeling, pumped hydro storage, hybrid power system, Renewable energy.

### 3.1 Introduction

Ramea is an island located off the south coast of Newfoundland, Canada. It is approximately 3.1 km long by 1 km wide. In 2004, Ramea was selected as the first pilot site for a Wind-Diesel hydrogen hybrid power system. The project was led by Newfoundland and Labrador Hydro in collaboration with Atlantic Canada Opportunities Agency, the Government of Newfoundland and Labrador, Natural Resources Canada, Memorial University of Newfoundland, University of New Brunswick and Frontier Power Systems with the support of CANMET Energy Technology Centre-Ottawa (CETC-Ottawa). The key objective of this project was to exhibit substantial improvement of energy efficiency and reliability after incorporating Wind-Diesel Integrated Control System (WDICS) in the island's grid which can reduce the use of diesel power by introducing green renewable wind energy in remote and isolated location. Annually, this

wind-diesel pilot system is generating almost one million kWh of electricity and offsetting approximately 750 tons of greenhouse gas emissions [1] [2].

Ramea hybrid system consists of six 65kW Windmatic 15s, three 100kW Northern power 100 wind turbines, three 925kW Diesel generators, Hydrogen Electrolyzer and Storage and a 250kW Hydrogen Powered Generator. When wind power generation exceeds the load, the electrolyzer produces hydrogen from water electrolysis which is stored in the storage tanks. And when harnessed wind power is inadequate to supply the total load the stored hydrogen is fed into a generator as a fuel which delivers electricity to the grid and maintains the stability [2]. A hydrogen electrolyzer and storage system produces hydrogen at 70% efficiency and a hydrogen fueled generator generate electricity at less than 35% efficiency. So the overall turn around conversion efficiency is less than 25% which is very low [3].

Reference [4] presented detailed information, analysis and dynamic simulation for the optimal size and site selection of a pumped hydro storage system replacing the hydrogen electrolyzer and storage as a permanent long term solution. About 37% renewable energy fraction can be achieved from a 150kW pumped hydro storage system with a 3932m<sup>3</sup> water reservoir at a height of 63m on the top of 'Man of War' hill. Topographical map of this hill shows that it has 2000m<sup>2</sup> of area to build a 2m high hydro storage reservoir. In that report only 24s of simulation has been shown as it took days of computer time. And the simulation didn't converge in the time period of 11s to 16s.

Modeling every component with simpler first order transfer function can considerably improve the required simulation time, makes the analysis easier and gives fairly accurate solutions.

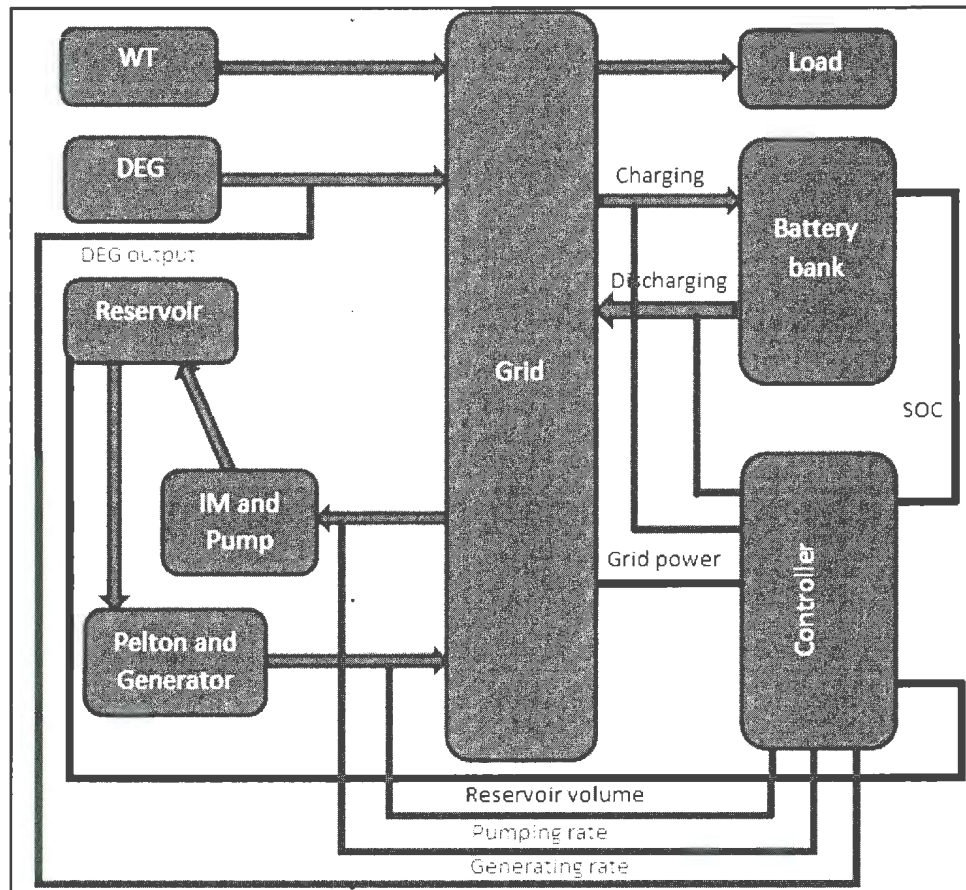


**Figure 3.1. A block diagram of Ramea hybrid power system with proposed pumped hydro storage system**

Reference [5] studied system stability by time-domain simulations of an autonomous hybrid renewable energy power generation and storage system connected with isolated loads. The mentioned hybrid system has a battery bank and a flywheel system as storage subsystems. Three mathematical models have been investigated for three different

operating points and disturbance conditions. But the mathematical model which has been used here has no connection with the real world model with friction, efficiency, response time and no controller is considered in this model. Modeling practical subsystems with simple first order models juxtaposing all efficiencies, dynamic frictions, different time constants according to the subsystem parameters is a real challenge.

In this study a simple, fast novel method has been introduced to simulate system dynamic of Ramea hybrid power system with a pumped hydro storage. A block diagram of Ramea hybrid power system is shown in Figure 3.1. A battery bank is also used to supply or store the intermittent power as induction motor and centrifugal pump or turbine and generator require some time to reach a certain rated operating point and have higher time constant than Lead Acid Battery. The introduced model here has proportional controllers with all of its subsystems. Characteristic data and parameters of the aforementioned wind turbines and diesel generator used in Ramea hybrid system are taken from the respective manufacturers. All the subsystem models e.g. Diesel Engine Generator, Battery bank, Pelton Wheel Turbine have been created after analyzing the parameters of the real world model. In this model 1st order simple model is considered. Simulation has been done for 10000s which is approximately 2.77 hour. Load demand and wind speeds are generated in such a way which emulates the real condition of Ramea.

## 3.2 Model description

### 3.2.1 Wind speed and Load data

Wind data has been taken from a website which stores 1s wind data [6]. From several available data arrays, suitable arrays have been selected which matches with the average wind speed in Ramea in the month of January-February. Average wind speed in the used wind data file is 9.65m/s. As shown in Figure 3.2 data has been taken for 10000s. Load data of Ramea has been collected from the Homer model file which has been used for simulation in Reference [4]. One 24 hour load curve of January-February is shrunk to 2.77 hour time to simulate both of the pumping and generating operation in off-peak and peak hour of load demand. As shown in Figure 3.3 load demand data has been taken for 10000s.

### 3.2.2 Wind turbine model

Wind turbine power curve has been collected from the manufacturers [Appendix A]. Taking several samples from the curve a 6th order polynomial fitting has been performed to generate the exact same curves for the turbines. As shown in Figure 3.4 necessary cut in and cut out wind speed conditions have been applied in the wind turbine model. Time constant is measured for two types of turbines using the following equation from the Reference [7]:

$$H = 1.87 * P^{0.0597}$$

3.1

In Equation 3.1,  $H$  is the mechanical inertia time constant and  $P$  is the power of the turbine in watts. So calculation gives 3.6s for 65kW Windmatic 15s turbine [8] and 3.7s for 100kW Northern Power 100 turbines [9]. In Figure 3.5 all the turbines and demand curve are added in the first adder 'add1'. Output of 'add1' represents power available or lack in the grid after the wind penetration which will be managed by the Diesel Engine Generator (DEG) first.

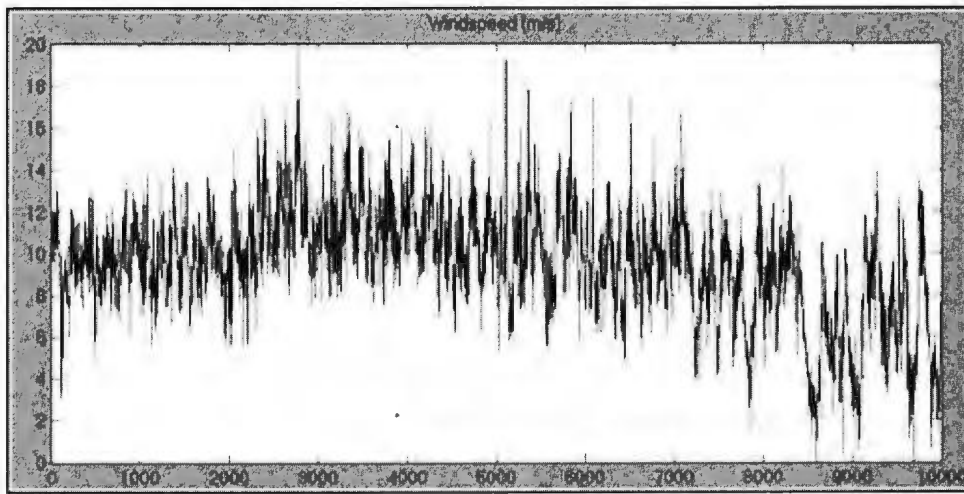


Figure 3.2. 1s Wind speed data

### 3.2.3 Diesel Engine Generator model

DEG in Ramea has a rated output of 925kW. There are three DEG but only one is used at a time. A DEG can be operated down to 30% of its rated output so here DEG is operating from 300kW to 925kW region which means any power requirement in this range can be met by DEG only. If DEG reaches to its maximum 925kW or minimum 300kW then

pump, turbine or battery will take over the responsibility of power balance in the grid. Time constant of DEG is taken as it is used in Reference [5]. Transfer function (TF) of DEG becomes  $TF_{DEG} = 1 / (2s + 1)$ .  $K_P = 100$  is used for DEG. This value of  $K_P$  is found suitable and used in all subsystems.

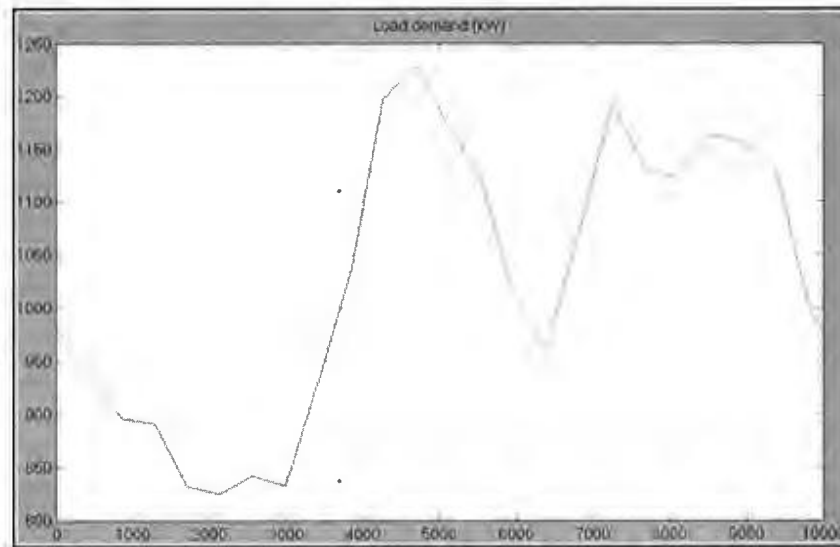


Figure 3.3. Load demand data

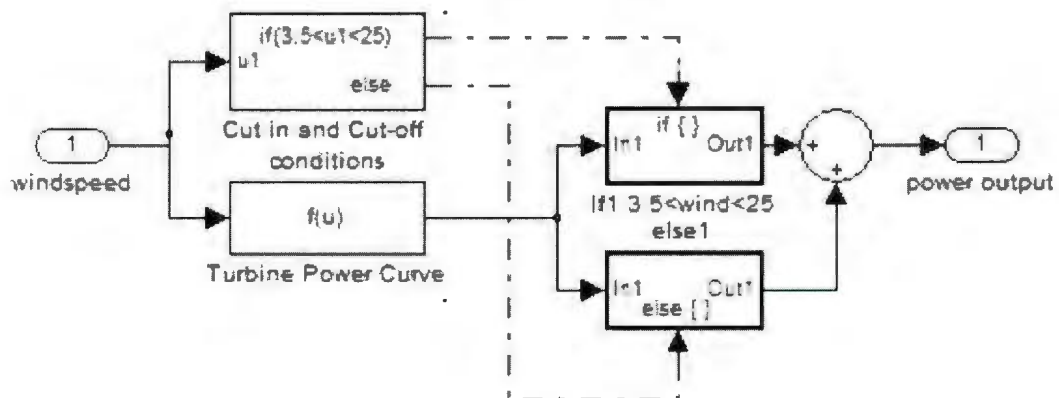
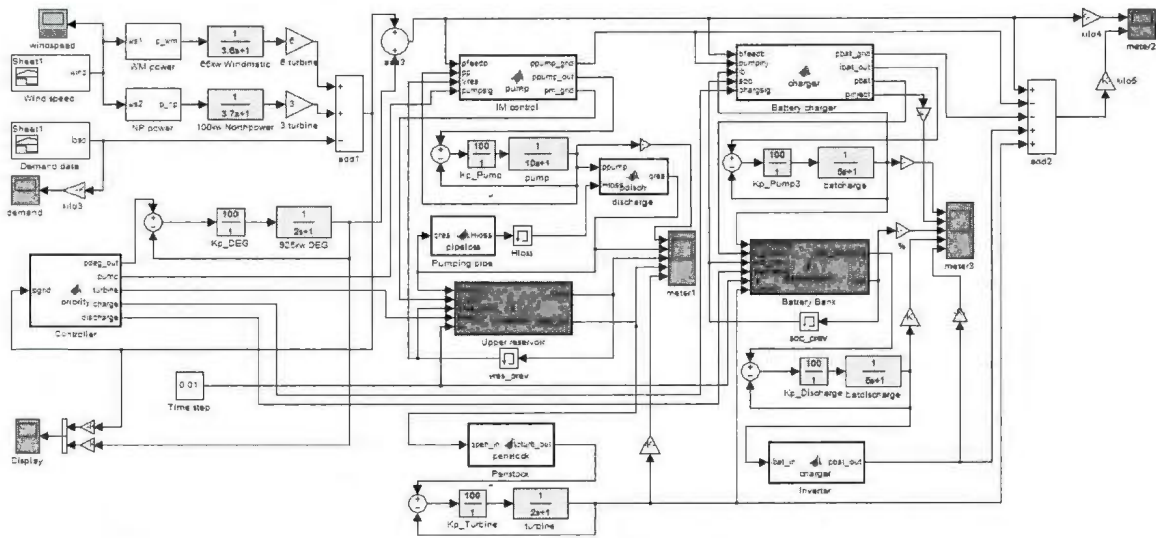


Figure 3.4. Wind turbine power curve and conditions



**Figure 3.5. Simulink - MATLAB embedded function blocks based dynamic model of Ramea hybrid power system with pumped hydro storage and battery bank**

### 3.2.4 Induction motor and Centrifugal Pump model

Induction motor (IM) and Centrifugal Pump (CP) are modeled together in the same block considering their individual characteristics. CP takes relatively large time to response for a sudden change than an IM. Comparing the starting time of a combination of IM and CP from reference [10], a 4000HP 1000RPM pumping system takes approximately two and half minutes to reach its rated output. Here we assumed the 200HP pumping system needs 1 minute to settle down. Transfer function of this block is  $TF_{PUMP} = 1/(10s+1)$  and  $K_P = 100$ . Efficiencies of IM and CP are considered as 95% and 80% respectively which gives a total efficiency of 75%. Equation 3.2 is used in MATLAB code to determine  $q_{res} =$  pumping water flow to reservoir after measuring  $p_{feedb}$  which is the available power in the grid after the DEG reaches its minimum of 300kW.

$$q_{res} = \frac{ppump * pmeff}{hres + Hloss} * dens * g \quad 3.2$$

Here,  $ppump$  = power delivered to the pumping system which can vary from 30% to 100% of the rated output, here it's 100kW to 300kW;  $pmeff = 75\%$ ;  $hres = 63\text{m}$ ; height of the reservoir;  $Hloss$  = penstock friction loss;  $dens = 1000 \text{ kgm}^{-3}$  and  $g = 9.81\text{ms}^{-2}$ .

### 3.2.5 Penstock model

Penstock is designed as  $L_{pipe} = 70\text{m}$  long and  $D_{pipe} = 0.3\text{m}$  in diameter. Reynolds number is chosen assuming that flow is laminar inside the pipe. A minor loss coefficient for water meter is used here as ' $klossco$ ' which is taken equal to 7 [11].

$$\begin{aligned} \text{Velowaterpump} &= q_{res}/A_{pipe}; && \% \text{water velocity in pipe} \\ \text{Re} &= 2000; && \% \text{Reynolds number} \\ \text{flam} &= 64/\text{Re}; && \% \text{Darcy Friction Factor for laminar flow} \\ \text{hpipefric} &= (8 * \text{flam} * L_{pipe} * q_{res}^2)/(g * \pi^2 * D_{pipe}^5); && 3.3 \\ \text{hlossmeter} &= klossco * (\text{Velowaterpump}^2)/(2 * g); \\ \text{Hloss} &= \text{hpipefric} + \text{hlossmeter}; \end{aligned}$$

Equation 3.3 used here is Darcy–Weisbach equation for friction [12].

### 3.2.6 Water reservoir model

The water reservoir has a total volume of  $4000\text{m}^3$ . Initial volume is considered as  $2000\text{m}^3$ . Pump action will be stopped if water volume exceeds  $3900\text{m}^3$  and turbine action will be terminated if water volume goes below  $100\text{m}^3$ .

### 3.2.7 Turbine model

A 150kW Pelton wheel turbine is used here which has very good partial flow efficiency as shown in Figure 3.6 [13]. The blue curve is for twin jet setup. Synchronous generator and turbine are modeled together using a combined efficiency of 70% and time constant of 2. TF of this block is  $TF_{\text{TURB}} = 1/(2s + 1)$  and  $K_P = 100$ .

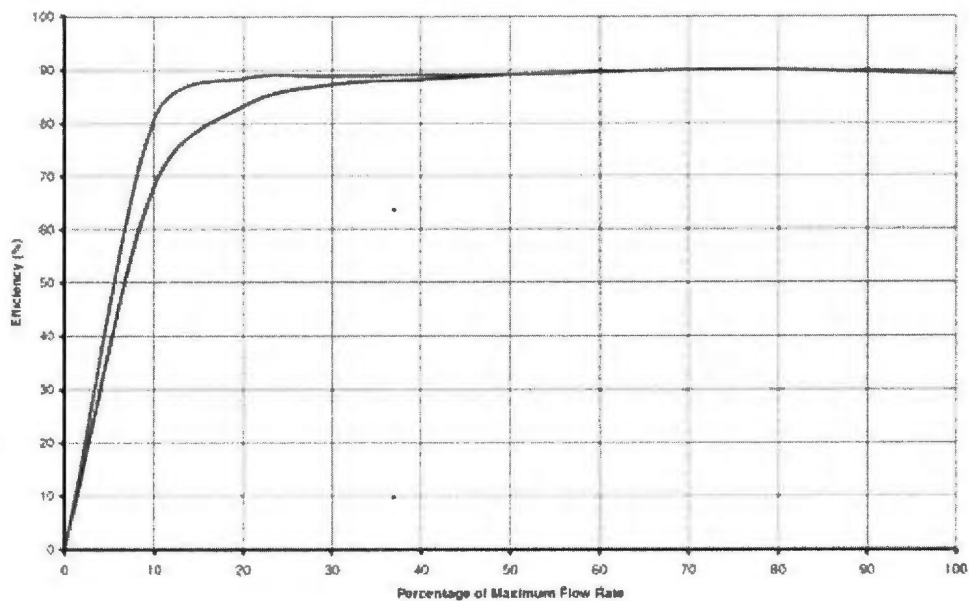


Figure 3.6. Part flow efficiency of a Pelton Wheel Turbine

The power output of the turbine generator block is as in Equation 3.4 below where  $pturb\_out$  = turbine output,  $qpen\_in$  = water flow coming to the turbine and  $turb\_eff$  = 70%.

$$pturb\_out = qpen\_in * hres * dens * g * turb\_eff \quad 3.4$$

### 3.2.8 Battery bank model

In an isolated grid batteries used as storage provide fast response which makes them favorable for dynamic operations to gain more system reliability and improve power quality. A bank of 300 batteries is used each having a capacity of 200Ahr. A set of 15 branches are connected in parallel where each branch consists of 20 batteries i.e. a dc battery bus voltage of 240V. A charging and discharging block have been created to control the current and monitor the State of Charge (SOC) of the battery. A Lead-Acid battery should not be discharged when SOC goes down to 40%. Total coulomb capacity can be found from the calculations below in Equation 3.5,

$$\begin{aligned} Total\ cap &= individual\ capacity * 360 * no.\ of\ branches & 3.5 \\ &= 200 * 3600 * 15 = 10800000\ C\ (at\ 100\% \text{ SOC}) \end{aligned}$$

So the operating region of the battery starts from 100% SOC to 40% SOC equivalent to 4320000 C. For charging 'one third of individual capacity' has been followed as in Equation 3.6 where  $ibat\_out$  = total charging current,  $ind\_cap$  = individual capacity and  $n\_para$  = no. of branches (here it is 15).

$$ibat\_out = 0.33 * ind\_cap * n\_para \quad 3.6$$

If more than 234kW power is available in the grid considering the pump is already operating, the battery will be charged with this rated current. Below charging current will be changed according to the available power. In this model initial SOC is chosen as 70% which is 7560000 C. While discharging, battery bank can be discharged at any rate but that will affect the effective capacity of battery following the '*Peukert's law*'. Thumb rule for optimal discharge rate is 10% of the individual capacity. In this model combined efficiency of battery and converters is considered as 80%. Equation 3.7 is used to calculate the power delivered ( $pbat\_out$ ) by the battery when required where  $v\_bat$  = 240V,  $ibat\_in$  = total discharging current and  $bateff$  = 80%.

$$pbat\_out = v\_bat * ibat\_in * bateff \quad 3.7$$

TF of battery block is  $TF_{BAT} = 1 / (0.5s + 1)$  and  $K_p = 100$ . Key point here is, due to the faster response, it always operate to cover the intermittent power changes caused by the delayed response of other mechanical subsystems.

### 3.3 Simulation and Result

Simulation has been run for 10000s. As shown in Figure 3.7 DEG output is being varied to compensate the load demand by a controller which sends signal to the other subsystems too. A simple algorithm used is as follows:

```
if pgrid >= -300000
    pdeg_out = 300000;
    pump = 1; charge = 1;
end

if pgrid > -925000 && pgrid < -300000
    pdeg_out = -pgrid;
    pump = 0; charge = 0;
    turbine = 0; discharge = 0;
end

if pgrid < -925000
    pdeg_out = 925000;
    turbine = 1; discharge = 1;
end
```

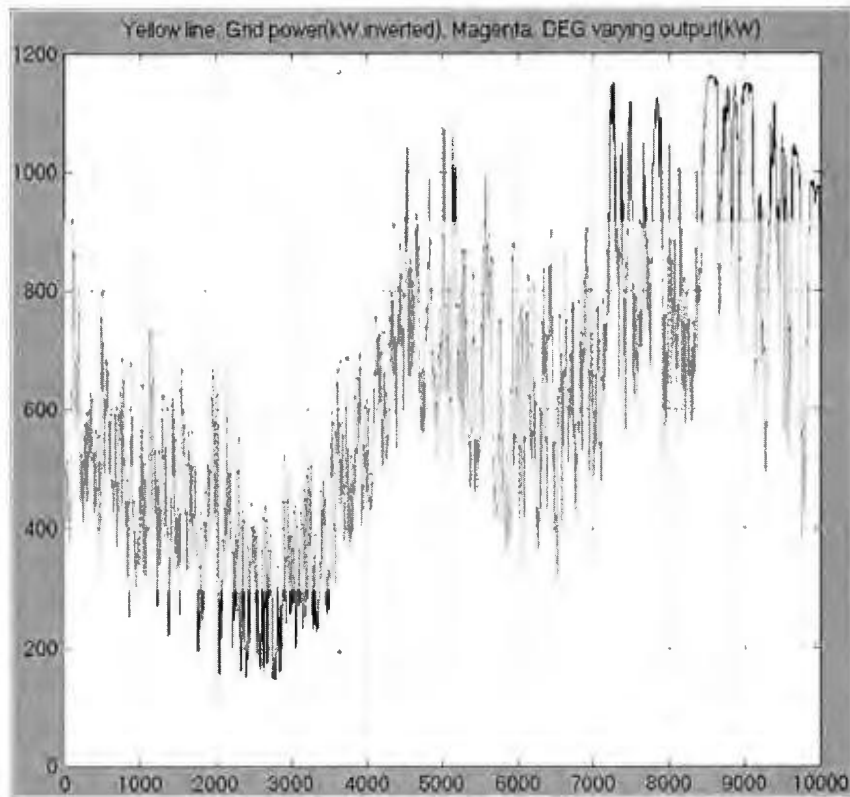


**Figure 3.7. Varying DEG output to cover load demand in between 300kW to 925kW**

From Figure 3.8 and Figure 3.9 it is observed that from 1200s to 3500s DEG is operating at 300kW and pump and battery start operating. Reservoir water volume and %SOC both are increasing that time. Power shortage is found from 4500s to 5500s and at next from 7200s to 10000s while DEG is operating at its rated 925kW condition. Both turbine and battery discharging start to deliver the required power to the grid to maintain system stability. The Final comparison can be seen in Figure 3.10 where upper output has no storage system and lower output has the proposed pumped hydro storage system. Power fluctuation is much more in the aforementioned system.

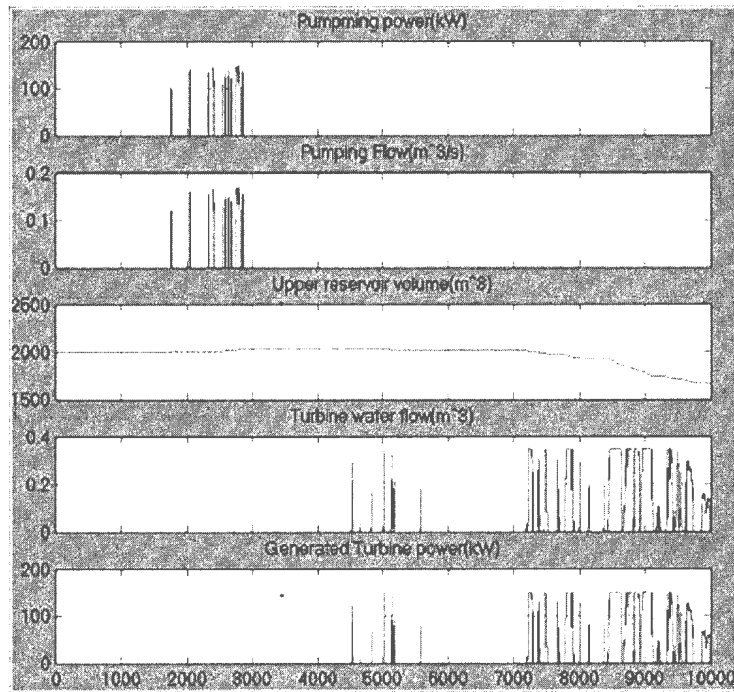


Figure 3.8. Pump and Turbine operation

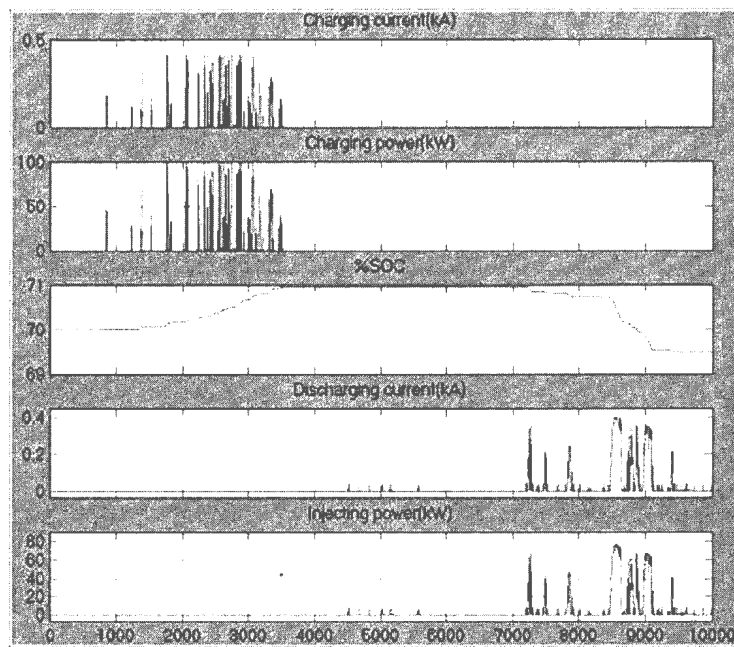
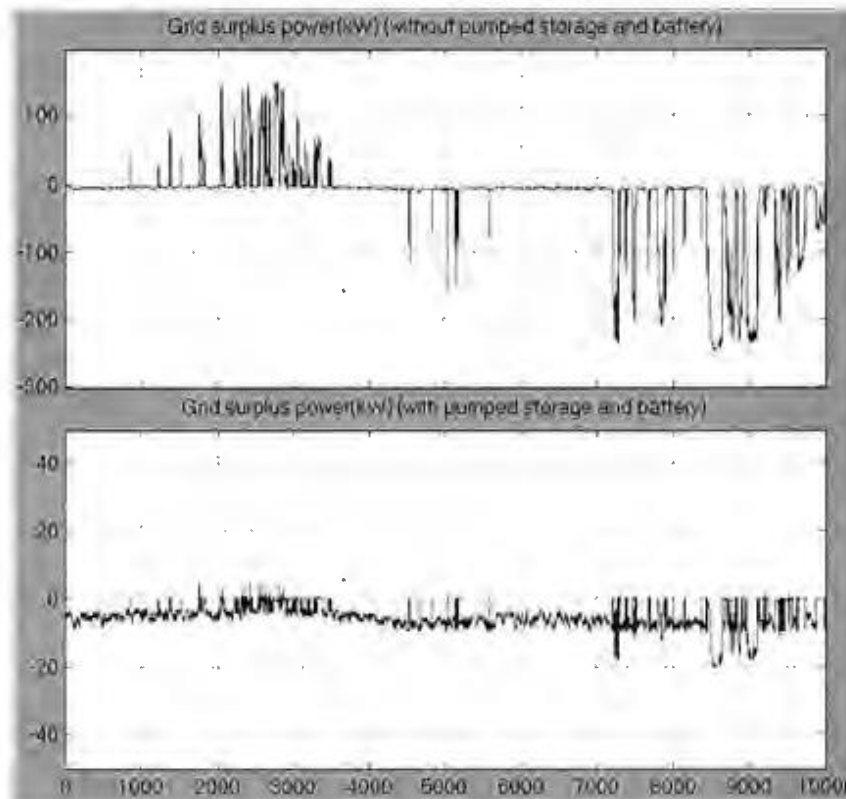


Figure 3.9. Battery discharge and charging operation



**Figure 3.10. Comparison between two scenarios where bottom curve is representing the grid power with pumped hydro and battery system**

### 3.4 Conclusion

The proposed hybrid system model is very fast in simulation. Using 0.01s time step, for 10000s simulation it takes only 3min to complete. All real world characteristics curves, efficiencies and losses are used in this model. This model can be used to check possible future extension to the hybrid system. Any wind data and load data can be used here. Given enough time to simulate the proposed model allows us to simulate few months of operations of Ramea hybrid system. This model can be improved further incorporating

higher order complicated models in the blocks and nonlinear efficiencies and AC analysis.

### 3.5 Acknowledgment

Authors thank The NSERC Wind Energy Strategic Network (WESNet) which is a Canada wide research network funded by industry and the Natural Sciences and Engineering Research Council of Canada (NSERC) for funding this research.

### 3.6 References

- [1] Govt. of Ramea, "Ramea Island," [Online]. Available: <http://www.ramea.ca/>. [Accessed 05 10 2012].
- [2] CANMET Energy, "Natural Resource Canada," Natural Resource Canada, 07-07-2007. [Online]. Available: <http://canmetenergy.nrcan.gc.ca/renewables/wind/464>. [Accessed 05 10 2012].
- [3] M. Oprisan, "IEA Wind," IEA Wind – KWEA Joint Workshop, 01 04 2007. [Online]. Available: [http://www.ieawind.org/wnd\\_info/KWEA\\_pdf/Oprisan\\_KWEA\\_.pdf](http://www.ieawind.org/wnd_info/KWEA_pdf/Oprisan_KWEA_.pdf). [Accessed 05 10 2012].
- [4] T. Iqbal, "Feasibility Study of Pumped Hydro Energy Storage for Ramea Wind-Diesel Hybrid Power System," The Harris Centre, St. John's, 2009.
- [5] D.-J. Lee and L. Wang, "Small-Signal Stability Analysis of an Autonomous Hybrid Renewable Energy Power Generation/Energy Storage System Part I: Time-

Domain Simulations," IEEE TRANSACTIONS ON ENERGY CONVERSION, vol. 23, no. 1, pp. 311-320, 2008.

[6] ALMA Site Characterisation Team. "Atacama Large Millimeter Array," 08 2000. [Online]. Available: [http://alma.sc.eso.org/htmls/wind\\_1Hz.html](http://alma.sc.eso.org/htmls/wind_1Hz.html). [Accessed 05 10 2012]

[7] A. G. Rodríguez, A. G. Rodríguez and M. B. Payán, "Estimating Wind Turbines Mechanical Constants," in INTERNATIONAL CONFERENCE ON RENEWABLE ENERGIES AND POWER QUALITY (ICREPQ'07), Bilbao, 2007.

[8] Windmatic, "Windmatic 15s," [Online]. Available: <http://windmatic.com/15s-brochure.pdf>. [Accessed 06 10 2012].

[9] Northern Power Systems, "Northern Power 100," [Online]. Available: [http://www.northernpower.com/pdf/NPS100-21\\_SpecSheet\\_EU-A4\\_English\\_2012.pdf](http://www.northernpower.com/pdf/NPS100-21_SpecSheet_EU-A4_English_2012.pdf). [Accessed 06 10 2012].

[10] Advantica Inc., "Moment of Inertia and Pump Startup/Failure," 14 03 2011.[Online].Available: [http://my.advanticagroup.com/support/allsecure/watersecure/releases\\_advisories/KBA\\_pump\\_moment\\_of\\_inertia.pdf](http://my.advanticagroup.com/support/allsecure/watersecure/releases_advisories/KBA_pump_moment_of_inertia.pdf). [Accessed 06 10 2012].

[11] "The Engineering Toolbox," [Online]. Available: [http://www.engineeringtoolbox.com/minor-loss-coefficients-pipes-d\\_626.html](http://www.engineeringtoolbox.com/minor-loss-coefficients-pipes-d_626.html). [Accessed 06 10 2012].

[12] G. Brown, "Henry Darcy and His Law," 22 06 2000. [Online]. Available: <http://biosystems.okstate.edu/darcy/index.htm>. [Accessed 06 10 2012].

[13] Renewables First, "Pelton & Turgo Turbines," Renewables First, [Online]. Available: <http://www.renewablesfirst.co.uk/pelton-and-turgo-turbines.html>. [Accessed 06 10 2012].

## 4 Dynamic Modeling and Analysis of a Remote Hybrid Power System with Pumped Hydro Storage

### Preface

A version of this manuscript has been accepted for publication in the *International Journal of Energy Science*. The co-author Dr. Tariq Iqbal supervised the principle author Md. Rahimul Hasan Asif to develop the research on this topic and assisted him to conceptualize the techniques and theories on the subject matter. Md. Rahimul wrote the paper, developed the dynamic model, organized the cases with extreme conditions, conducted simulation for different extreme cases and associated analyses while Dr. Iqbal reviewed the manuscript and suggested many corrections and recommendations. Some overlap with the previous chapter should be noticed in this chapter.

### Abstract

In this research dynamic modeling of a remote hybrid power system and feasibility of a pumped hydro storage system is presented. Current hybrid system in Ramea, Newfoundland has an electrolyzer, storage and hydrogen generator system. This research proposes a pumped hydro storage as a replacement to the hydrogen system. Detailed MATLAB-Simulink modeling has been done for every component of the Ramea hybrid power system. Incorporation of a pumped hydro system and some lead acid batteries will eliminate the low turn around efficiency of the electrolyzer and hydrogen generator

system. The system dynamic model presented here is fast, accurate and includes dynamic and supervisory controllers. The proposed real time supervisory controller algorithm observes the available surplus/missing power in the system and regulates pump/turbine and charging/discharging of the battery bank to maintain a stable system frequency. This paper presents dynamic model, supervisory controller design and algorithm, six case studies and detailed simulation results.

**Keywords:** Dynamic Modeling; Wind-diesel systems; Pumped Hydro Storage; Hybrid Power Systems; Renewable Energy .

#### **4.1 Introduction**

Ramea is a small island located off the south coast of Newfoundland, Canada. In 2004, Ramea was selected as the first pilot project site for a Wind-Diesel hydrogen hybrid power system which was led by the Newfoundland and Labrador Hydro. The main objective of this project was to demonstrate substantial improvement of energy efficiency and reliability after incorporating Wind-Diesel Integrated Control System (WDICS) in the island's grid which can reduce the use of diesel power by hosting green renewable wind energy in remote and isolated location. This wind-diesel pilot system is generating almost 1million kWh of electricity and offsetting nearly 750 tons of greenhouse gas emissions per annum [1] [2].

Wind energy system in Ramea has six 65kW Windmatic 15s and three 100kW NorthernPower100 wind turbines (WT). Three 925kW Diesel engine generators (DEG) are used as the main power source. A Hydrogen Electrolyzer and Storage (HES) and a 250kW Hydrogen Powered Generator (HPG) have been installed to increase the renewable energy penetration. When wind power generation exceeds the load, the electrolyzer produces hydrogen from water electrolysis which is stored in the storage tanks. And when harnessed wind power is inadequate to supply the total load the stored hydrogen is fed into a HPG as a fuel which delivers electricity to the grid and maintains the stability [2]. This HES system produces hydrogen at 70% efficiency and HPG generates electricity at less than 35% efficiency. Overall it gives a poor turn around conversion efficiency that is less than 25% [3]. Ramea system has many operational issues due to its complexity. So far, it never operated as designed. Detailed information, analysis and dynamic simulation for the optimal size and site selection of a pumped hydro storage (PHS) system replacing the HES and HPG has been presented in Ref. [4]. It has been explained that almost 37% renewable energy fraction can be attained using a 150kW PHS system with a 3932m<sup>3</sup> water reservoir at 63m height on top of 'Man of War' hill [4]. Topographical map of that hill shows that it has 2000m<sup>2</sup> of area to build a 2m high hydro storage reservoir. In Ref. [4] only 24s of dynamic simulation had been presented as it took days of computer time to simulate 1min of system operation. Moreover the simulation didn't converge in the time period of 11s to 16s. Simple first order modeling of every system component can considerably reduce the simulation time, make the analysis easier and gives fairly accurate solutions. Research [5] shows the system stability

of a self-governing hybrid renewable power generation and storage system connected with isolated loads by time-domain simulations. As storage subsystems, that hybrid system had a battery bank (BB) and a flywheel system. Three mathematical models have

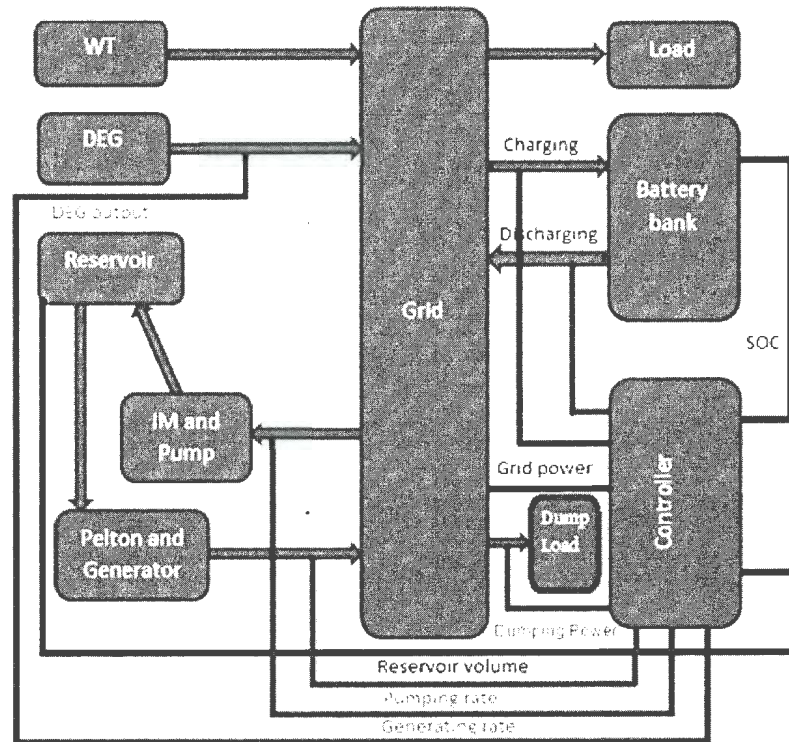


Figure 4.1. Block diagram of Ramea hybrid power system with a proposed pumped hydro storage system, battery bank and dump load

been investigated for three different sets of operating points and disturbance conditions. But the presented mathematical subsystems are too simple where nonlinear efficiency, friction and response time are ignored and there is no controller in the model. The real challenge is to model practical subsystems with simple first order models juxtaposing all

efficiencies, dynamic frictions, different time constants related to the subsystem parameters.

A simple, fast and novel method has been introduced in this research work to simulate system dynamics of Ramea hybrid power system with a proposed PHS. A block diagram of Ramea hybrid power system is shown in Figure 4.1. Some system details may be found in [6]. A BB has been used to supply or store the intermittent power as induction motor (IM) and centrifugal pump (CP) or turbine and generator require some time to reach a certain rated operating point and have larger time constant than a battery bank. A controllable dump load (DL) has also been used to dump the excess power. The presented model has PID controllers with all its subsystems. Characteristic data and parameters of the aforementioned WTs and DEG used in Ramea hybrid system are taken from the respective manufacturers. All other subsystem models e.g. CP, Pelton Wheel Turbine (PWT), BB have been created using first principle and data obtained from manufactures. In this study dynamic models with 1st order transfer functions (TF) are considered. Simulations have been done for one day (86400s) for six extreme cases. Detailed results and analyses are presented in the later part of this paper.

## 4.2 Dynamic Modeling

### 4.2.1 Wind Speed Data

Wind speed data (1Hz) from the Prince Edward Island (PEI), Newfoundland, Canada is used. Average value of the data was adjusted to represent wind speed at Ramea. Two wind speed average have been considered here e.g. 2.9m/s and 13.75m/s.

### 4.2.2 Load Data

Ramea load data for two days is used from Ref. [4]. Two 24 hour load curves are used from the data array with averages of 303kW and 800kW.

### 4.2.3 Wind Turbine Model

WT power curves have been collected from the corresponding manufacturers. Power curve data was fitted with a 6th order polynomial.

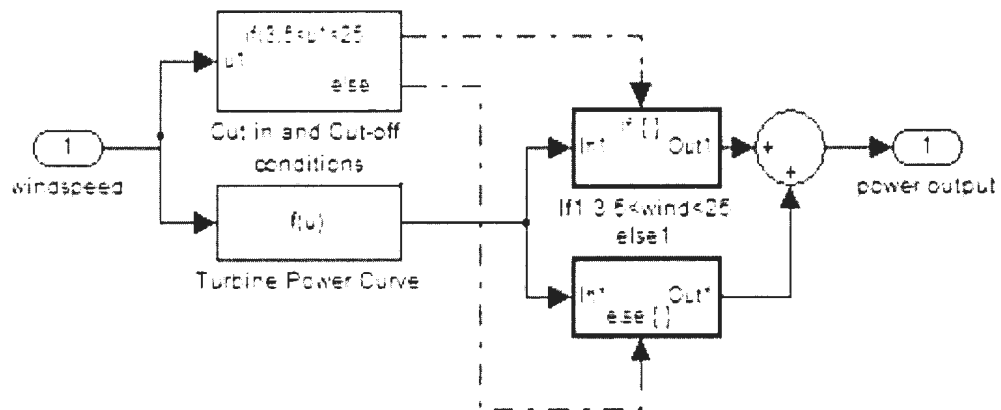
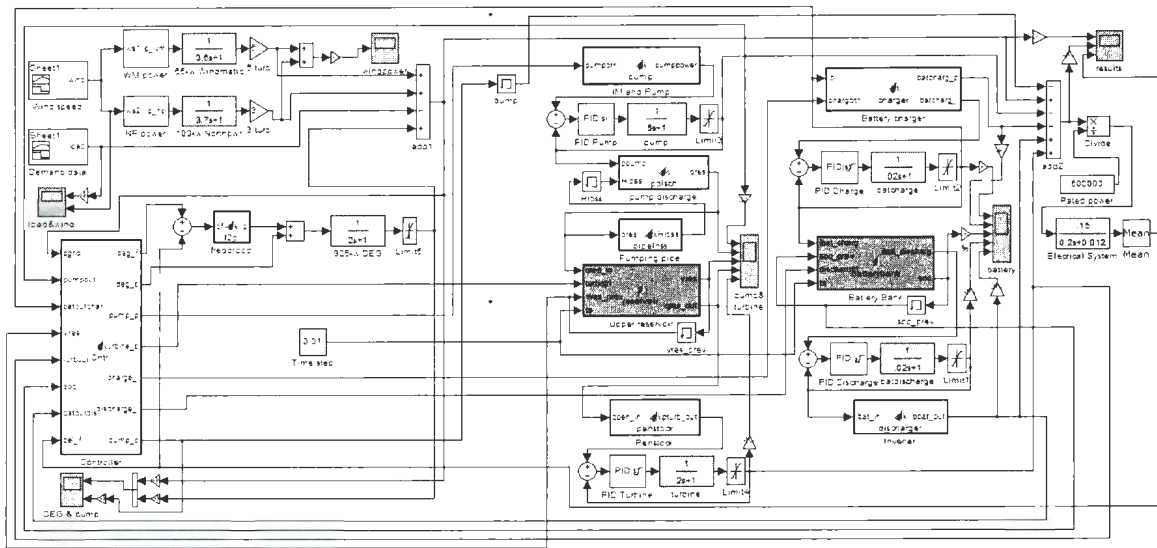


Figure 4.2. Wind turbine power curve and limiting conditions

As shown in Figure 4.2 necessary cut in and cut out wind speed conditions have been applied in the WT model. Wind turbine time constants are used following the equation from the Ref. [7]:

$$H_{WT} \cong 1.87 * P_{WT}^{0.0597} \quad 4.1$$

In Equation 4.1  $H_{WT}$  is the mechanical inertia time constant and  $P_{WT}$  is the power of the WT in watts. So calculation gives 3.6s for 65kW Windmatic 15s [8] and 3.7s for 100kW Northern Power 100 [9]. In Figure 4.3 all WTs, load demand and varying DEG output are connected with an adder 'add1'. Output of 'add1' represents the power available or lack in the grid which has to be managed by the PHS or BB.



**Figure 4.3. Simulink - MATLAB embedded function blocks based dynamic model of Ramea hybrid power system with pumped hydro storage, battery bank and dump load**

#### 4.2.4 Diesel Engine Generator Model

DEG in Ramea has a rated output of 925kW. There are three DEG but only one is used at a time. A DEG can be operated down to 30% of its rated output i.e. the DEG can operate from 300kW to 925kW. However, a DEG always keeps running at 300kW (a minimum), whatever the case, to maintain a stable system frequency. Time constant of DEG is taken as it is used in Ref. [5] so  $T_{DEG} = 1/(2s + 1)$ . This value has been verified from the datasheet of a DEG of almost same rating. The acceleration time constant of DEG is calculated by the following Equation 4.2,

$$J = \frac{S_n T_{DEG}}{\omega_n^2} \quad 4.2$$

Here,  $J$  is the moment of inertia;  $\omega_n$  is the rated angular velocity, which equals  $2\pi f$ ;  $S_n$  is the DEG nominal apparent power;  $T_{DEG}$  is the acceleration time constant rated to  $S_n$ . In the datasheet of the DEG,  $J = 20\text{kg.m}^2$ . That results in the acceleration time constant of DEG of  $T_{DEG} \cong 2$  s. With this time constant this DEG needs about 10s to reach its steady state value.

Frequency droop curve has been introduced considering that this DEG has a  $\Delta P/\Delta f$  ratio of 300kW/1Hz. The MATLAB code used here is,

$$dpu = 1 - (62 - (df + 60))/2 \quad 4.3$$

In Equation 4.3  $dpu$  is per unit excess power that will be injected to balance out the frequency deviation,  $df$  in the grid.

#### 4.2.5 Induction Motor and Centrifugal Pump Model

Considering their individual characteristics IM and CP are modeled together in a block (IM and Pump block in Figure 4.3). The CP takes relatively large time to respond to a sudden change than an IM. Comparing the starting time of a combination of IM and CP from Ref. [10], a 4000hp – 1000rpm pumping system takes approximately 2:30 minutes to reach its rated output. Here we assumed that a 200hp pumping system needs 30s to settle down to its steady state. Therefore transfer function of this block is  $TF_{CP} = 1/(5s + 1)$ .  $K_P = 0.4732$ ,  $K_I = 0.3391$  and  $K_D = 0$  are used in PID controller of CP. Built in tuner of Simulink PID block has been used for this block as well as rest of the blocks in this model to determine suitable controller parameters. Efficiencies of IM and CP are considered as 95% and 80% respectively which gives a total efficiency of 75%. Equation 4.4 is used in MATLAB code to determine  $q_{res}$  = pumping water flow to reservoir.

$$q_{res} = \frac{p_{pump} * p_{meff}}{h_{res} + H_{loss}} * dens * g \quad 4.4$$

Here,  $p_{pump}$  = power delivered to the pumping system which can vary from 30% to 100% of the rated output e.g. 100kW to 300kW;  $p_{meff} = 75\%$ ;  $h_{res} = 63\text{m}$  (height of the reservoir);  $H_{loss}$  = penstock friction loss;  $dens = 1000\text{kgm}^{-3}$  and  $g = 9.81\text{ms}^{-2}$ .

#### 4.2.6 Penstock Model

Penstock is designed as  $L_{pipe} = 70\text{m}$  in length and  $D_{pipe} = 0.3\text{m}$  in diameter. Reynolds number is selected assuming that water flow is laminar inside the pipe. A minor loss coefficient for water meter is used here as  $k_{lossco}$  which is taken equal to 7 [11].

$Vel_{waterpump} = q_{res}/A_{pipe}$ ; %water velocity

$Re = 2000$ ; %Reynolds number

$flam = 64/Re$ ; %Darcy Friction Factor for laminar flow

$h_{pipefric} = (8 * flam * L_{pipe} * q_{res}^2) / (g * \pi^2 * D_{pipe}^5)$ ; 4.5

$h_{lossmeter} = k_{lossco} * (Vel_{waterpump}^2) / (2 * g)$ ;

$H_{loss} = h_{pipefric} + h_{lossmeter}$ ;

Equation 4.5 used here is Darcy–Weisbach equation for friction inside the penstock [12].

Here  $H_{loss}$  is calculated in each step for new  $q_{res}$ .

#### 4.2.7 Water Reservoir Model

The proposed water reservoir has a total volume of  $4000\text{m}^3$ . In simulations initial volume is considered as  $2000\text{m}^3$ . Pump action will be stopped if water volume exceeds  $3950\text{m}^3$  and turbine action will be terminated if water volume goes below  $150\text{m}^3$ . Total water volume in the reservoir can be determined from water flows in both ways or from the height of water in the reservoir (see upper reservoir block in Figure 4.3).

#### 4.2.8 Turbine Model

A 150kW PWT has been used here which has very good partial flow efficiency as shown in Figure 4.4 [13]. The blue curve here is for a twin jet setup. Synchronous generator and PWT are modeled together using a combined efficiency of 70% and time constant of 2s as DEG. TF of this block is  $TF_{\text{TURB}} = 1/(2s + 1)$ .  $K_P = 0.4732$ ,  $K_I = 1.6955$  and  $K_D = 0$  are used in PID controller of PWT (turbine block in Figure 4.3). The power output of the turbine generator block is as in Equation 4.6

$$pturb\_out = qpen\_in * hres * dens * g * turbeff \quad 4.6$$

Here,  $pturb\_out$  = turbine output power,  $qpen\_in$  = incoming water flow to the turbine and  $turbeff = 70\%$  as turbine efficiency.

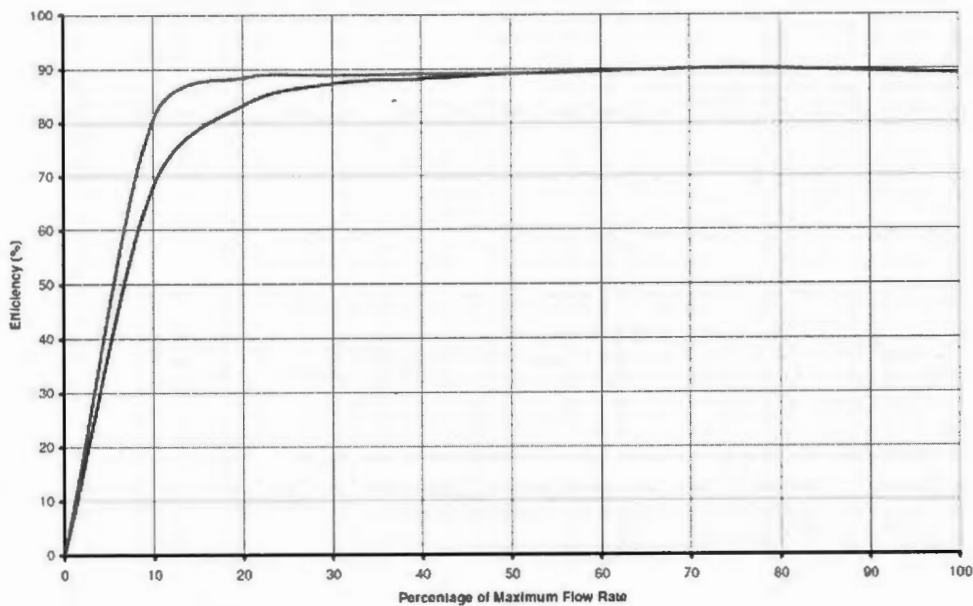


Figure 4.4. Part flow efficiency of a Pelton wheel turbine

#### 4.2.9 Battery Bank Model

In an isolated grid BB used as storage provides fast response which makes them favorable to improve power quality and gain system reliability. A bank of 300 batteries has been used here each having a capacity of 200Ahr. Total 15 branches are connected in parallel where each branch consists of 20 batteries in series delivering a DC battery bus voltage of 240V. A charging and a discharging block have been created to control the current and monitor the State of Charge (SOC) of the battery. A SLA battery should not be discharged when SOC goes down to 40%. Total coulomb capacity can be determined from the calculations below in Equation 4.7, (battery bank block in Figure 4.3)

$$\begin{aligned}
 \text{Total cap} &= \text{individual cap} * 3600 * \text{no. of branch} & 4.7 \\
 &= 200 * 3600 * 15 \\
 &= 10800000C \text{ (at 100\% SOC)}
 \end{aligned}$$

So the BB operates from 100% SOC to 40% SOC (4320000C). For charging current a maximum 10% of the individual capacity will be allowed as in Equation 4.8 where  $\text{charge}_i$  = total charging current,  $\text{ind\_cap}$  = individual capacity and  $\text{nbat\_para}$  = no. of branches.

$$\text{charge}_i = 0.1 * \text{ind\_cap} * \text{nbat\_para} \quad 4.8$$

$$\text{discharge}_i = 0.33 * \text{ind\_cap} * \text{nbat\_para} \quad 4.9$$

A maximum of 72kW surplus power can be utilized to charge the BB almost instantaneously. For a maximum power shortage of 234kW can be supplied from the BB by discharging it to 'one third of the individual capacity'. In Equation 4.9  $\text{discharge}_i$  = total discharging current. In this model initial SOC is chosen as 70% which is equivalent to 7560000C. While discharging, battery bank can be discharged at any rate below 0.33CA but that will affect the effective capacity of battery following the 'Peukert's law'.

$$I_t = C \left( \frac{C}{I_H} \right)^{k-1} \quad 4.10$$

Here, ' $I$ ' is the effective capacity at discharge rate of  $I$ ,  $H$  is the rated discharge time, in hours,  $k$  is the Peukert constant which is 1.2 for SLA battery. Along with this in this model the combined efficiency of battery and converters is considered as 80%. Equation 4.11 is used to calculate the power delivered ( $p_{bat\_out}$ ) by the battery where  $v_{bat} = 240V$ ,  $ibat\_in =$  total discharging current and  $bateff = 80\%$ .

$$p_{bat\_out} = v_{bat} * ibat\_in * bateff \quad 4.11$$

TF of Battery Discharge block (Figure 4.3) is  $TF_{BB} = 1/(0.02s + 1)$ . As SLA battery has a very fast response in the range of milliseconds [14], here modeled BB takes less than 100ms to reach steady state. Coefficients for the PID controller of this block are  $K_P = 0.0001$ ,  $K_I = 213617.933$  and  $K_D = 0$ . The BB will provide power while mechanical subsystems are starting up.

#### 4.2.10 Dump Load Model

A 1MW (maximum) controllable dump load has been used to curtail the excess power from the grid while the wind speed is considerably high and/or the load demand is low. Maximum power dissipation in the dump load is 800kW (in the case 2 where wind speed is high and load is low). A PWM controller can be used to dump the surplus power from the grid to the dump load. The dump load help reduce the frequency spikes in the grid.

#### 4.2.11 Model of the Electrical System

The system inertia constant  $M$  and load-damping constant  $D$  have been used same as in Ref. [5]. The gain has been changed from 1.0 to 0.15 as 1.0 makes the system too sensitive. TF of the electrical system has been considered as  $TF_{ELEC} = 0.15/(0.2s + 0.012)$ . Therefore, 0.05pu power deviation will cause 0.01pu or 0.6Hz frequency deviation (see electrical system block in Figure 4.3).

#### 4.3 Supervisory Controller

PID controllers have been used to control all individual subsystems. To determine the optimum coefficients for the PID controllers, Simulink built in PID tuner has been used. Limiters have been used to clip all out of range values. A simple flowchart of the algorithm used in this model as the supervisory controller is shown in Figure 4.5. It is shown as a block 'controller' in the Figure 4.3. DEG has the last priority to take control. Pump and Pelton wheel operate with the highest priority as per the requirement and BB compensates for the intermittent deviations due to the inertial delay of rotating mechanical devices. In each step supervisory controller keeps measuring the reservoir water volume, SOC and the grid power. When DEG takes control, a differential block measures the frequency deviation from the set value and according to the frequency droop characteristics curve of the DEG it adjusts its output power.

#### 4.4 Results: Six Case Studies

For different conditions of wind speed and load six cases are proposed in Table 4.1. These six cases cover possible normal and extreme operation of the hybrid power system. Simulation of the developed system model shown in Figure 4.3 has been done for one day i.e. 86400s. Site wind speed data and load data have been used [4]. Data is from the year 2001. Inspecting site wind speed data and load data the lowest 24 hours average load was found to be 303kW on September 3, 2001 which is referred as 'Low load' in this paper. Load varies between 200kW to 330kW from 12:00:00AM to 11:59:59PM. And the highest load found in the year of 2001 is 800kW on December 29, 2001 where load varied from 590kW to 990kW throughout the day. This is referred as 'High load' in this paper.

Observing all daily average of wind speed data it has been found that on September 17, 2001 a lowest daily average of wind speed was recorded which was 2.9m/s and wind speed stayed between 0m/s to 9m/s. This is referred here as 'Low wind'. Highest daily average wind speed has been found to be 13.75m/s on February 26, 2001 where it varied between 10m/s to 20m/s. This wind speed pattern is referred as 'High wind' in this paper. As an abrupt change of load, it is assumed that for a 1000s time period load changes to 700kW from 500kW at  $t = 200s$  and drops to 500kW again at  $t = 700s$  while wind speed stays steady at 5m/s. On the other hand, abrupt change of wind speed has been considered as a rise to 11m/s from 8m/s at  $t = 200s$  and again dropping back to 8m/s at  $t = 700s$ . For

this change the load has been assumed a constant at 500kW. Results for all six case studies with these extreme conditions are presented below.

**Table 4.1. Six different cases of load and wind speed**

<b>Case</b>	<b>Load</b>	<b>Wind speed</b>
<b>1</b>	Low (200kW to 330kW)	Low (0m/s to 9m/s)
<b>2</b>	Low (200kW to 330kW)	High (10m/s to 20m/s)
<b>3</b>	High (590kW to 990kW)	Low (0m/s to 9m/s)
<b>4</b>	High (590kW to 990kW)	High (10m/s to 20m/s)
<b>5</b>	Abrupt load change (500kW to 700kW at 200s and vice versa at 700s)	Steady in midrange (5m/s)
<b>6</b>	Steady in midrange (500kW)	Abrupt wind speed change (8m/s to 11m/s at 200s and vice versa at 700s)

#### **4.4.1 Case 1: Low Load and Low Wind**

In Case 1, Low load and low wind speed have been used as inputs to the dynamic model and system outputs are observed. From Figure 4.6 to Figure 4.10 it can be observed that in the first 30000s load was very low so CP and BB charger worked to store the excess energy. From 30000s to 50000s load was increasing and PWT and BB delivered the

necessary power. After 50000s reservoir is empty so DEG takes control and supply a maximum of 450kW for some time.

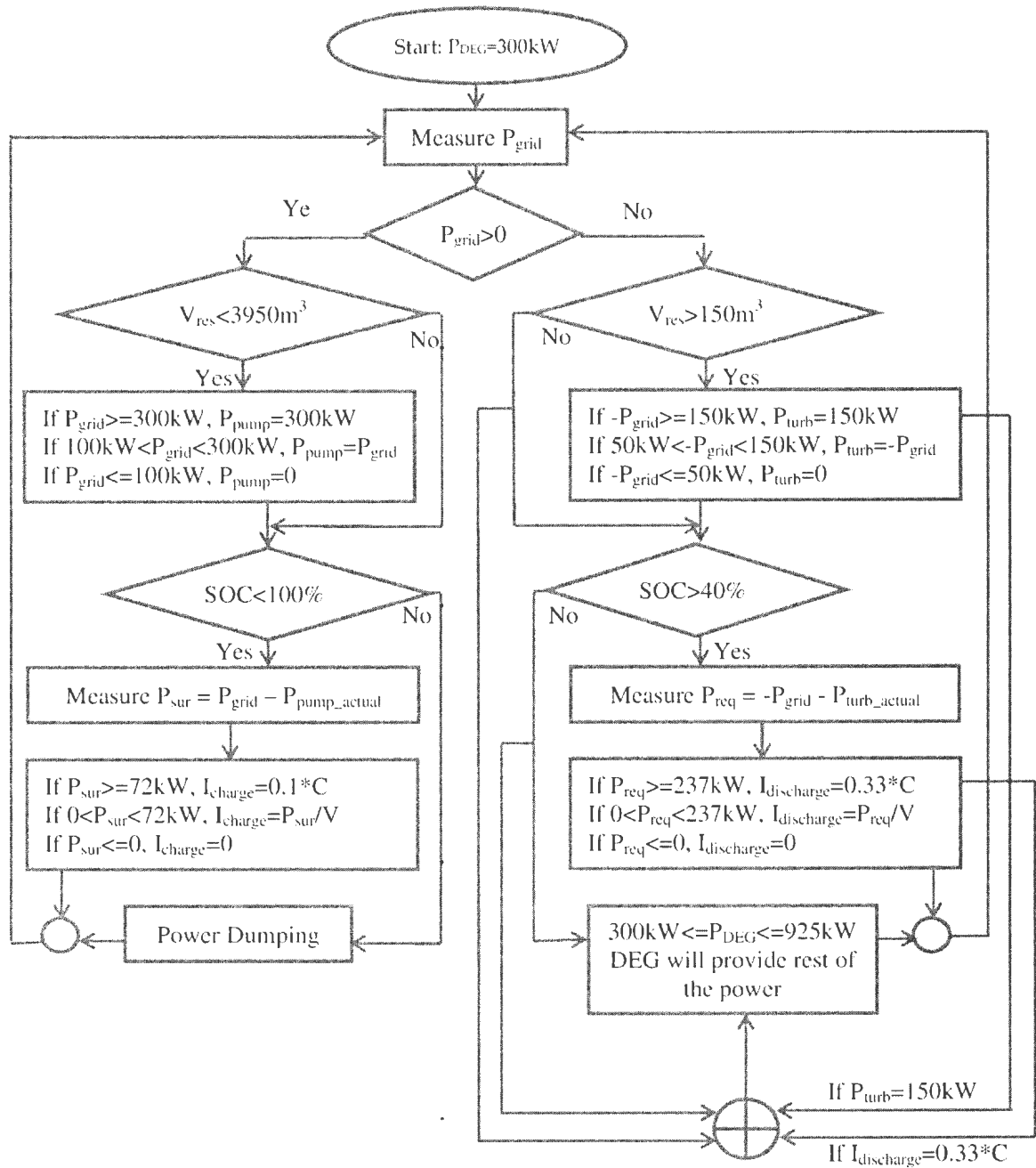


Figure 4.5. Simple flowchart of the algorithm used as supervisory controller

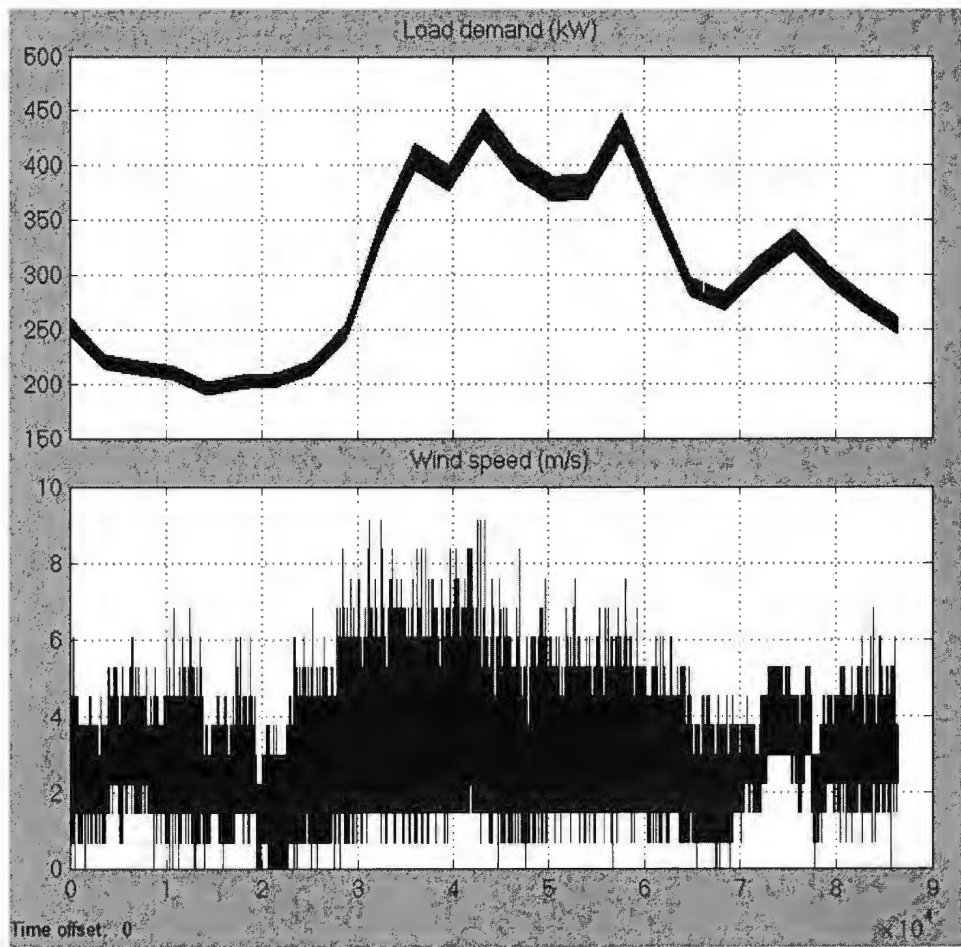
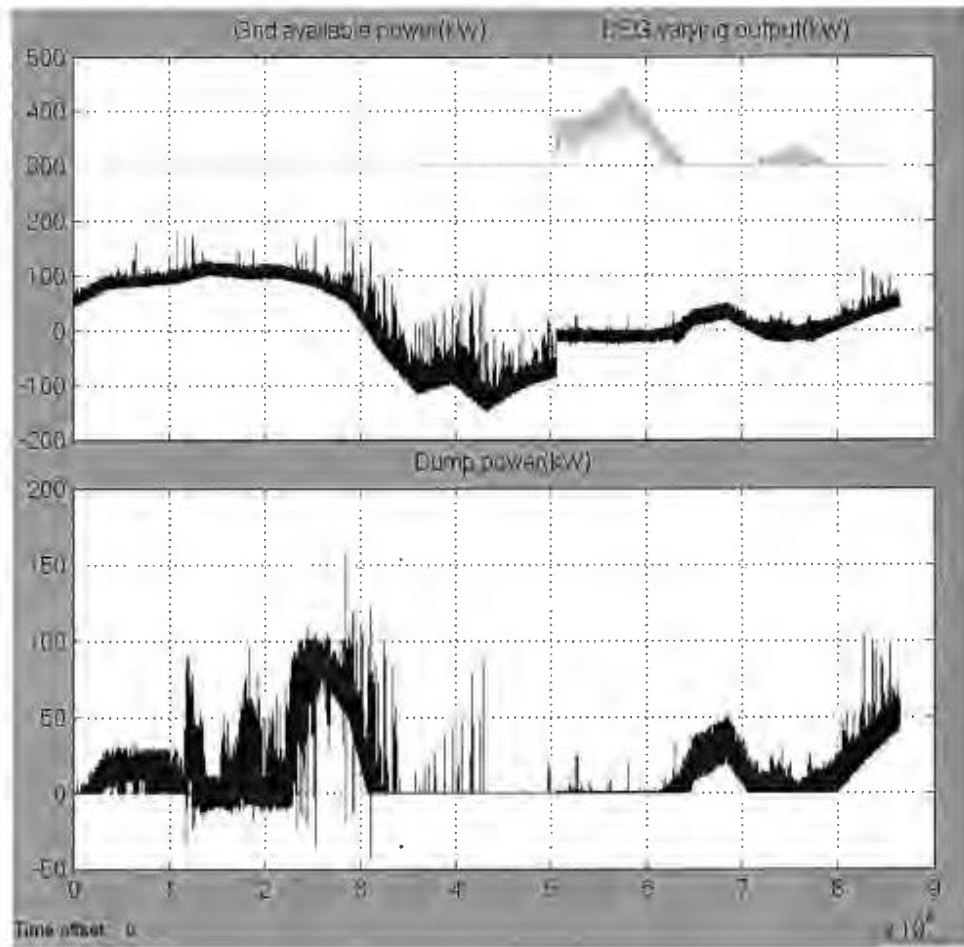


Figure 4.6. Load demand (kW) and wind speed (m/s) data for the case 1

System frequency remains almost stable that day. A sudden frequency dip of 1.3Hz is observed in Figure 4.10 when load is increasing rapidly after  $t = 30000s$  and PWT respond slowly. Such a frequency dip is acceptable in remote hybrid power systems. This case study indicates that the developed model and supervisory controller is capable of correctly simulating the hybrid power system. The transients observed in these figures are not instantaneous rather slow variations. The x-axes cover a whole day simulation

(86400s) so these spikes are basically steady variations lasting minutes. In Figure 4.11, a zoomed result from 57700s to 57800s has been shown.



**Figure 4.7.** In top figure, the grid available power (kW) and DEG varying output (kW) (with a minimum 300kW value) is shown and in the lower figure dump power (kW) is shown for the case 1

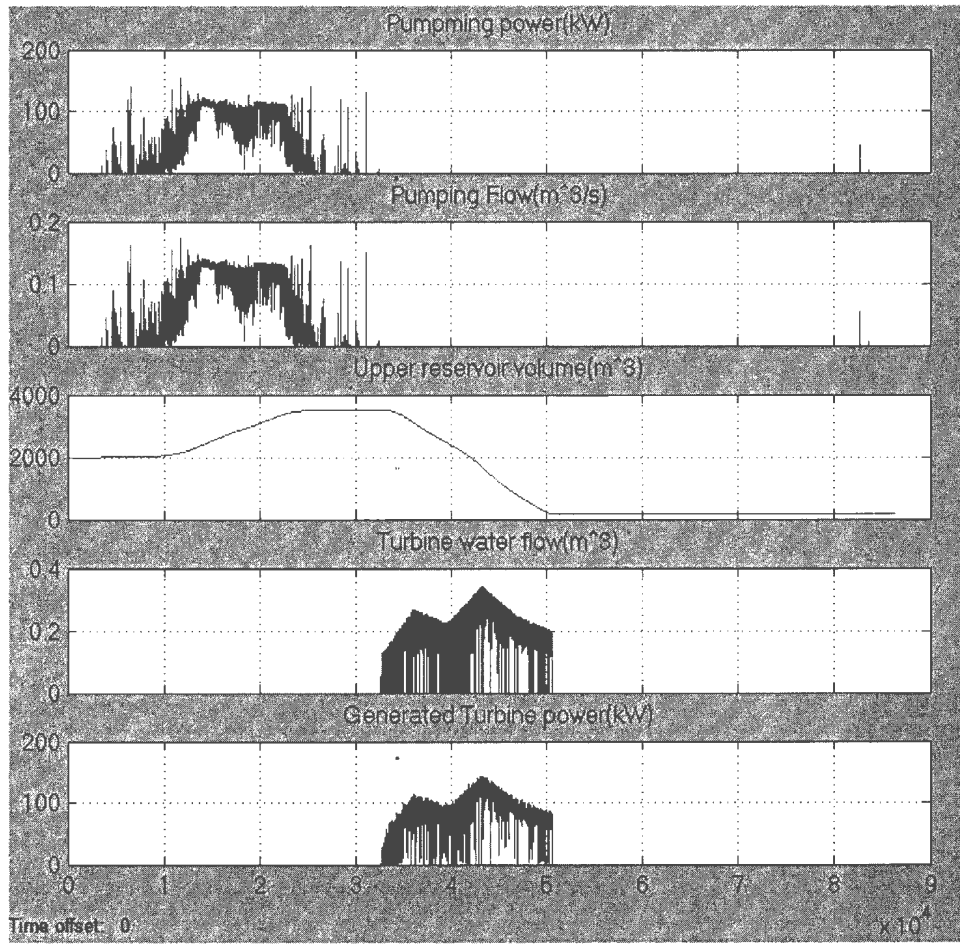


Figure 4.8. Pump power consumption (kW), pump water flow ( $\text{m}^3/\text{s}$ ), the upper reservoir water volume ( $\text{m}^3$ ), turbine water flow rate ( $\text{m}^3/\text{s}$ ) and the turbine generated power (kW) for the case 1

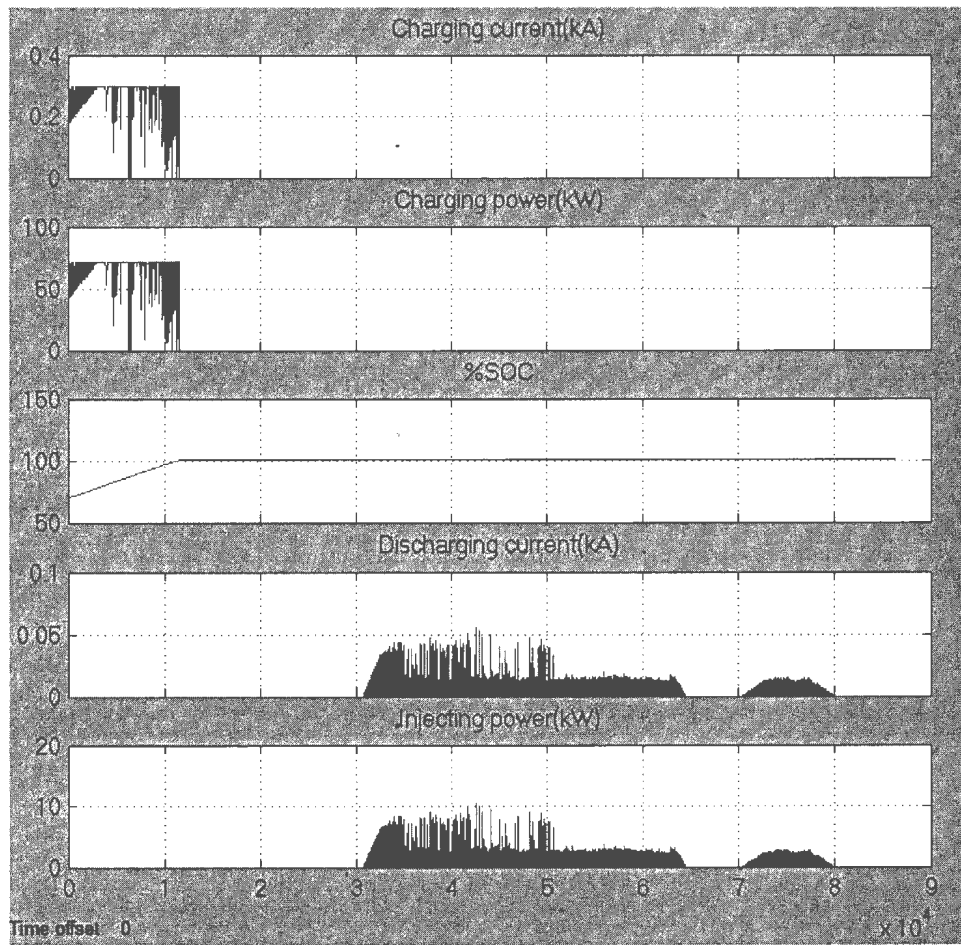
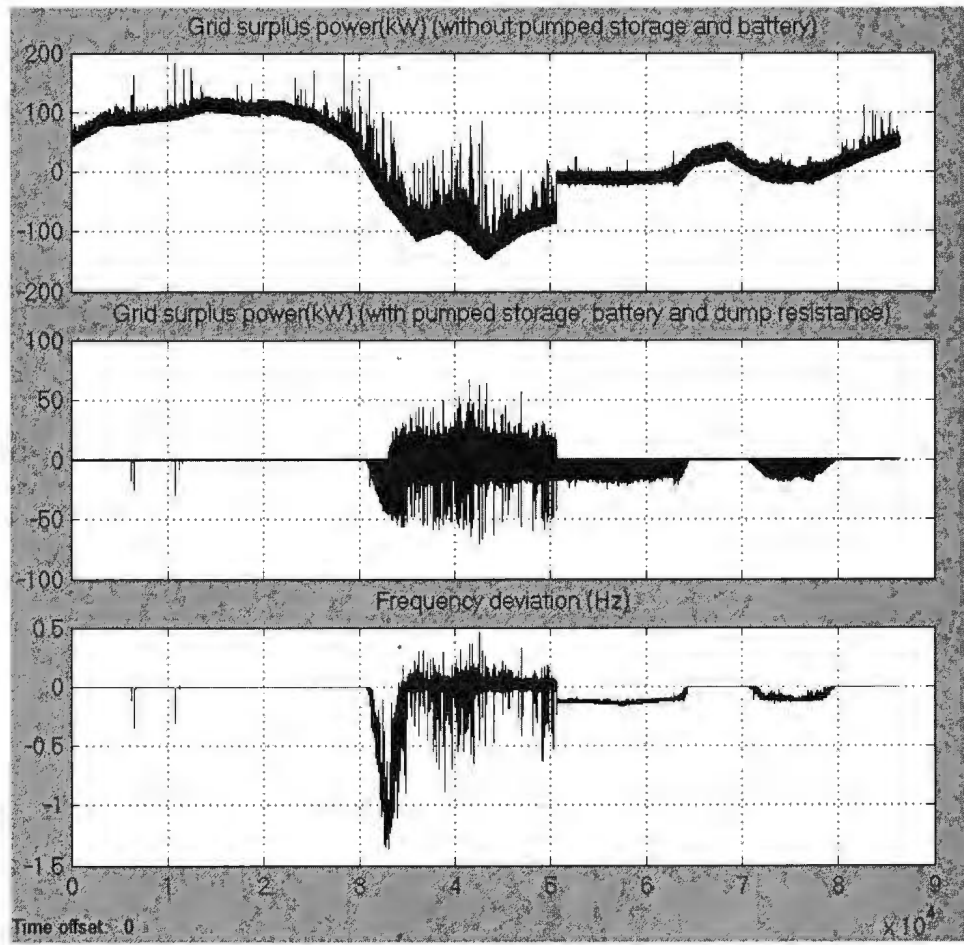
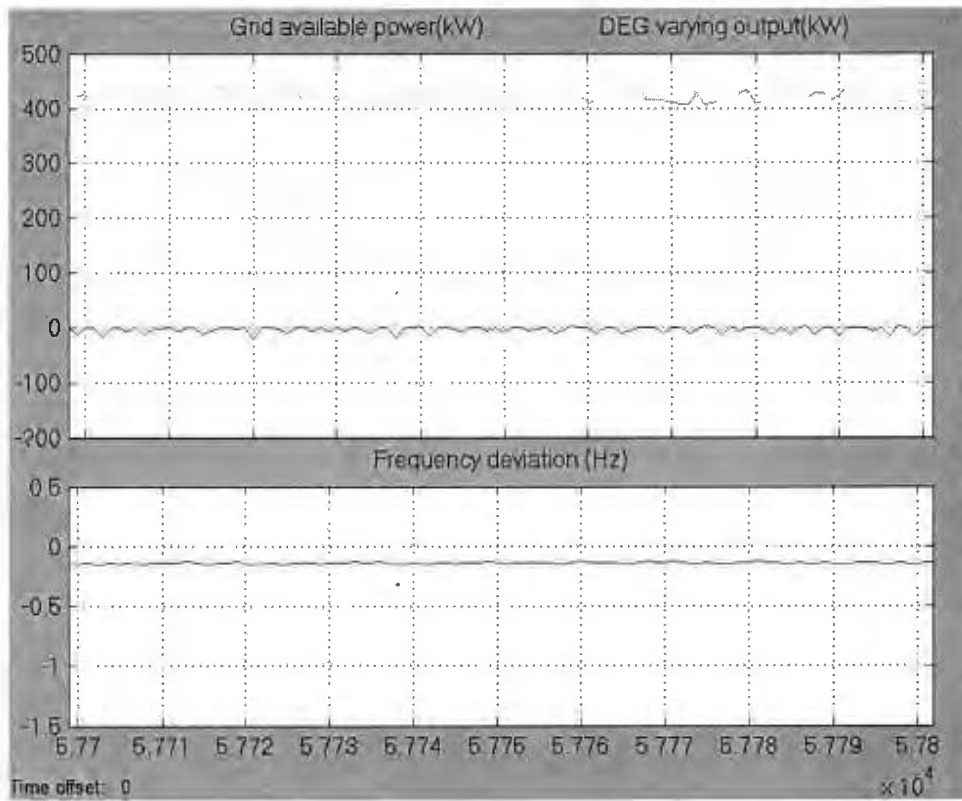


Figure 4.9. Charging current (kA), charging power (kW), percentage of state of charge, discharging current (kA) and the power to the grid (kW) due to the discharging of the battery are shown for the case 1



**Figure 4.10. Grid surplus power (kW) with and without pumped storage, battery and dump load and the resultant frequency deviation for the case 1**



**Figure 4.11.** Simulation result has been zoomed from 57700s to 57800s to show the transients. In top figure, the grid available power (kW) and DEG varying output (kW) is shown and in the lower figure the resultant frequency deviation is shown for the case 1

#### 4.4.2 Case 2: Low Load and High Wind

In case 2, a low load and high wind speed have been used in the dynamic model to observe the system outputs and responses. Figure 4.12 shows the selected data. Daily load cycle and random variation is shown in the top section of Figure 4.12. From Figure 4.13 to Figure 4.16 it can be observed that as wind is high and load is low, the water reservoir and BB become fully charged in the first 8000s and 10000s respectively. After that all the excess power goes to the dump load. The maximum power dissipation in the dump load is

800kW. System frequency is totally stable for all time as it is maintained by the diesel. These results also show that the developed model is capable of correctly simulating the complex Ramea hybrid power system.

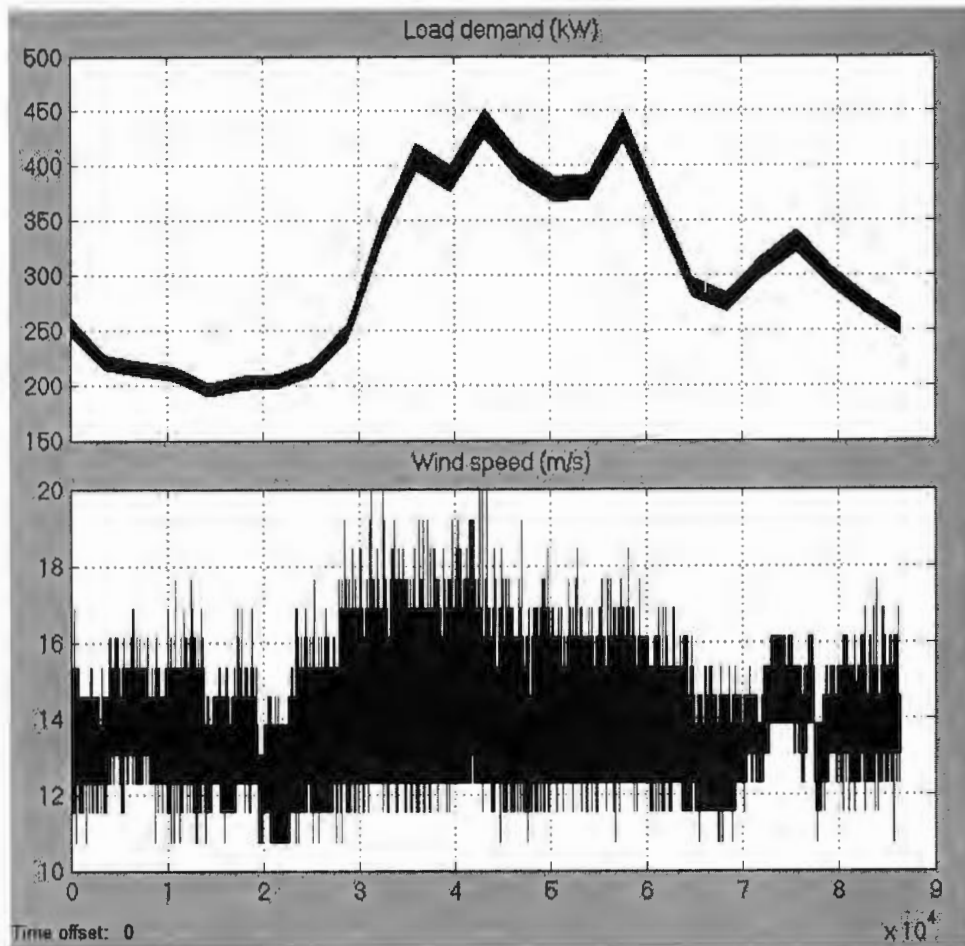


Figure 4.12. Load demand (kW) and wind speed (m/s) data for case 2

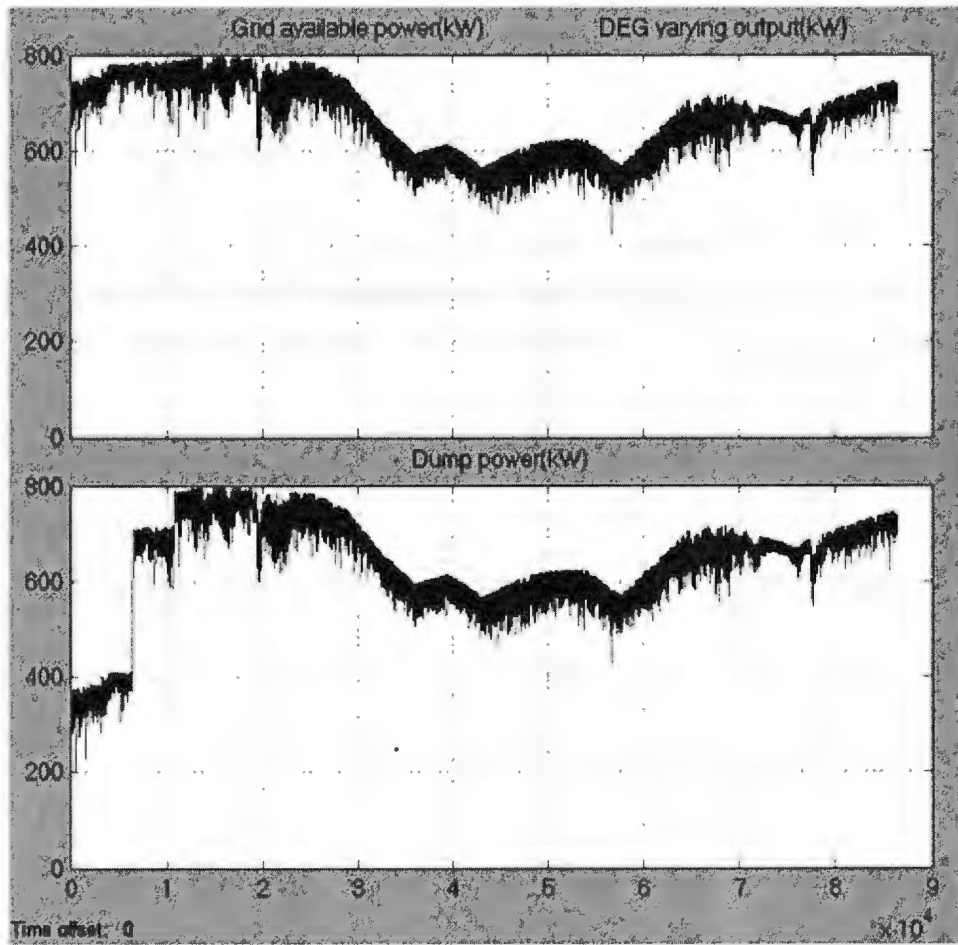


Figure 4.13. In the top part, grid available power (kW) and DEG output (kW) (with flat 300kW value) are shown and in the lower part dump power (kW) is shown for the case 2

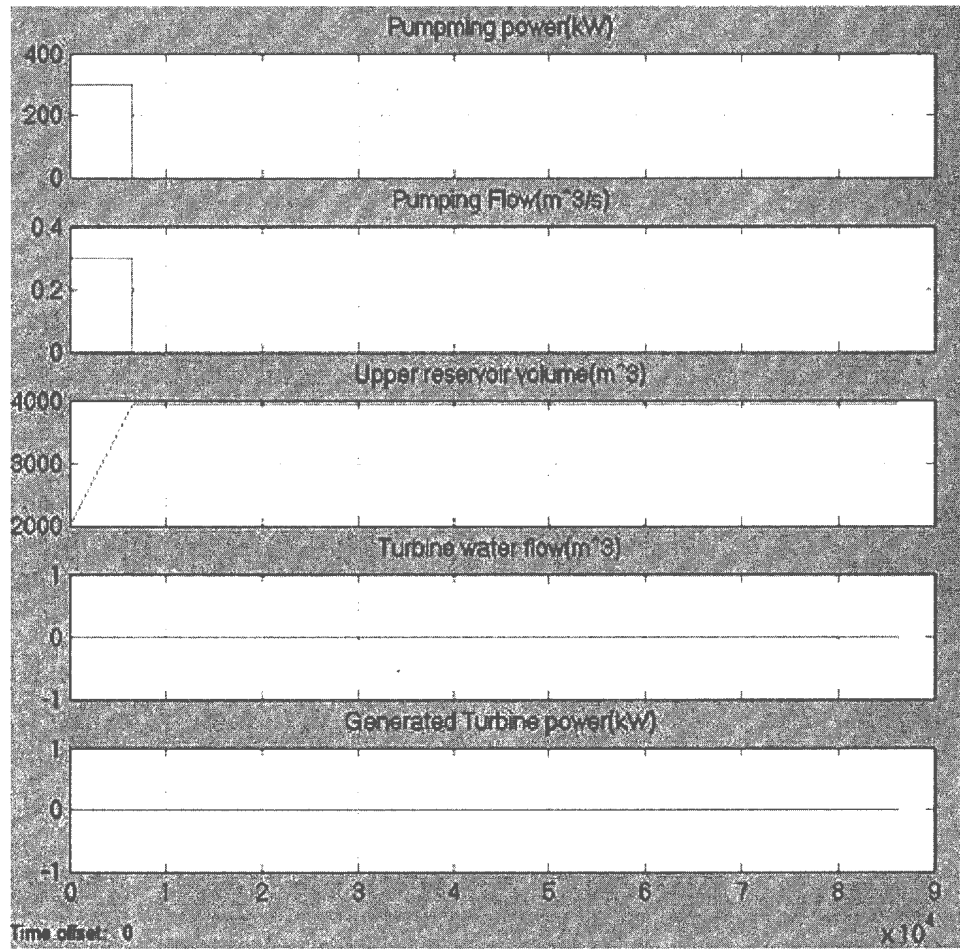


Figure 4.14. Pumping power (kW), pumping water flow rate ( $m^3/s$ ), upper reservoir water volume ( $m^3$ ), turbine water flow ( $m^3/s$ ) and turbine generated power (kW) for the case 2

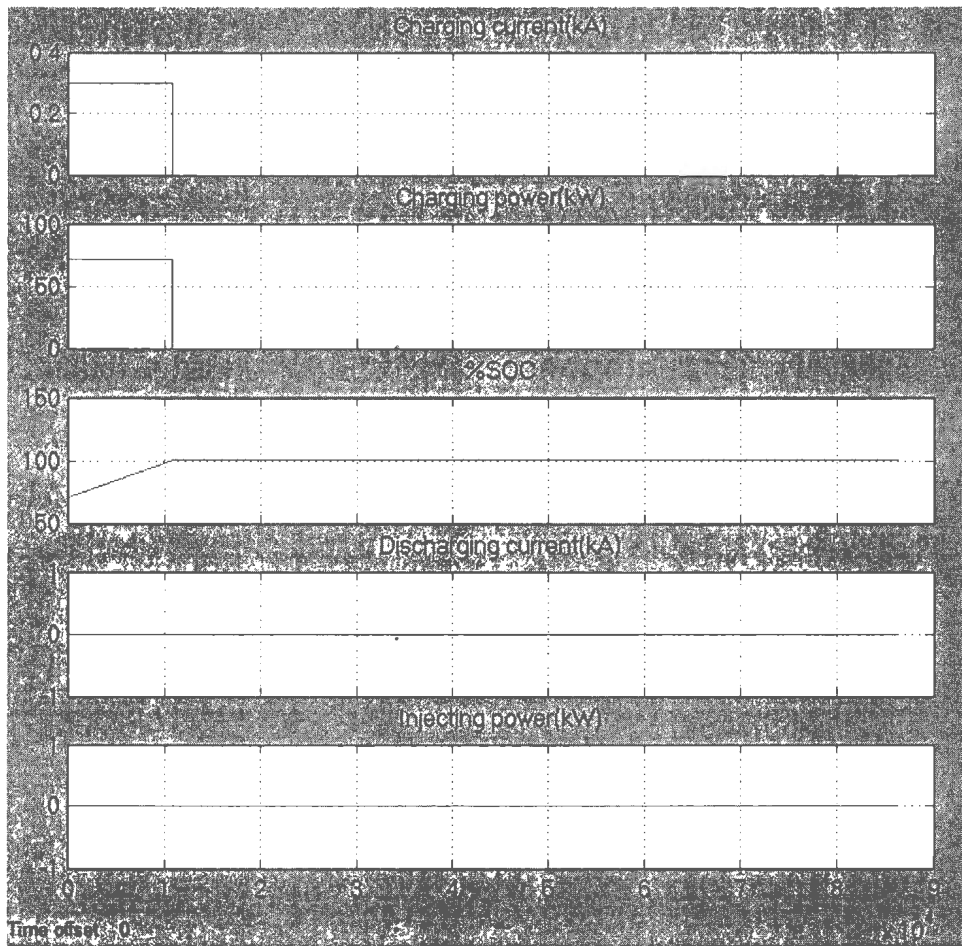
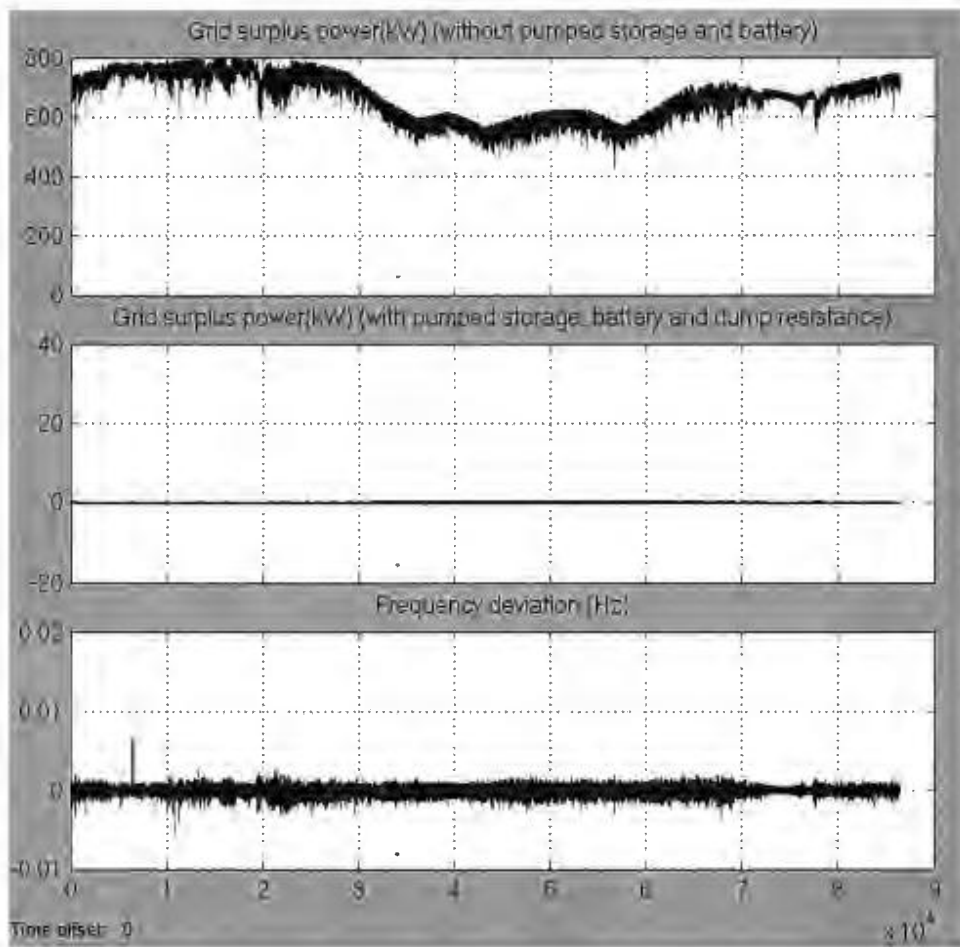


Figure 4.15. Charging current (kA), charging power (kW), percentage of state of charge, discharging current (kA) and the power injected to the grid (kW) due to the discharging of the battery are shown above for the case 2



**Figure 4.16. Grid surplus power (kW) with and without pumped storage, battery and dump load and the resultant frequency deviation are shown above for the case 2**

#### 4.4.3 Case 3: High Load and Low Wind

In case 3, high load and low wind speed have been used as inputs to the dynamic model to observe the outputs and system responses. Selected one day load data and wind speed are shown in Figure 4.17 below.

From Figure 4.17 to Figure 4.21 it has been observed that in first 5500s reservoir becomes empty and by 10000s BB almost discharged. This is because load is very high and WT are not delivering enough power due to very low wind speed. DEG delivers the required amount No power dumping happened in this case. System frequency remains quite stable though two frequency dips of 0.6Hz and 0.9Hz are observed when load suddenly dips around 40000s and 60000s. Such small frequency dips are considered acceptable for remote hybrid power system.

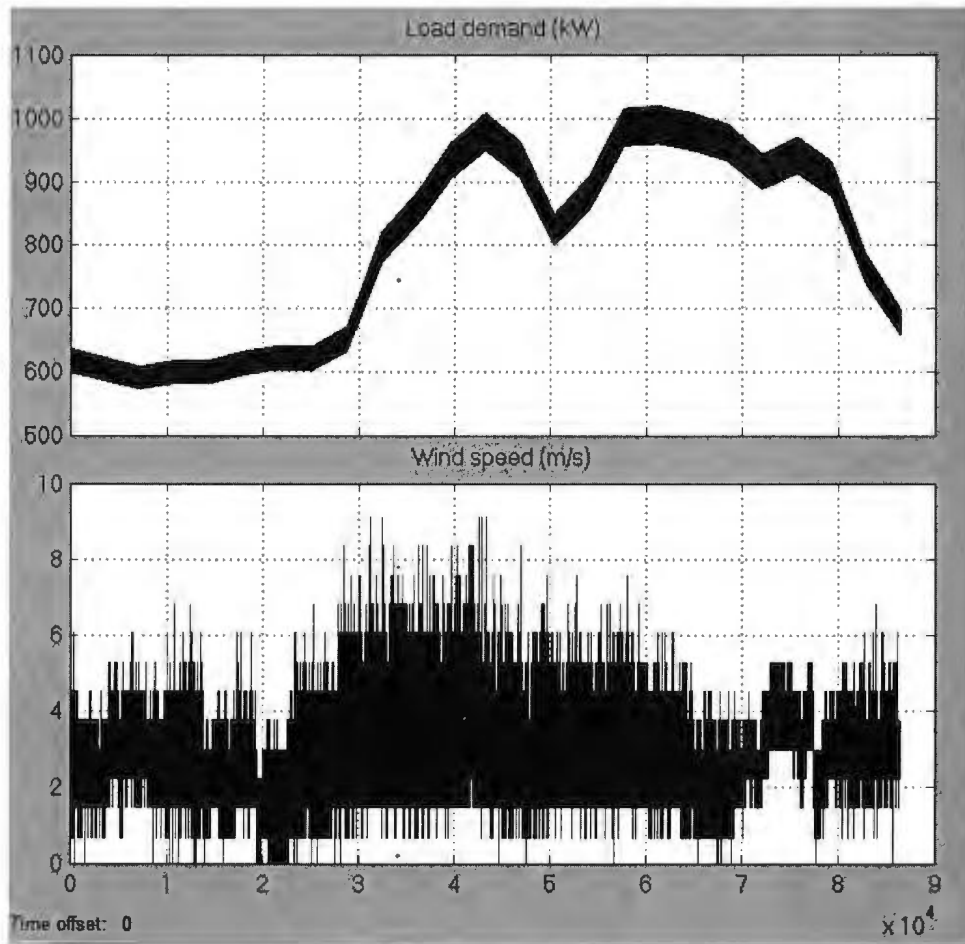


Figure 4.17. Load demand (kW) and wind speed (m/s) data for the case 3

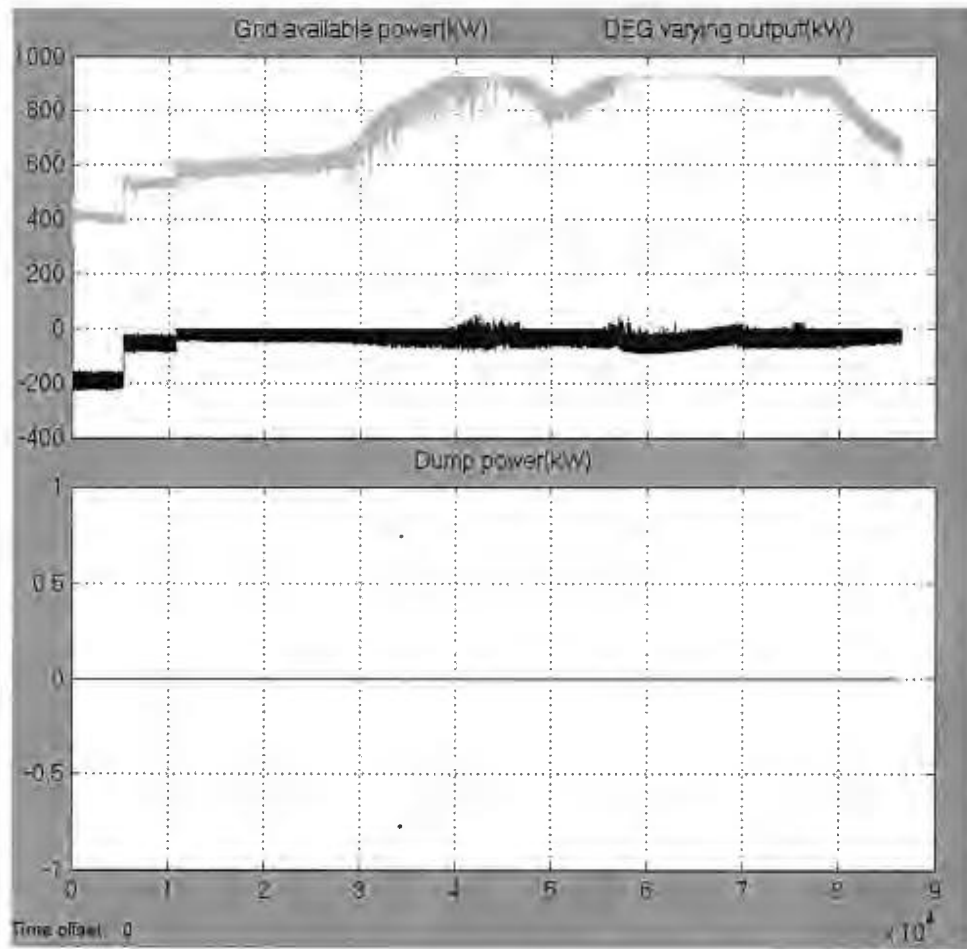


Figure 4.18. In top figure, grid available power (kW) and DEG varying output (kW) (from 400kW to 925kW) are shown and in the bottom part dump power (kW) is shown for the case 3

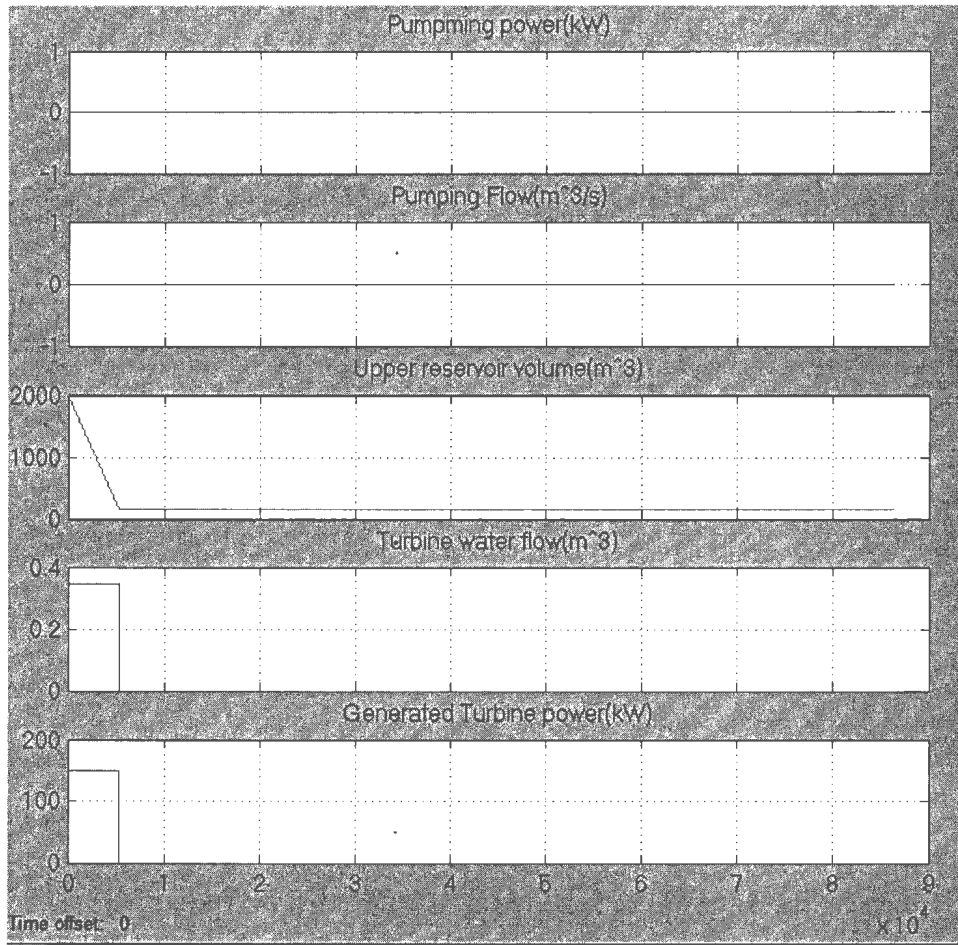


Figure 4.19. Pumping power (kW), pumping water flow ( $m^3/s$ ), upper reservoir water volume ( $m^3$ ), turbine water flow ( $m^3/s$ ) and turbine generated power (kW) are shown for the case 3

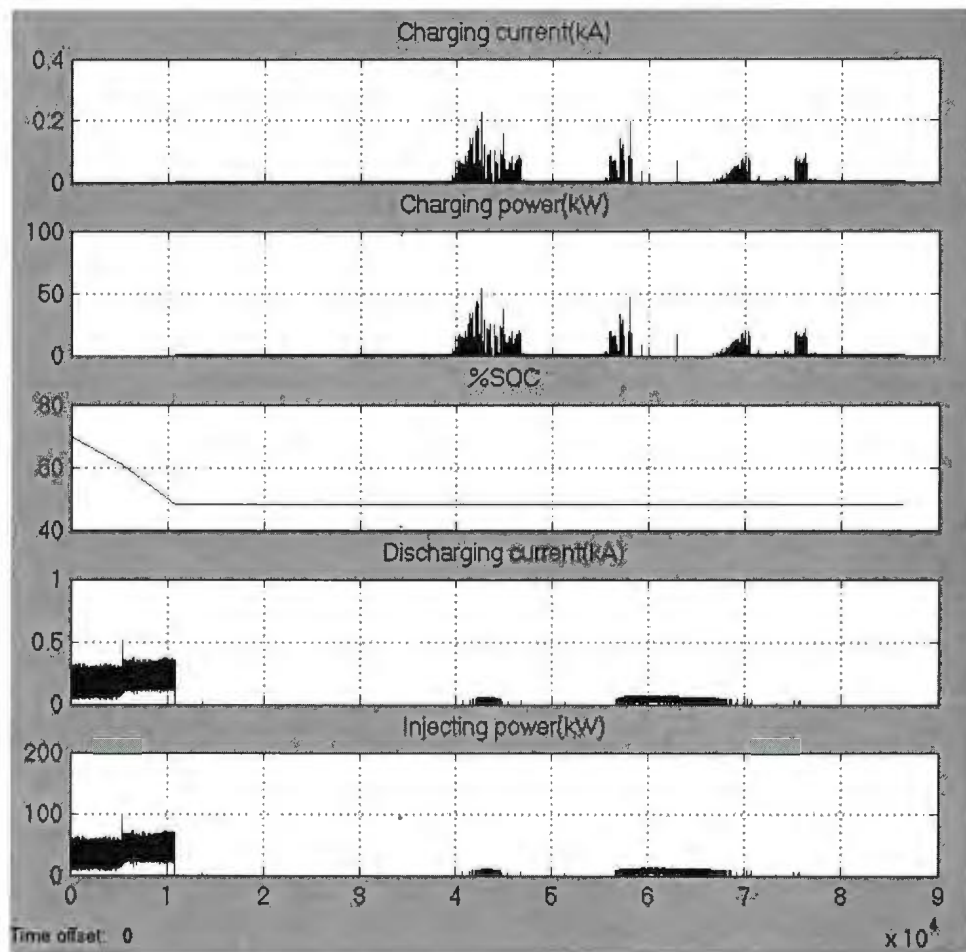
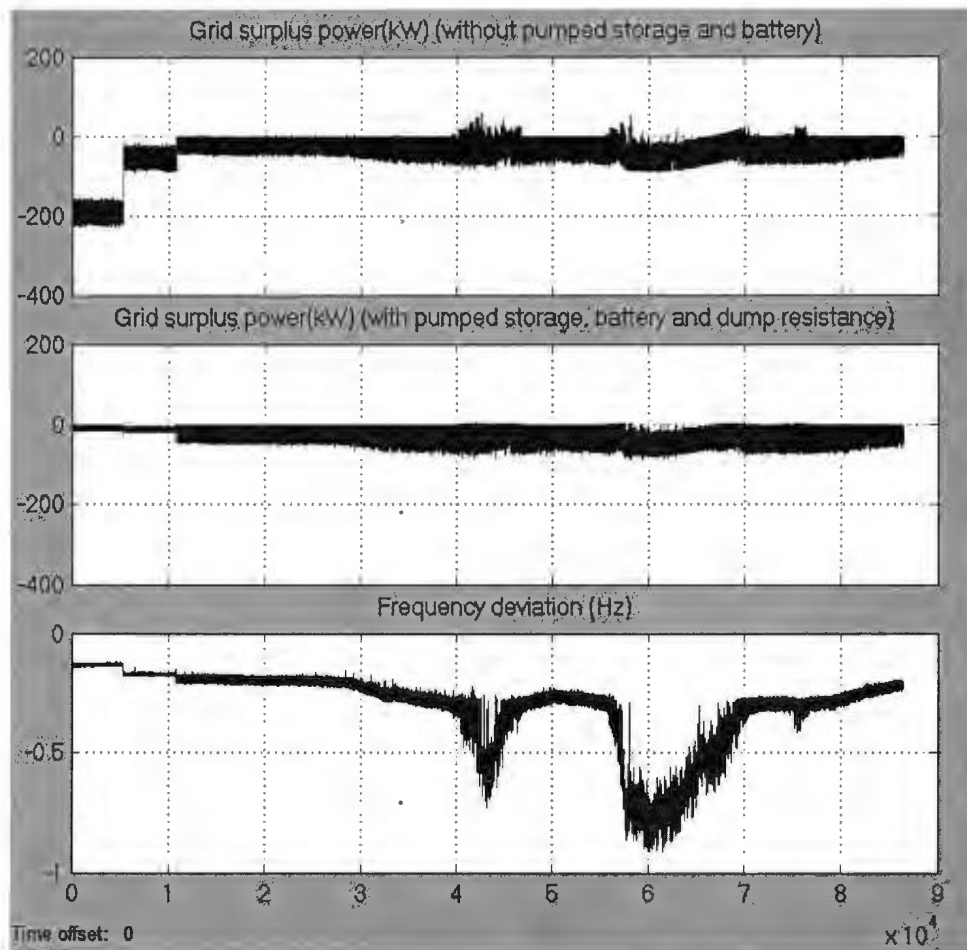


Figure 4.20. Charging current (kA), charging power (kW), percentage of state of charge, discharging current (kA) and injected power to the grid (kW) due to the discharging of the battery are for the case 3



**Figure 4.21. Grid surplus power (kW) with and without pumped storage, battery and dump load and the resultant system frequency deviation for the case 3**

#### 4.4.4 Case 4: High Load and High Wind

For case 4, high load and high wind speed have been used as inputs to the dynamic model and observe the outputs and system responses. Figure 4.22 shows the selected load and wind speed data for the case 4. The system simulation results are shown in the Figure 4.23 to Figure 4.26 below. From Figure 4.22 to Figure 4.26 it has been observed that in

the first 7000s reservoir becomes full and by 12000s BB is showing 100% SOC. As wind is very high WTs are generating enough power to the system so DEG delivers only 300kW and maintains the system stability. Remaining excess power is being dumped depending on the load changes. System frequency is stable for the whole time. One frequency dip of 0.4Hz is observed at 65000s. This happens when hydro generation turns on for a while.

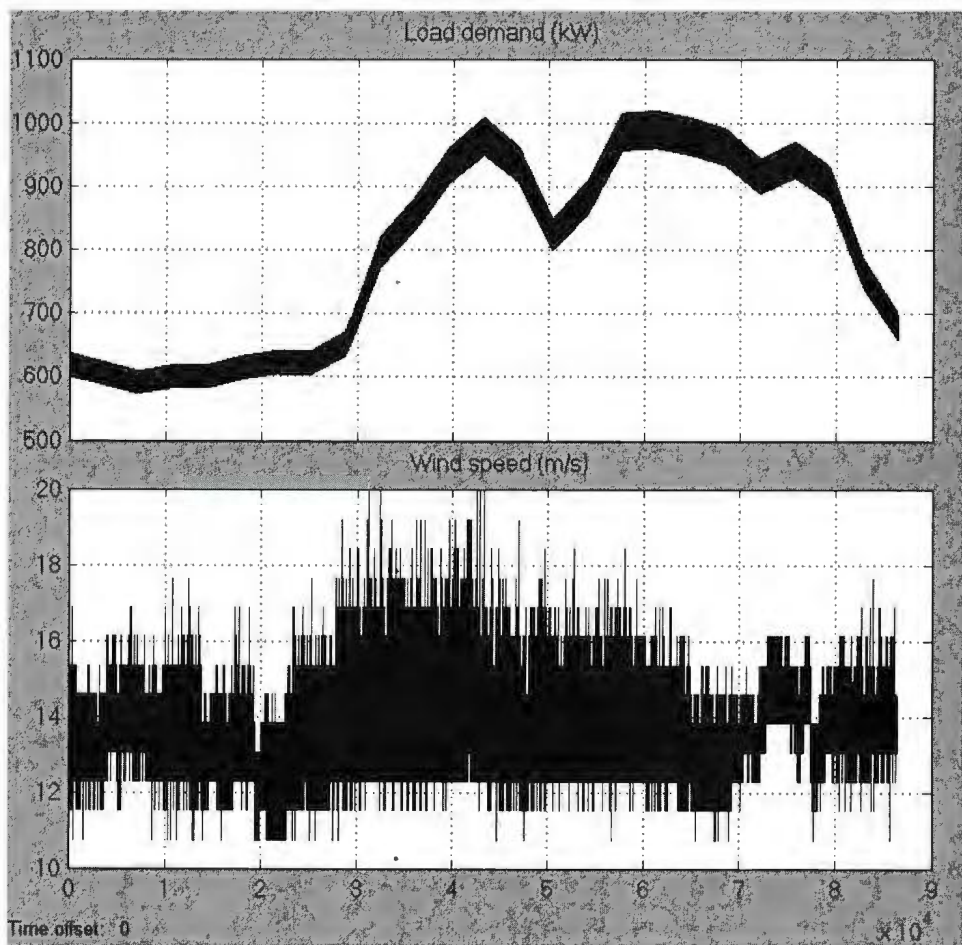
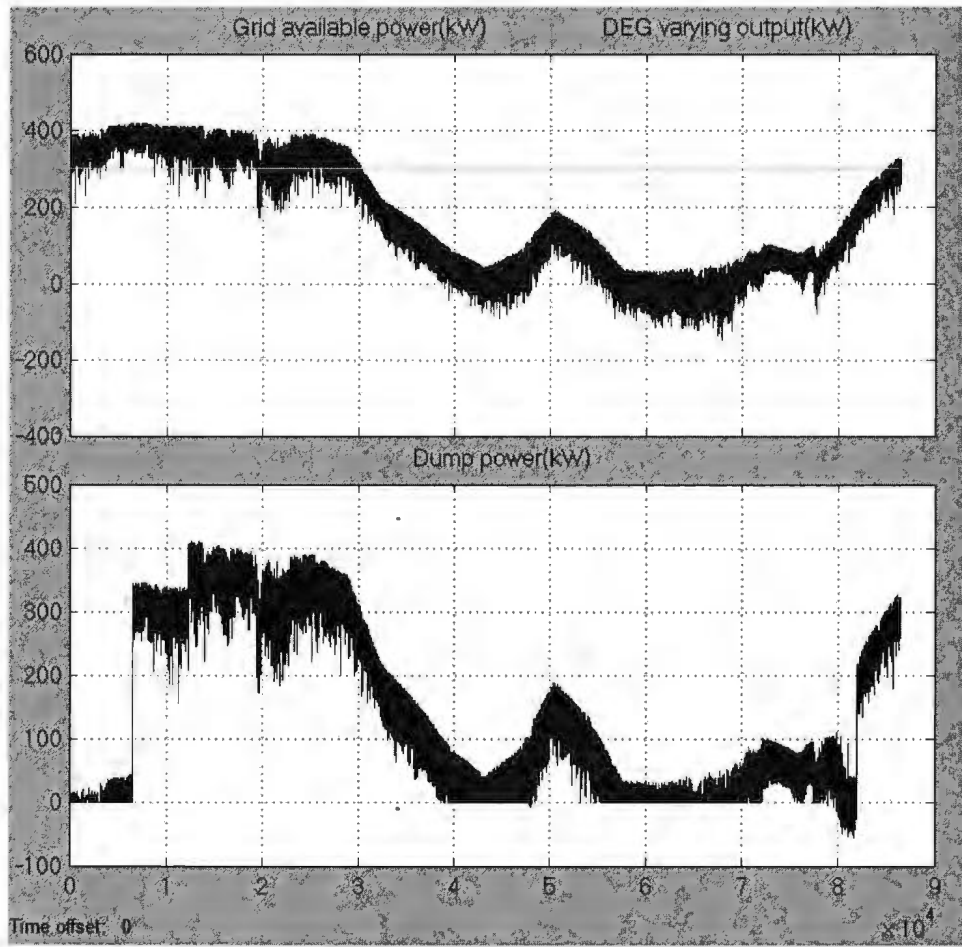


Figure 4.22. Load demand (kW) and wind speed (m/s) data for the case 4



**Figure 4.23.** In top figure grid available power (kW) and DEG output (kW) (flat 300kW value) are shown and in the lower part dump power (kW) is shown for the case 4

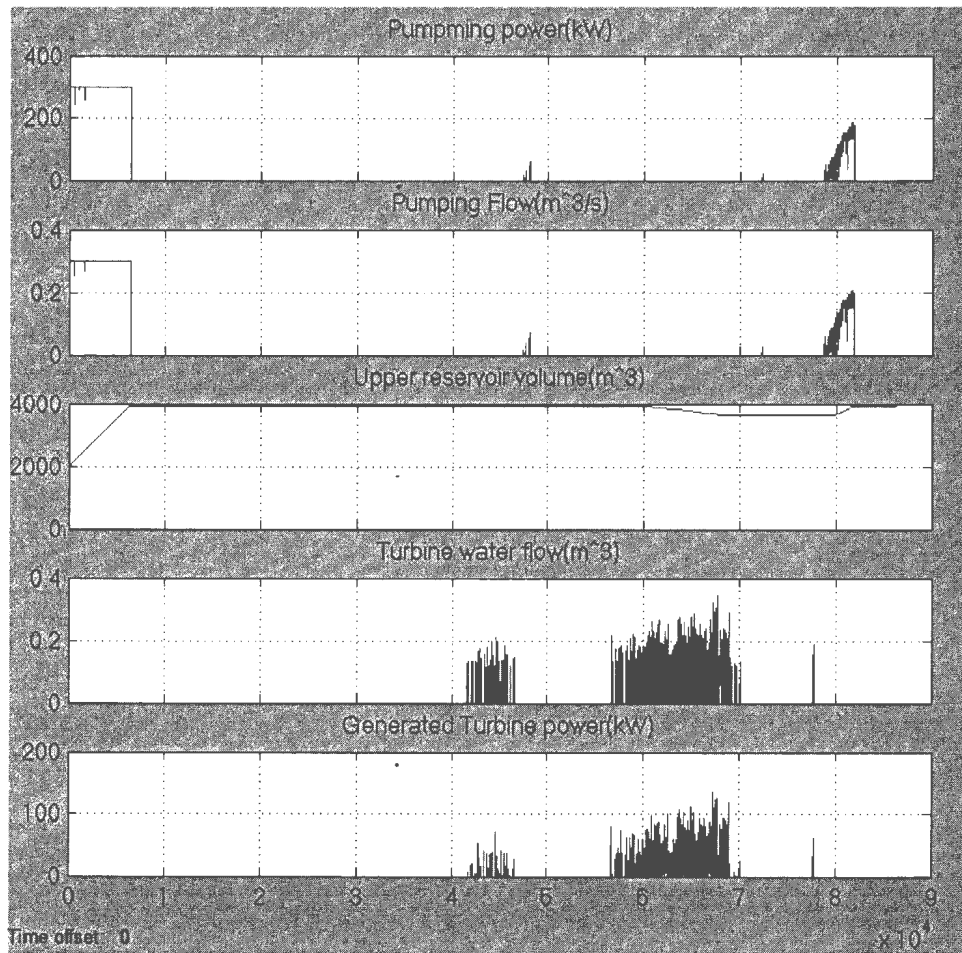


Figure 4.24. Pumping power (kW), pumping water flow (m<sup>3</sup>/s), upper reservoir water volume (m<sup>3</sup>), turbine water flow (m<sup>3</sup>/s) and turbine generated power (kW) for the case 4 are shown above

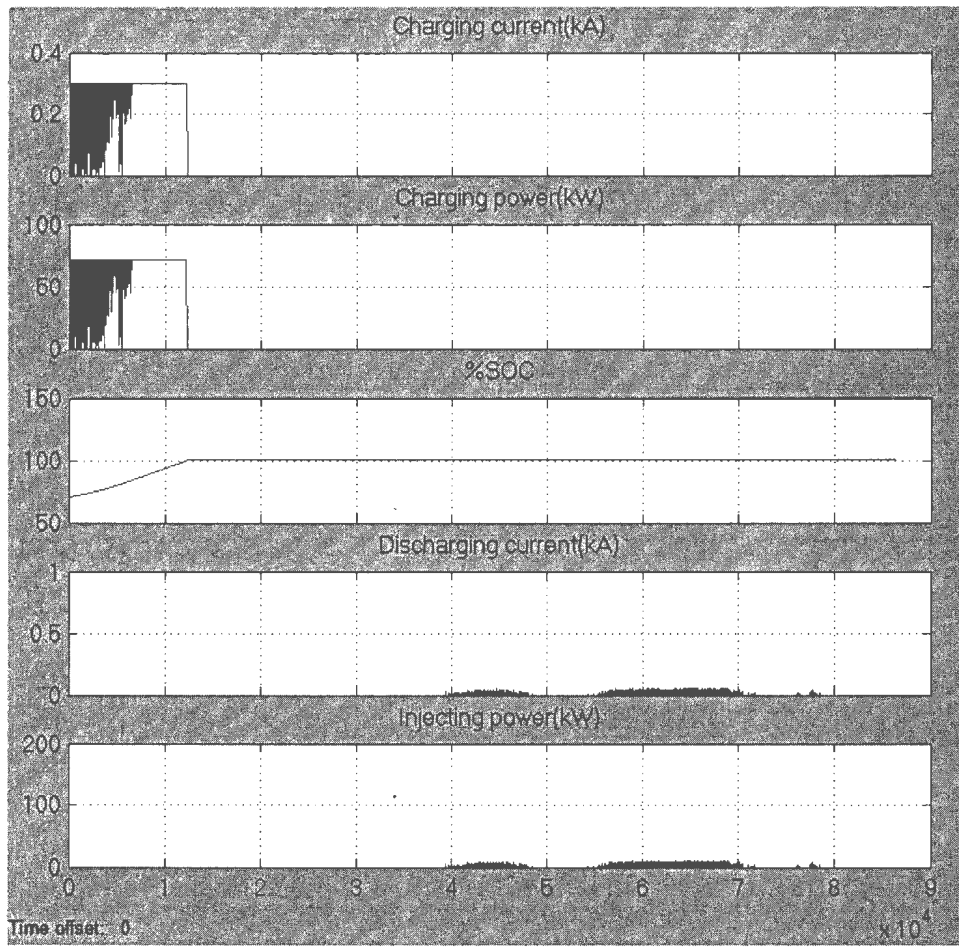


Figure 4.25. Charging current (kA), charging power (kW), percentage of state of charge, discharging current (kA) and the power injected to the grid (kW) due to the discharging of the battery are shown above for the case 4

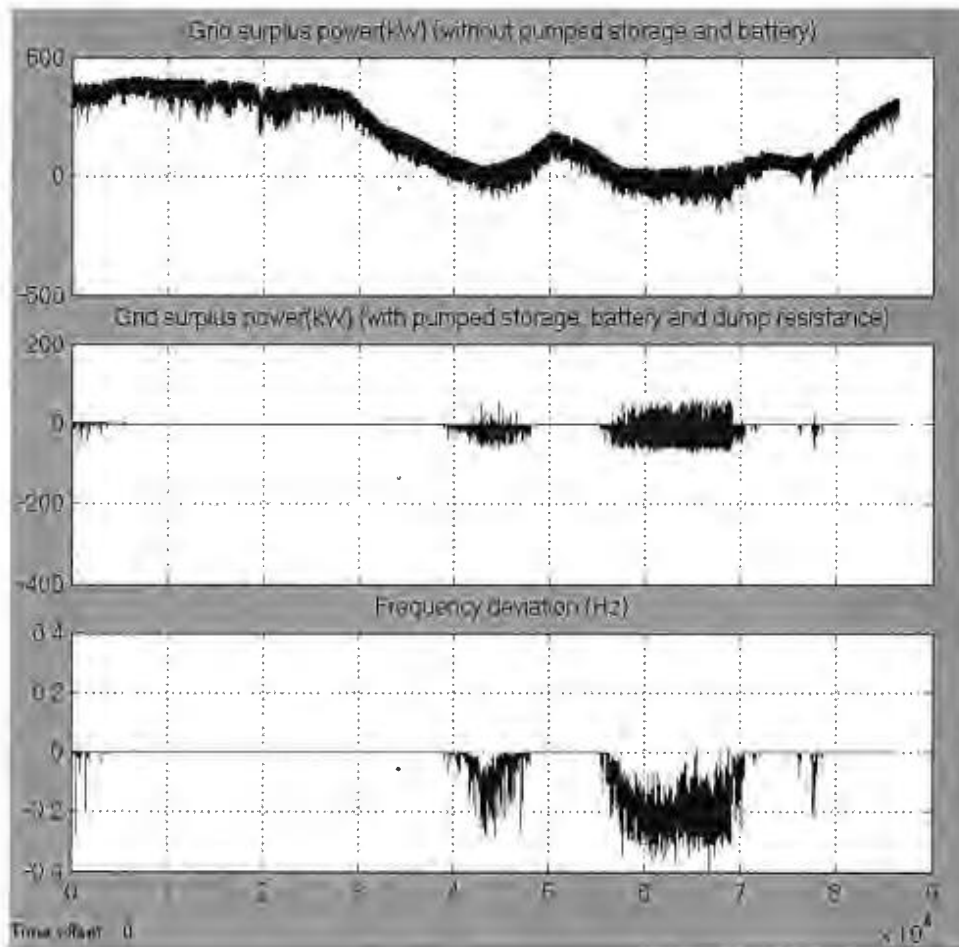


Figure 4.26. Grid surplus power (kW) with and without pumped storage, battery and dump load are shown above. The resultant frequency deviation is also plotted for the case 4

#### 4.4.5 Case 5: Abrupt Change of Load While Wind Speed is Steady in the Midrange

For this case study a simple step change in the load is assumed. This case study is done to observe the system dynamics in case of a change in the load. From Figure 4.27 to Figure 4.31 it has been found that PWT supplies a maximum of 150kW power for the whole time and DEG delivers the excess required amount from 200s to 700s. No water pumping

and no power dumping occur. Such sudden load change of 200kW leads to a frequency fluctuation of 0.2Hz that dies down in 40s. System is capable of maintaining an almost stable frequency in such rare event.

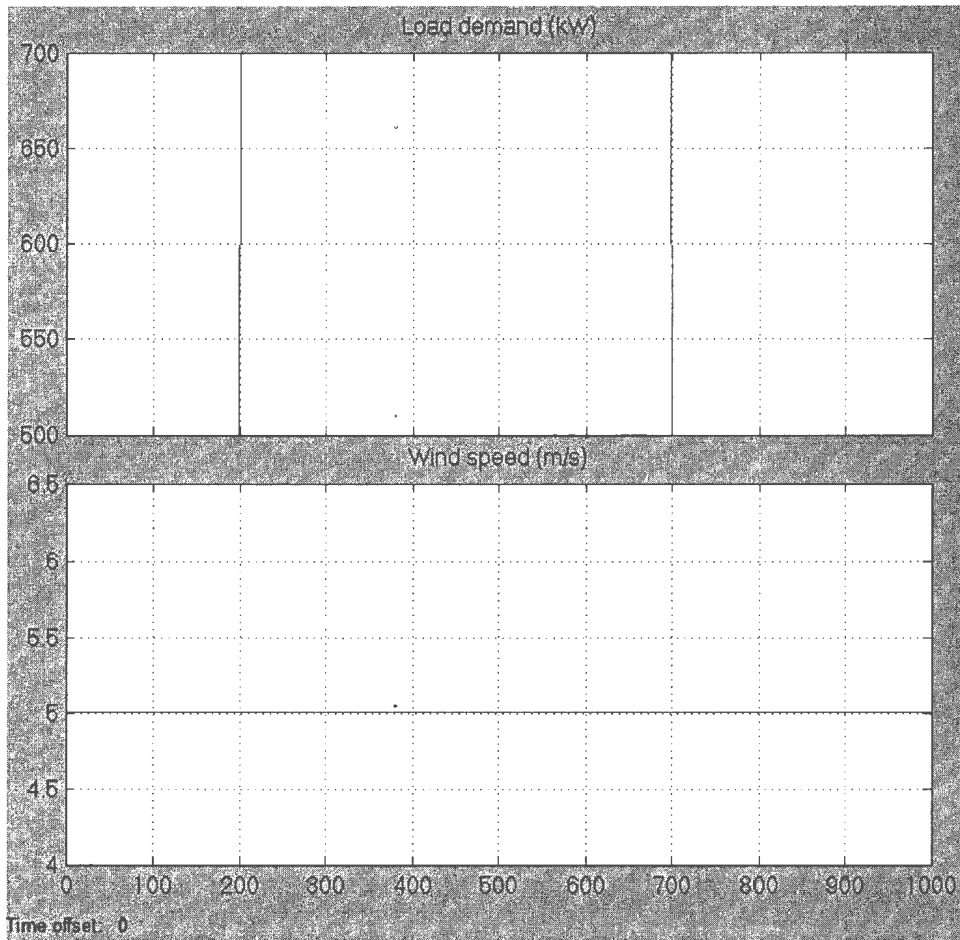


Figure 4.27. Load demand (kW) and wind speed (m/s) data for the case 5

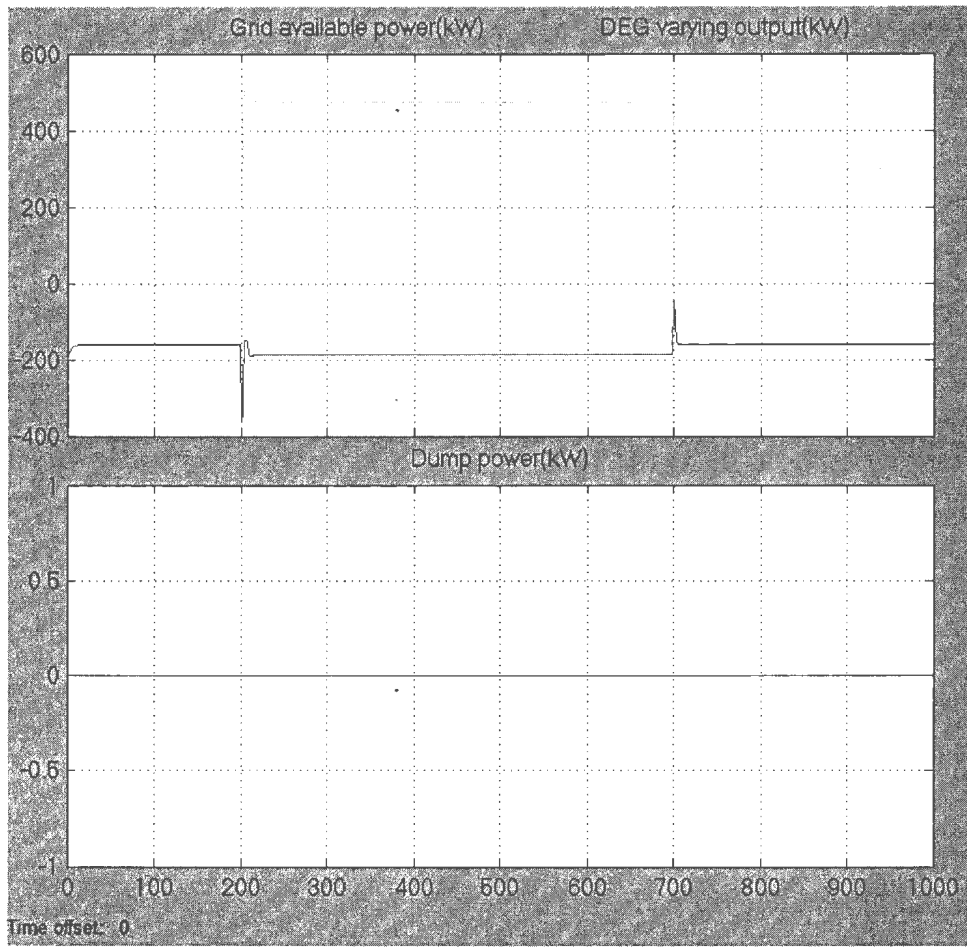


Figure 4.28. In top part, grid available power (kW) and DEG varying output (kW) (that changes from 300kW to 500kW) are shown. In the lower part dump load power (kW) is plotted for the case 5

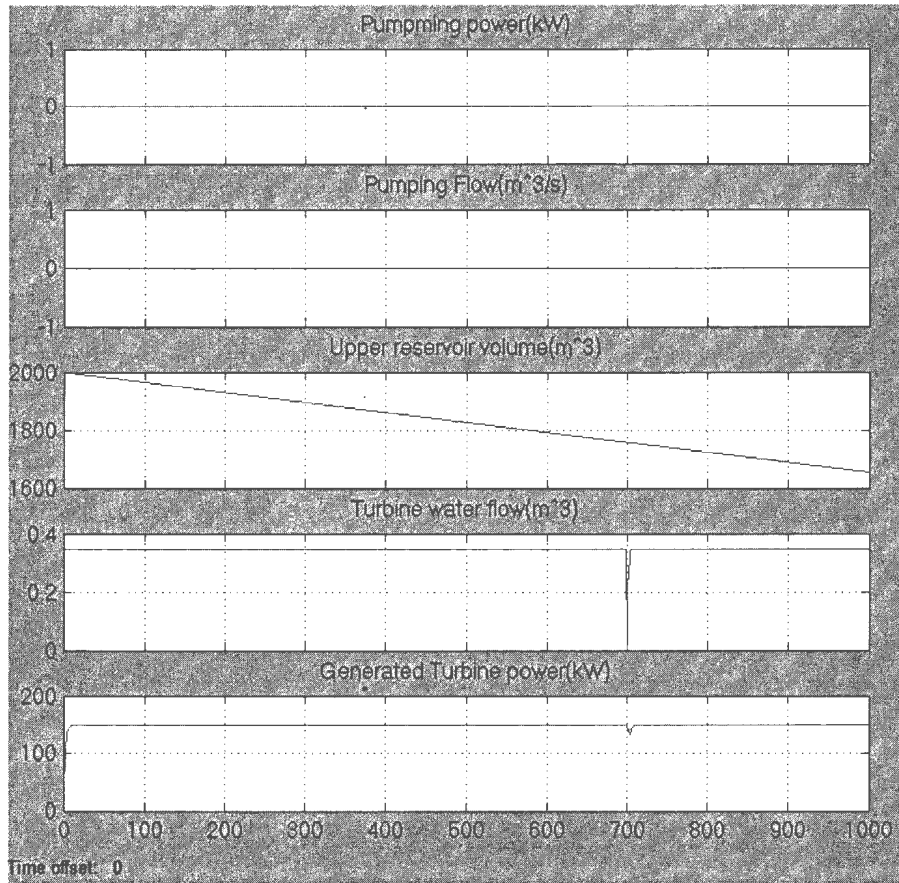


Figure 4.29. Pumping power (kW), pumping water flow ( $\text{m}^3/\text{s}$ ), upper reservoir water volume ( $\text{m}^3$ ), turbine water flow ( $\text{m}^3/\text{s}$ ) and turbine generated power (kW) are plotted above for the case 5

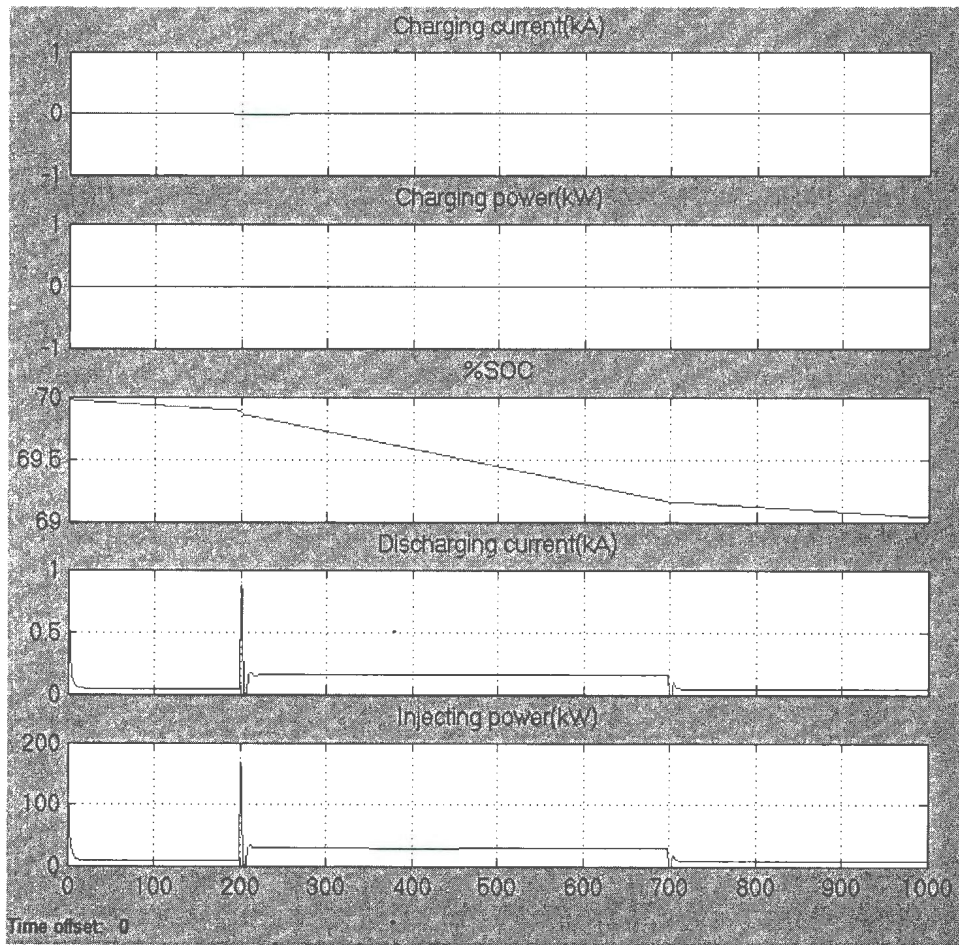


Figure 4.30. Charging current (kA), charging power (kW), percentage of state of charge, discharging current (kA) and injecting power to the grid (kW) due to the discharging of the battery are plotted above for the case 5

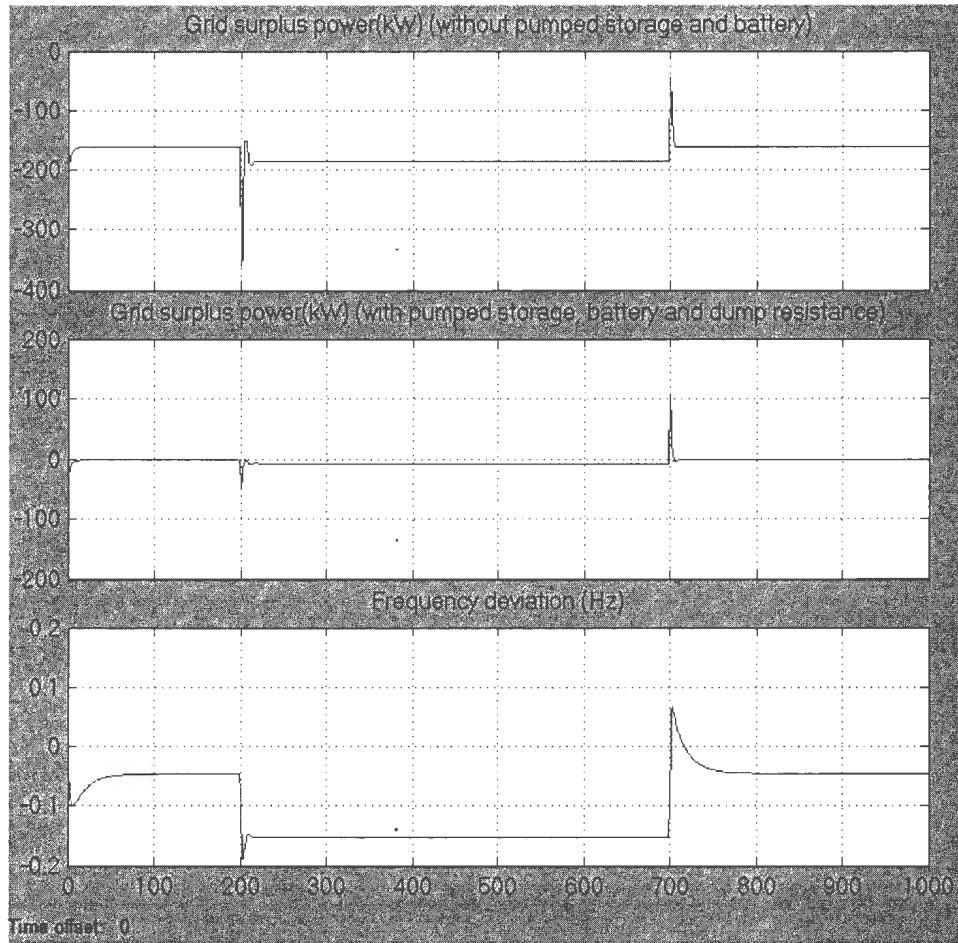


Figure 4.31. The grid surplus power (kW) with and without pumped storage, battery and dump load and the resultant frequency deviation for the case 5

#### 4.4.6 Case 6: Load is Steady in the Midrange and Wind Speed is Changed Abruptly

In this case study load is a constant while wind speed is increased and then decreased. The system inputs are shown in the Figure 4.32. Simulation results are shown in Figure 4.32 to Figure 4.36.

From Figure 4.32 to it has been found that as wind speed increases the water pumping starts and operates of its maximum rating from  $t=200s$  to  $700s$ . BB is charging too for a while. DEG is supplying 300kW all time.

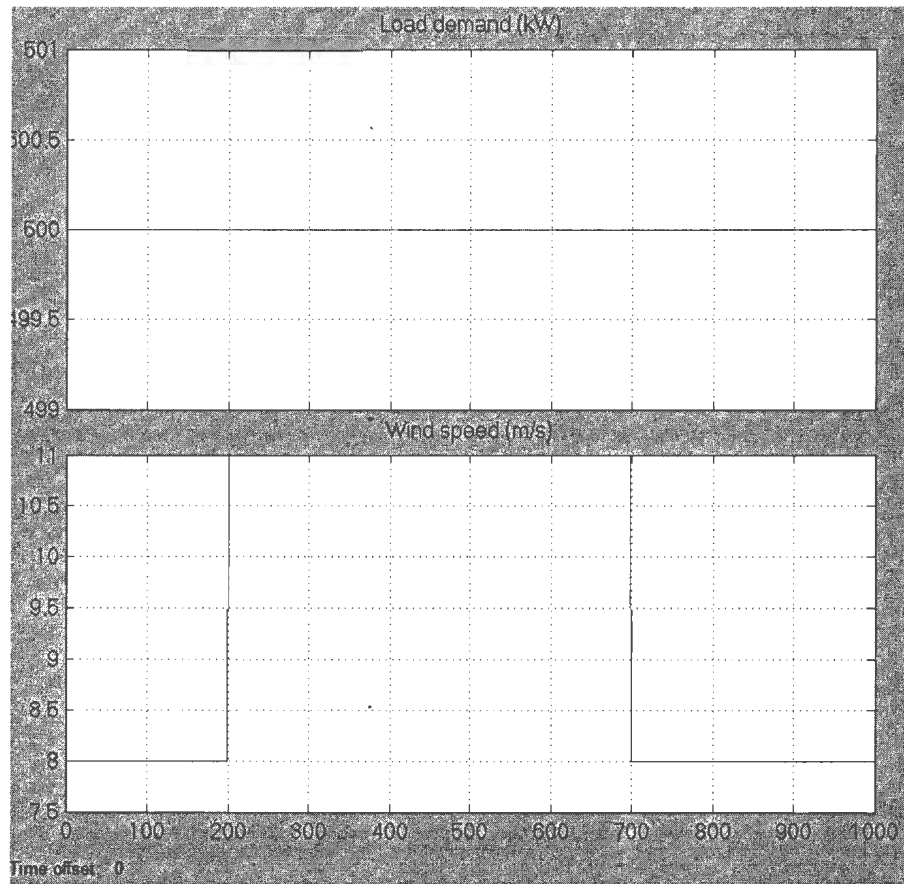


Figure 4.32. Load demand (kW) and wind speed (m/s) data for the case 6

At 700s a sudden 1.1Hz system frequency dip is found when wind speed drops from to 8m/s from 11m/s. Such a large dip may not be acceptable. But a sudden wind speed drop of 3m/s is impossible. This case study shows that the proposed supervisory controller is capable of controlling the system in extreme conditions.

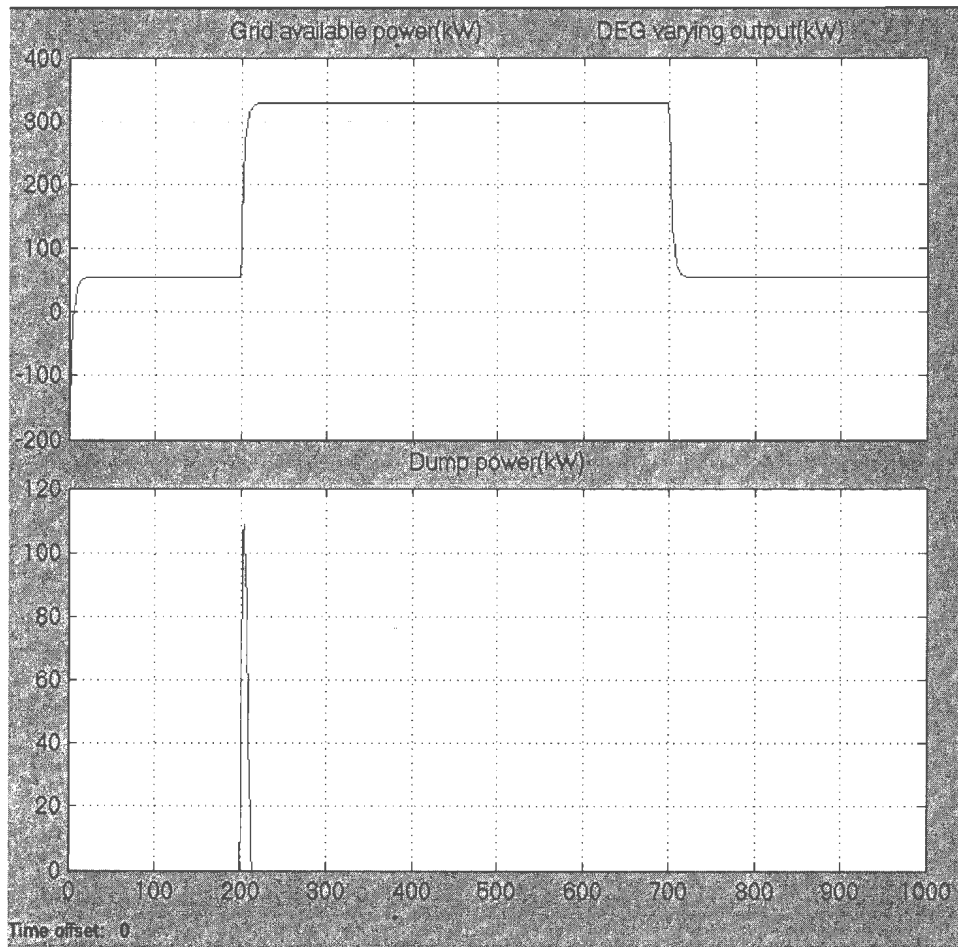


Figure 4.33. In the top part, grid available power (kW) and DEG varying output (kW) (with a flat 300kW) and in bottom part dump power (kW) is shown for the case 6

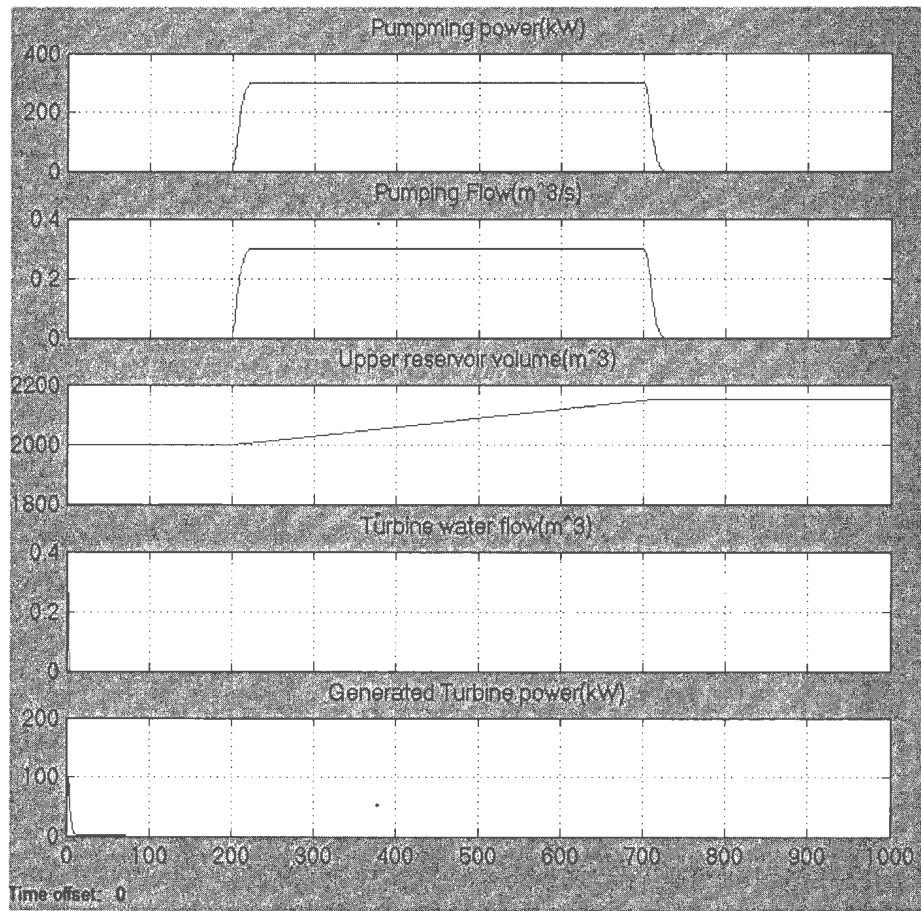
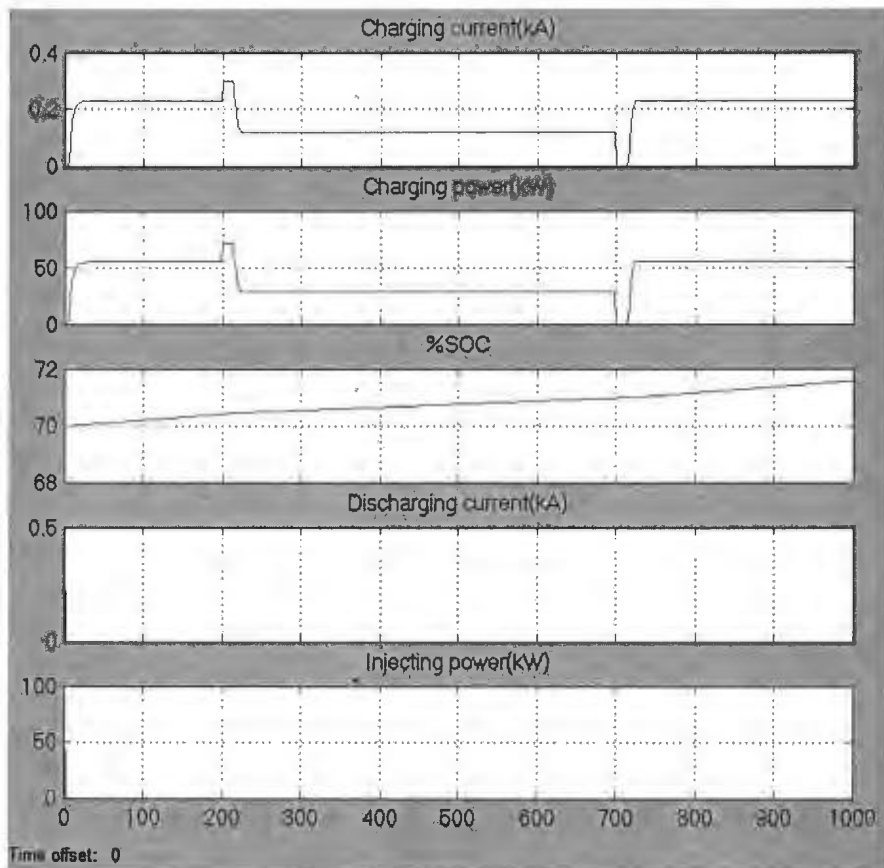
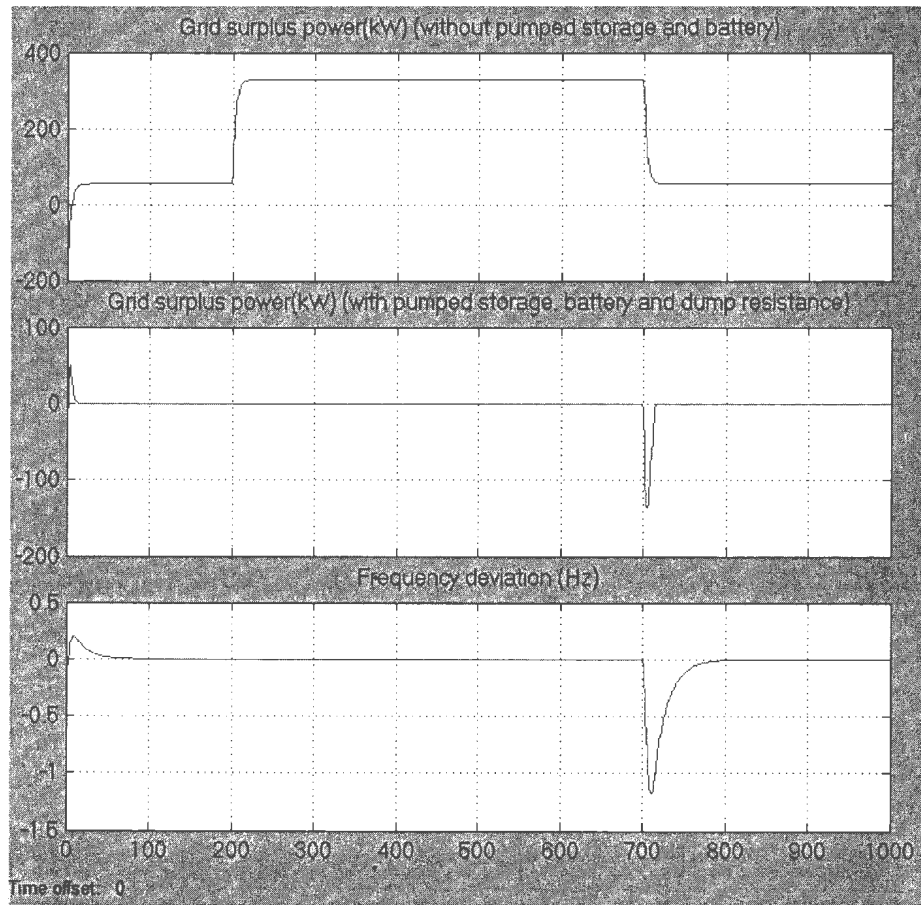


Figure 4.34. Pumping power (kW), pumping water flow (m<sup>3</sup>/s), upper reservoir water volume (m<sup>3</sup>), turbine water flow (m<sup>3</sup>/s) and turbine generated power (kW) are shown above for the case 6



**Figure 4.35. Charging current (kA), charging power (kW), percentage of state of charge, discharging current (kA) and injected power to the grid (kW) due to the discharging of the battery are plotted above for the case 6**



**Figure 4.36. Grid surplus power (kW) with and without pumped storage, battery and dump resistance and the resultant frequency deviation are shown above for the case 6**

All above discussed 6 cases show almost steady system frequency for extreme conditions. These are extreme situations for the load demand and wind speed data in a year. Real situations may be much milder than above selected cases.

#### 4.5 Conclusions

This paper presented a dynamic simulation model and a supervisory controller for a remote hybrid power system with a proposed pumped hydro storage. From the simulation results, based on six possible extreme cases, it can be concluded a) a minimum of 300kW operation of DEG permits higher penetration of wind energy and leads to a low diesel consumption and maintains a fairly stable system frequency b) proposed dump load addition will prevent the system frequency spikes in high wind and make the system operation easier and results in less frequency deviations. Expected response of pump hydro system with battery storage is acceptable for a remote location like Ramea Island. Simulation of the presented dynamic model with proposed PHS, BB and dump load is significantly fast. Using a 0.01s time step, a day i.e. 86400s simulation takes about 30min to complete on a computer with Intel Core2Duo 2.1GHz processor. The system model presented in this paper includes all real world characteristics curves, nonlinear efficiencies, losses and a supervisory controller. Moreover, this model can be used to check system stability and be modified easily for possible future extension to the hybrid power system. Wind data and load data of any day can be used with the model to determine the system expected response. This model allows us to simulate few months of operations of Ramea hybrid system and study parameters such as fuel consumption. Such a study is not possible in any commercially available software. Incorporating higher order complicated system components models in the blocks of this model can improve this model but that will considerably increase the simulation time. As a future work, system AC voltage analysis can be done to observe the voltage variations in the system.

#### 4.6 Acknowledgment

Authors thank The Wind Energy Strategic Network (WESNet) (which is a Canada wide research network, funded by industry and the Natural Sciences and Engineering Research Council of Canada (NSERC)) for funding this research.

#### 4.7 References

- [1] Introduction to the Ramea Island, [Online]. Available: <http://www.ramea.ca/>. [Accessed 30-01-2013].
- [2] CANMET Energy, "Natural Resource Canada," Natural Resource Canada, 07-07-2007. [Online]. Available: <http://canmetenergy.nrcan.gc.ca/renewables/wind/464>. [Accessed 30-01-2013].
- [3] M. Oprisan, "IEA Wind," IEA Wind – KWEA Joint Workshop, 01-04-2007. [Online]. Available: [http://www.ieawind.org/wnd\\_info/KWEA\\_pdf/Oprisan\\_KWEA\\_.pdf](http://www.ieawind.org/wnd_info/KWEA_pdf/Oprisan_KWEA_.pdf). [Accessed 30 01 2013].
- [4] T. Iqbal, "Feasibility Study of Pumped Hydro Energy Storage for Ramea Wind-Diesel Hybrid Power System," The Harris Centre, St. John's, 2009.
- [5] D.-J. Lee and L. Wang, "Small-Signal Stability Analysis of an Autonomous Hybrid Renewable Energy Power Generation/Energy Storage System Part I: Time-Domain Simulations," IEEE TRANSACTIONS ON ENERGY CONVERSION, vol. 23, no. 1, pp. 311-320, 2008.

- [6] Md. Rahimul Hasan Asif and Tariq Iqbal, "A novel method to model a hybrid power system with pumped hydro storage for Ramea, Newfoundland", IEEE, Newfoundland Electrical and Computer Engineering Conference, St. John's, 2012
- [7] A. G. Rodríguez, A. G. Rodríguez and M. B. Payán, "Estimating Wind Turbines Mechanical Constants," in International Conference on Renewable Energies and Power Quality (ICREPQ'07), Bilbao, 2007.
- [8] Windmatic, "Windmatic 15s," [Online]. Available: <http://windmatic.com/15s-brochure.pdf>. [Accessed 30 01 2013].
- [9] Northern Power Systems, "Northern Power 100," [Online]. Available: [http://www.northernpower.com/pdf/NPS100-21\\_SpecSheet\\_EU-A4\\_English\\_2012.pdf](http://www.northernpower.com/pdf/NPS100-21_SpecSheet_EU-A4_English_2012.pdf). [Accessed 10 01 2013].
- [10] Advantica Inc., "Moment of Inertia and Pump Startup/Failure," 14 03 2011. [Online]. Available: [http://my.advanticagroup.com/support/allsecure/watersecure/releases\\_advisories/KBA\\_pump\\_moment\\_of\\_inertia.pdf](http://my.advanticagroup.com/support/allsecure/watersecure/releases_advisories/KBA_pump_moment_of_inertia.pdf). [Accessed 30 01 2013].
- [11] "The Engineering Toolbox," [Online]. Available: [http://www.engineeringtoolbox.com/minor-loss-coefficients-pipes-d\\_626.html](http://www.engineeringtoolbox.com/minor-loss-coefficients-pipes-d_626.html). [Accessed 30 01 2013].
- [12] G. Brown, "Henry Darcy and His Law," 22 06 2000. [Online]. Available: <http://biosystems.okstate.edu/darcy/index.htm>. [Accessed 30 01 2013].

- [13] Renewables First, "Pelton & Turgo Turbines," Renewables First, [Online]. Available: <http://www.renewablesfirst.co.uk/pelton-and-turgo-turbines.html>. [Accessed 30 01 2013].
- [14] Chen, H., Cong, T., Yang, W., Tan, C., Li, Y., and Ding, Y., Progress in electrical energy storage system: a critical review. *Progress in Natural Science* 19 (2008), 291–312.

## **5 Diesel Consumption in a High Penetration Remote Hybrid Power System with a Pumped Hydro and Battery Storage**

### **Preface**

A version of this manuscript has been accepted for the conference proceedings of *IEEE Electrical Power and Energy Conference 2013, Halifax, Nova Scotia, Canada*. This paper is going to be presented in the conference on August 21-23 2013. The co-author Dr. Tariq Iqbal supervised the principle author Md. Rahimul Hasan Asif to conduct the research on this topic and helped him with research techniques and to understand theories available on this topic. Md. Rahimul wrote the paper, developed the dynamic model, conducted simulation and associated analyses while Dr. Iqbal reviewed the manuscript and provided necessary suggestions and many recommendations.

### **Abstract**

In this research diesel consumption for three operational modes of a remote Hybrid Power System (HPS) is studied. The system consists of a 925kW diesel engine generator, a proposed pumped hydro storage system, battery bank and dump load. The proposed system is a replacement of the existing inefficient electrolyzer, hydrogen storage and generator system for Ramea Newfoundland. The hybrid system has been modeled with detailed customized function blocks in Simulink. Different modes of diesel engine generator have been studied here to estimate the fuel consumption, no of switching and

system frequency deviation. The HPS dynamic model presented here is fast, accurate and includes dynamic and supervisory controllers. The proposed real time control algorithm observes the surplus/missing power in the grid and regulates all components to maintain high penetration of wind energy while maintaining a stable system frequency. This paper presents three different operational modes of diesel engine and HPS simulation results.

**Index Terms**—Hybrid Power System; Dynamic Modeling; Wind Power; Pumped Hydro Storage; Renewable Energy; Wind-diesel systems.

## 5.1 Nomenclature

HPS - Hybrid Power System

PHS - Pumped Hydro Storage

WT - Wind Turbine

DEG - Diesel Engine Generator

HES - Hydrogen Electrolyzer and Storage

HPG - Hydrogen Powered Generator

BB - Battery Bank

SOC - State of Charge

IM - Induction Motor

CP - Centrifugal Pump

DL - Dump Load

PWT - Pelton Wheel Turbine

TF - Transfer Functions

TC - Time Constant

PID - Proportional-Integral-Derivative

## 5.2 Introduction

RAMEA is a small island located off the south coast of Newfoundland, Canada. In 2004, Ramea was selected as the first pilot project site for a remote Wind-Diesel-Hydrogen HPS which was led by the Newfoundland and Labrador Hydro. The major objective of this project was to demonstrate substantial improvement of energy efficiency and reliability after incorporating Wind-Diesel Integrated Control System (WDICS) to the island's grid which can reduce the use of diesel power by using wind energy in remote and isolated location. This wind-diesel pilot system is generating almost 106 kWh of electricity and offsetting nearly 750 tons of greenhouse gas emissions per annum [1] [2].

Hybrid system in Ramea has six 65kW Windmatic 15s and three 100kW NorthernPower100 WT. Three 925kW DEG are available but only one is used as the main power source. A Hydrogen Electrolyzer and Storage (HES) and a 250kW Hydrogen Powered Generator (HPG) have been installed to achieve high wind penetration. This HES and HPG have efficiencies respectively 70% and 35%. In overall they give a poor turn around conversion efficiency of less than 25% [3] and leads to many safety issues. Optimal sizing and site selection of a Pumped Hydro Storage (PHS) system replacing the HES and HPG with detailed information, analysis and dynamic simulation has been presented in [4]. It has been explained in [4] that using a 150kW PHS system with a

3932m<sup>3</sup> water reservoir at 63m height on the top of 'Man of War' hill, it is possible to achieve almost 37% renewable energy fraction. In [4] only 24s of system dynamic simulation was presented that took days of computer time to simulate the system. Simulation also had convergence issues from 11s to 16s. To reduce simulation time simple first order models have been used here which makes the analysis easier and gives fairly accurate solutions. Ref. [5] shows the stability of a self-governing HPS with battery bank (BB) and flywheel by time-domain simulations. But, the presented three mathematical subsystems had no controller and nonlinear efficiency, friction and response times are ignored. This paper presents the system with components modeled with simple first order Transfer Function (TF) juxtaposing all nonlinear efficiencies, dynamic frictions and TCs related to the subsystem. Some system details may be found in [6].

A BB has been used to supply or store the intermittent power as Induction Motor (IM) and Centrifugal Pump (CP) or Pelton Wheel Turbine (PWT) and DEG have higher time constant (TC) than BB. A controllable dump load (DL) has also been used to dump the excess power instantaneously. Presented model has PID controllers and all its subsystems. Built in PID tuner of Simulink has been used to determine the PID parameters. Parameters and characteristic data of the WTs and DEG used in Ramea HPS are taken from the respective manufacturers. All other subsystem models e.g. CP, PWT, BB have been formed using data obtained from data sheets of actual devices.

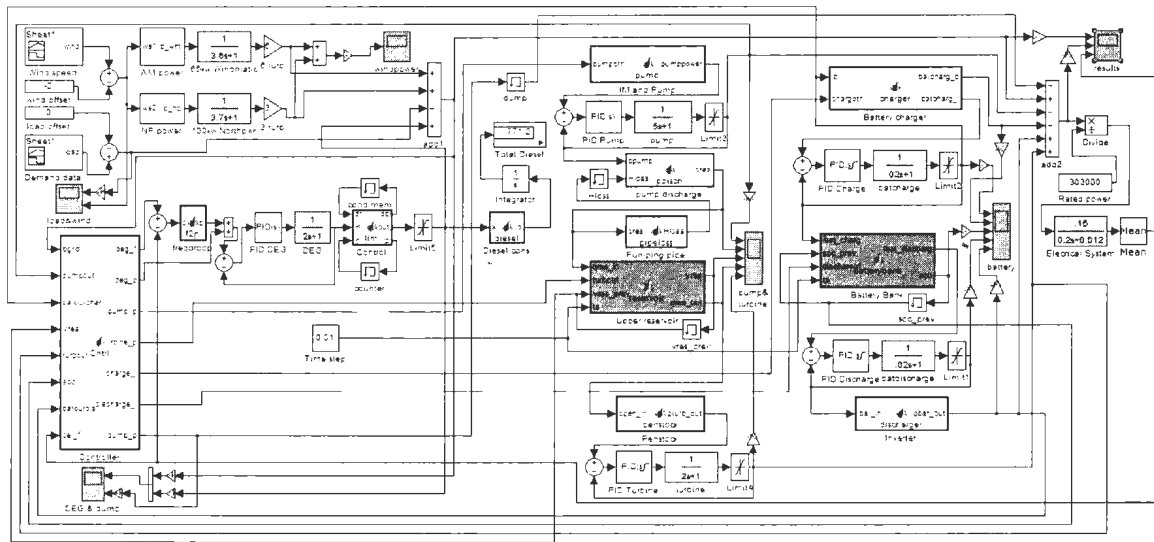


**Figure 5.1. Simulink - MATLAB embedded function block based dynamic model of Ramea hybrid power system with PHS, BB and DL**

### 5.3 Dynamic Model Description

In this study simulations have been done for 86400s (one day) with models with simple 1st order TFs to simulate the transient behavior of the HPS. In Figure 5.1 all subsystems represent the exact real world components with all nonlinear losses.

#### 5.3.1 Inputs: Wind Speed and Load Data

In this model 1Hz wind speed data from the Prince Edward Island (PEI), Newfoundland, Canada is used (such data for Ramea was not available). Average value of the one day data was adjusted to represent yearly average wind speed at Ramea e.g.  $4.9\text{ms}^{-1}$ . Ramea load data for one day is used from [4] with an average of 303kW as shown in Figure 5.2.

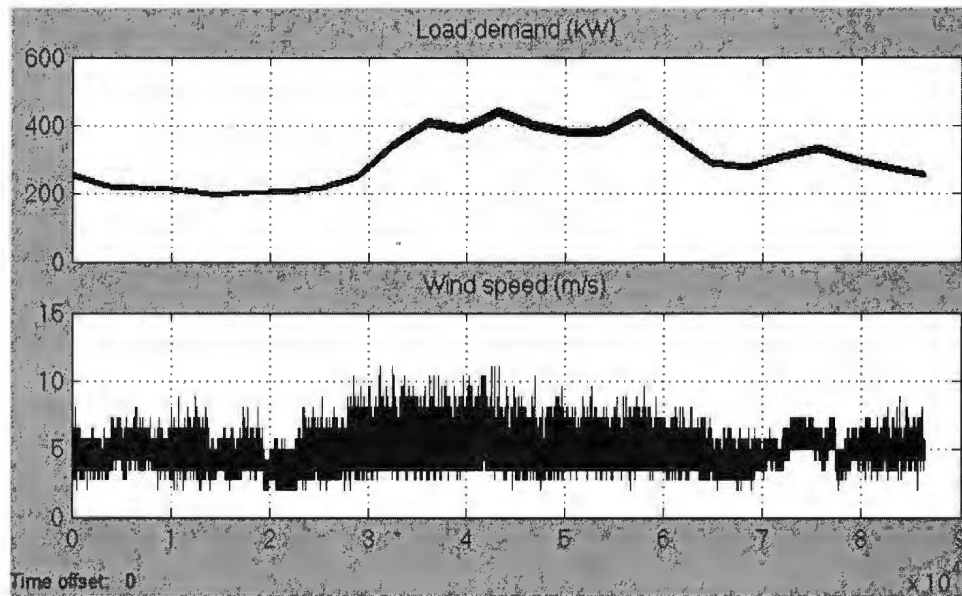


Figure 5.2. Load demand data and Wind speed data for one day (86400s)

### 5.3.2 Subsystem Blocks

Six 65kW Windmatic and three 100kW Northern Power WTs are modeled where WT TCs are used following the equation from [7].

$$H_{WT} \cong 1.87 * P_{WT}^{0.0597} \quad 5.1$$

In Equation 5.1  $H_{WT}$  is the mechanical inertia TC and  $P_{WT}$  is the power of the WT in watts. So calculation gives 3.6s for 65kW Windmatic 15s [8] and 3.7s for 100kW Northern Power 100 [9]. A 925kW DEG has been modeled with acceleration TC calculated by the following equation.

$$J = \frac{S_n T_{\text{DEG}}}{\omega_n^2}$$

Here,  $J$  is the moment of inertia;  $\omega_n$  is the rated angular velocity, which equals  $2\pi f$ ;  $S_n$  is the DEG nominal apparent power;  $T_{\text{DEG}}$  is the acceleration TC rated to  $S_n$ . In the datasheet of the DEG,  $J = 20\text{kg.m}^2$  which results in  $T_{\text{DEG}} \cong 2$  s. With this TC the DEG needs about 10s to reach its steady state value. Frequency droop curve has been introduced considering that this DEG has a  $\Delta P/\Delta f$  ratio of 300kW/1Hz. A DEG can operate from 30% to 100% of its rated power. In operating mode 2 with proposed continuous control, the DEG can operate below 30% with the help of a controllable inverter. Diesel consumption curve has been produced for this DEG from the manufacturer provided data.

A 200hp IM and CP system have been modeled assuming that this pumping system needs 30s to settle down comparing the starting time of a 4000hp – 1000rpm pumping system which takes 2:30 minutes to reach its rated output [10]. A 150kW PWT combined with a synchronous generator has been modeled having 70% efficiency and TC of 2s. A 70m in length and 15cm in radius penstock has been modeled assuming laminar flow inside the pipe. Darcy–Weisbach equation for friction inside the penstock has been used here.

A BB with 300 of 200Ahr Sealed Lead Acid batteries has been introduced where 20 batteries are connected in a branch making the DC bus voltage of 240V. These batteries can operate from 40% to 100% SOC and charging and discharging rate can be up to 10%

and 33% of the capacity respectively. Effect of '*Peukert's law*' on the effective capacity has been considered too. Conversion efficiency has been considered as 80%.

A 1MW controllable dump load has been modeled to stabilize the system frequency by removing excess power from the grid. As in [5] system inertia constant  $M$  and damping constant  $D$  have been used and gain has been adjusted so that 0.05pu power deviation will cause 0.01pu or 0.6Hz frequency deviation. This is acceptable for remote hybrid power systems.

### **5.3.3 Outputs**

System stability has been judged by the frequency variation in the grid. As in a small isolated HPS, a maximum of 2Hz sudden frequency dip is tolerable. Operational curves for all components with frequency deviation have been shown later for four different mode of operation of DEG.

### **5.4 Study of diesel consumption**

Diesel consumptions have been studied for 3 different modes. In mode 1, DEG is always turned on and operating in between 300kW to 925kW as required. In mode 2 DEG can be switched off but if it's on it will operate from 300kW to 925kW. In mode 3, DEG will be operated under continuous control where it can operate below 300kW. And in mode 4 DEG will stay in its present state for at least 10min after the recent switch over.

#### 5.4.1 Mode 1: DEG always ON

System simulation results are shown in Figure 5.3 to Figure 5.6. It can be observed that, in this mode DEG is operating at least 300kW for the whole time as power requirement was low. Surplus power has been dumped in DL. Maximum frequency dip is found to be 1.5Hz. Total diesel consumption in this mode in one day is expected as 2323L.

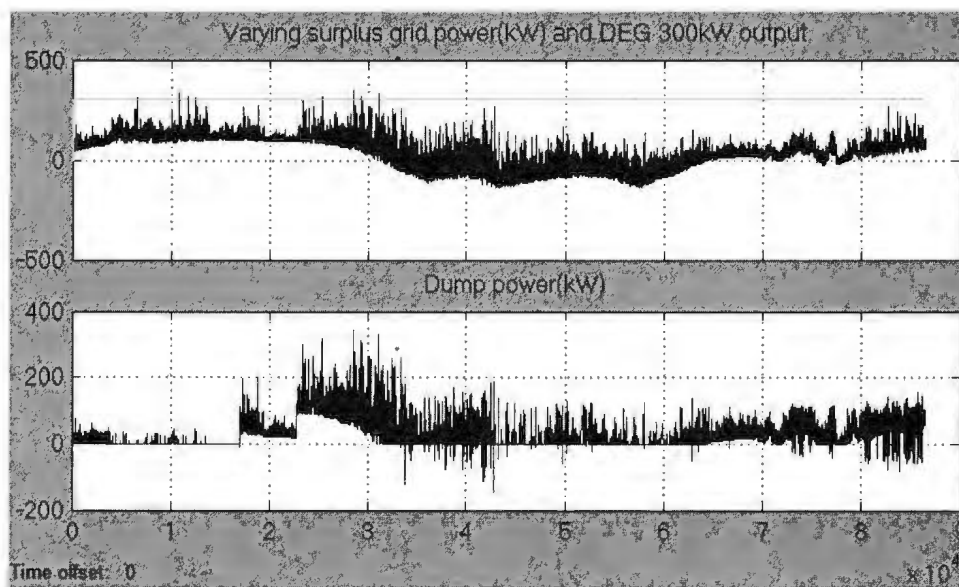
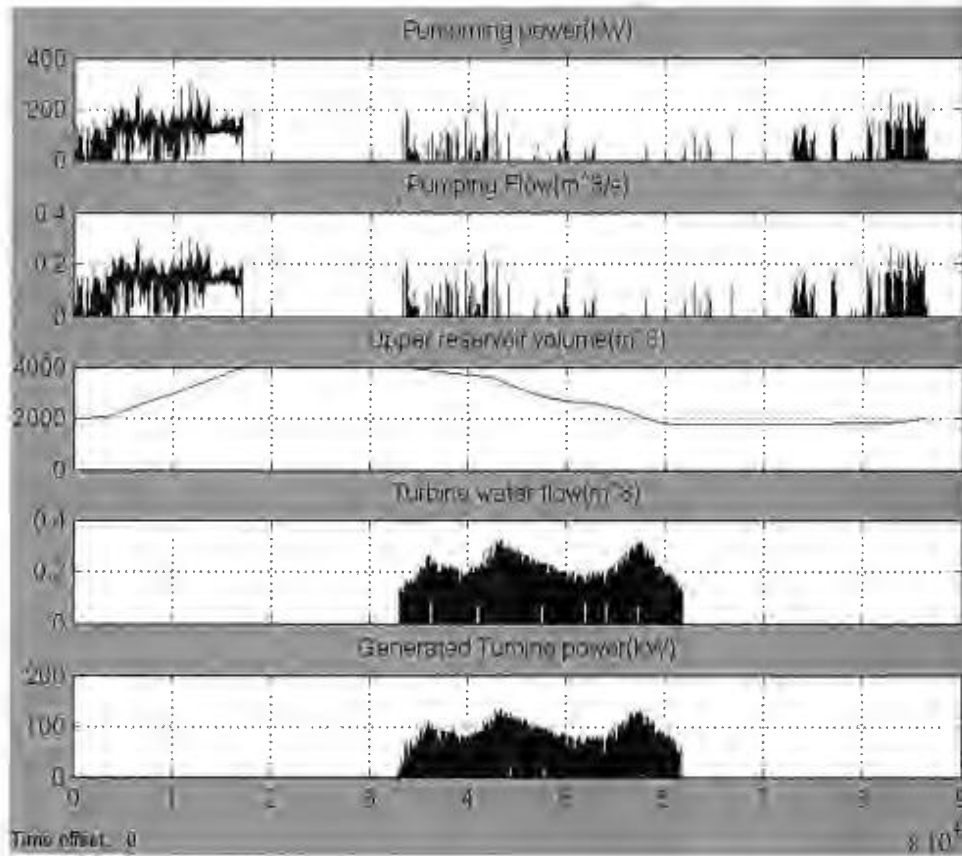


Figure 5.3. In top figure, the grid available power (kW) and DEG output (kW) (with a minimum 300kW value) is shown and in the lower figure dump power (kW) is shown for mode 1



**Figure 5.4. Pump power consumption (kW), pump water flow ( $m^3/s$ ), the upper reservoir water volume ( $m^3$ ), turbine water flow rate ( $m^3/s$ ) and the turbine generated power (kW) for the Mode 1**

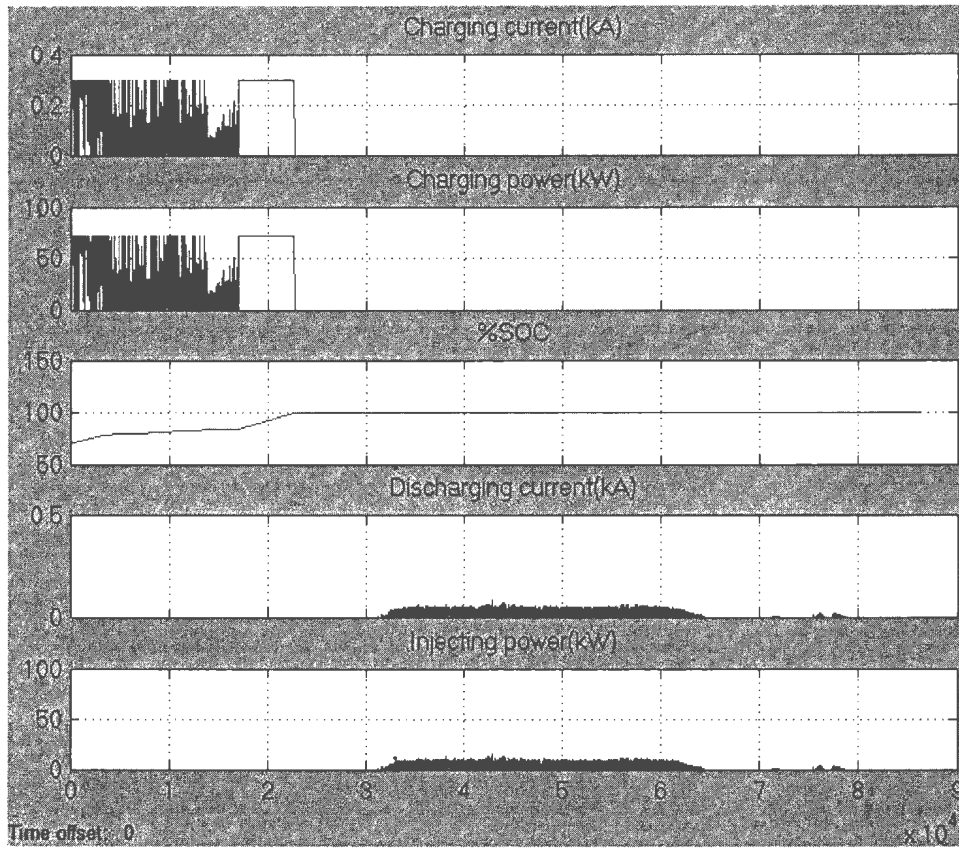
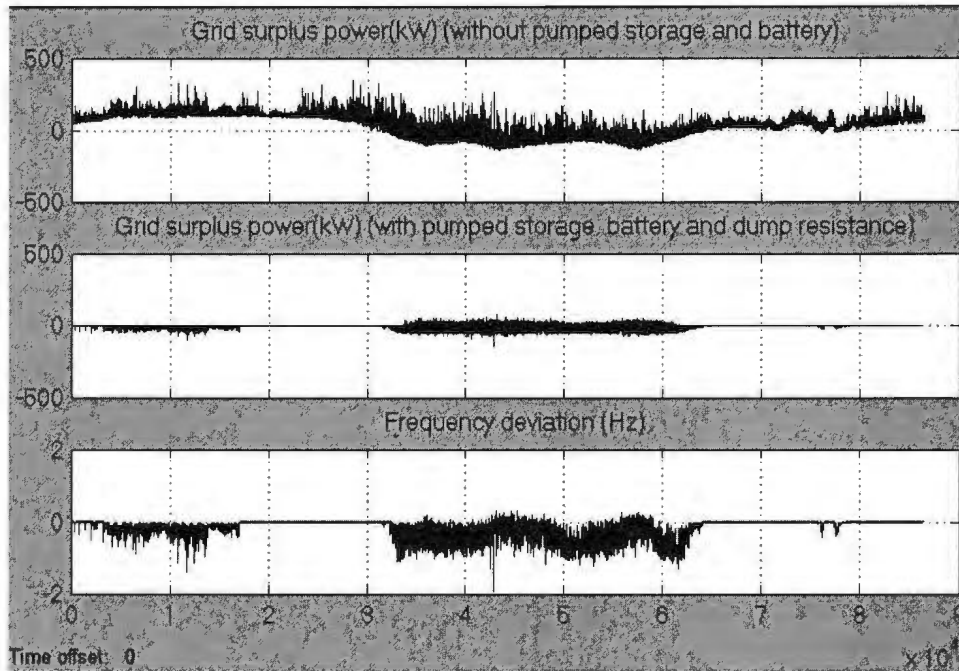


Figure 5.5. BB charging current (kA), charging power (kW), percentage of state of charge, discharging current (kA) and the power to the grid (kW) due to the discharging of the battery are shown for the mode 1



**Figure 5.6. Grid surplus power (kW) with and without pumped storage, battery and dump load and the resultant frequency deviation for the mode 1**

#### **5.4.2 Mode 2: DEG is operating independently without time constraint**

In this mode DEG is operating as needed for the whole time. System simulation results are shown from Figure 5.7 to Figure 5.10. In simulation results it can be observed that DEG is switching over frequently from 0 to 300kW as there is no continuous control. Maximum frequency deviation is found to be -7Hz from 10000s to 30000s for the unsteady supply from DEG. Total fuel consumption is reduced to 1866L. In Figure 5.11 (zoomed figure) the frequent switching of the DEG has been shown. Such a switching operation is not recommended for diesel generators. A continuous control of DEG power can solve this problem which is shown in Figure 5.12. This can be achieved by using a

variable speed diesel with an AC-DC-AC link. With this type of control fuel consumption is little bit higher than ON/OFF operation which is 2039L but the system provides better system stability e.g. maximum 0.15Hz frequency dip.

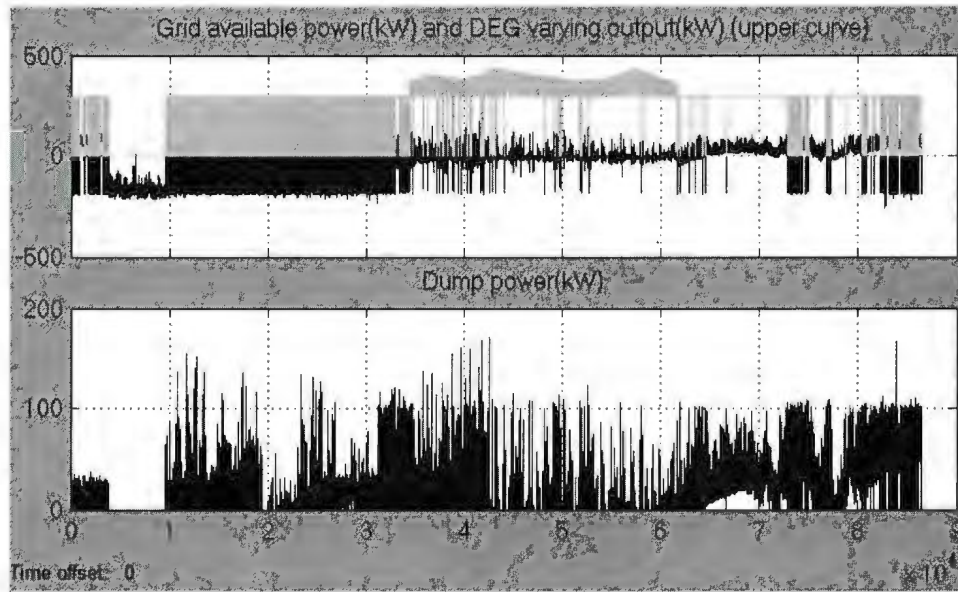


**Figure 5.7. In the top part, grid available power (kW) and DEG output (kW) (with flat 300kW value) are shown and in the lower part dump power (kW) is shown for the mode 2**

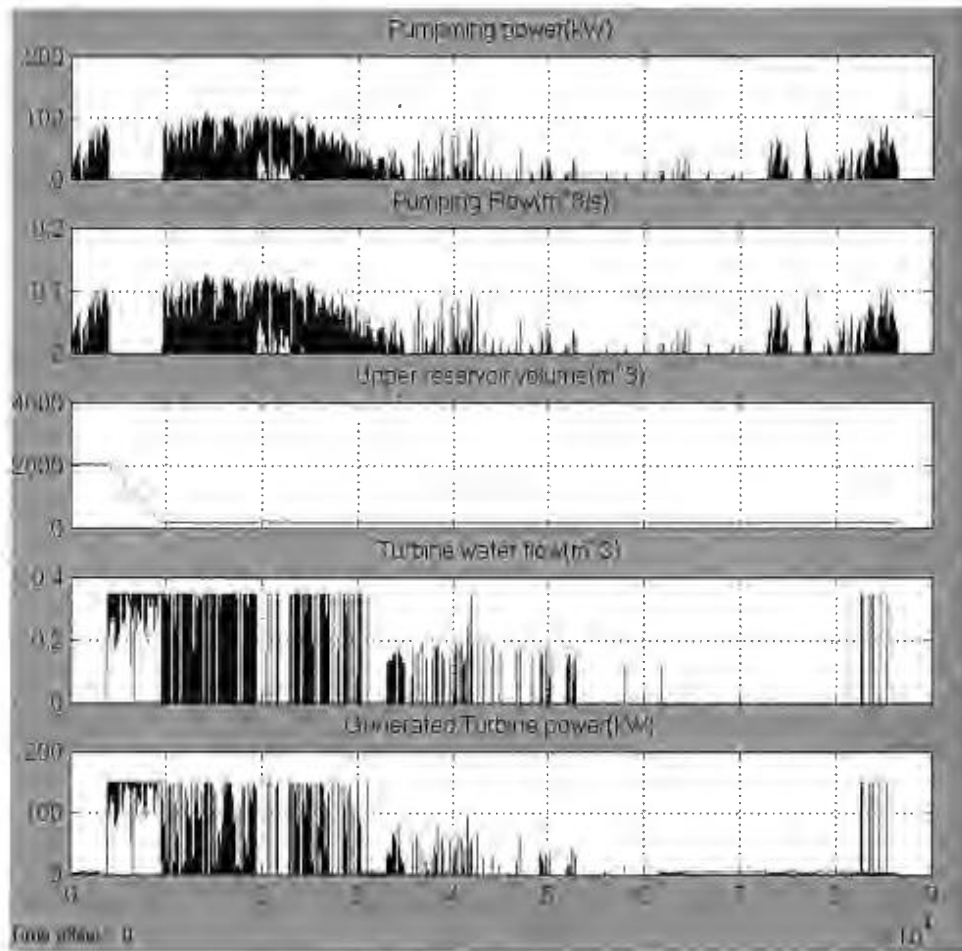


**Figure 5.8. Pumping power (kW), pumping water flow rate (m<sup>3</sup>/s), upper reservoir water volume (m<sup>3</sup>), turbine water flow (m<sup>3</sup>/s) and turbine generated power (kW) for the mode 2**

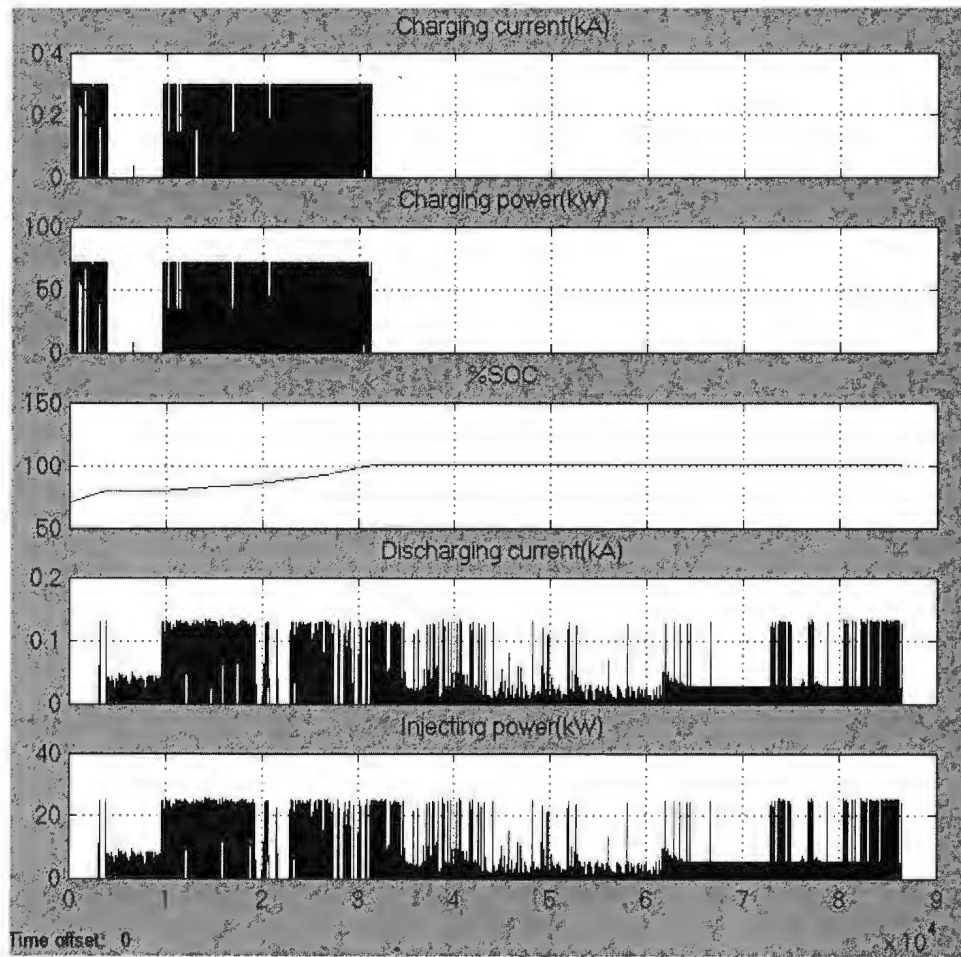


**Figure 5.9. BB charging current (kA), charging power (kW), percentage of state of charge, discharging current (kA) and the power injected to the grid (kW) due to the discharging of the battery are shown above for the mode 2**

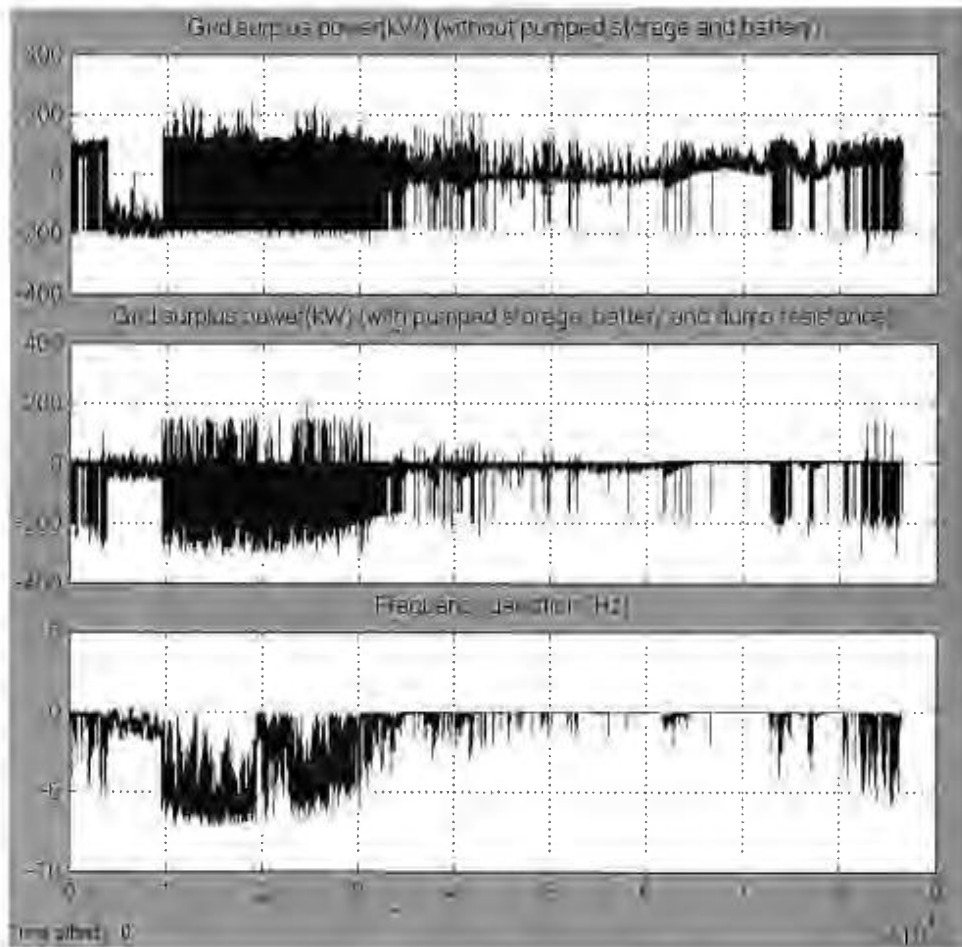


**Figure 5.10. Grid surplus power (kW) with and without pumped storage, battery and dump load and the resultant frequency deviation are shown above for the mode 2**

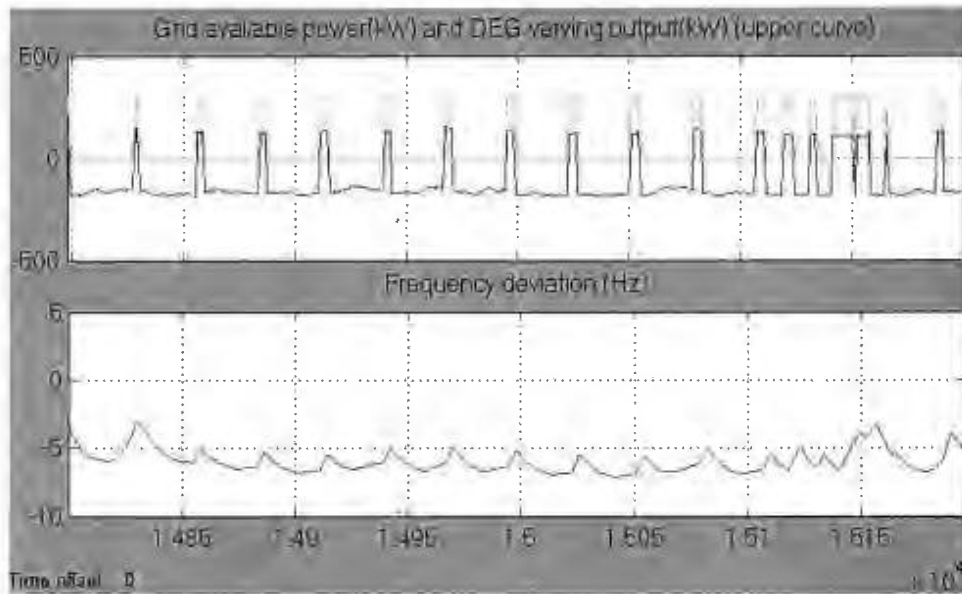


**Figure 5.11.** In the top part, grid available power (kW) and DEG output (kW) are shown and in the lower part the resultant frequency deviation (Hz) are shown for 14800s to 16000s in mode 2

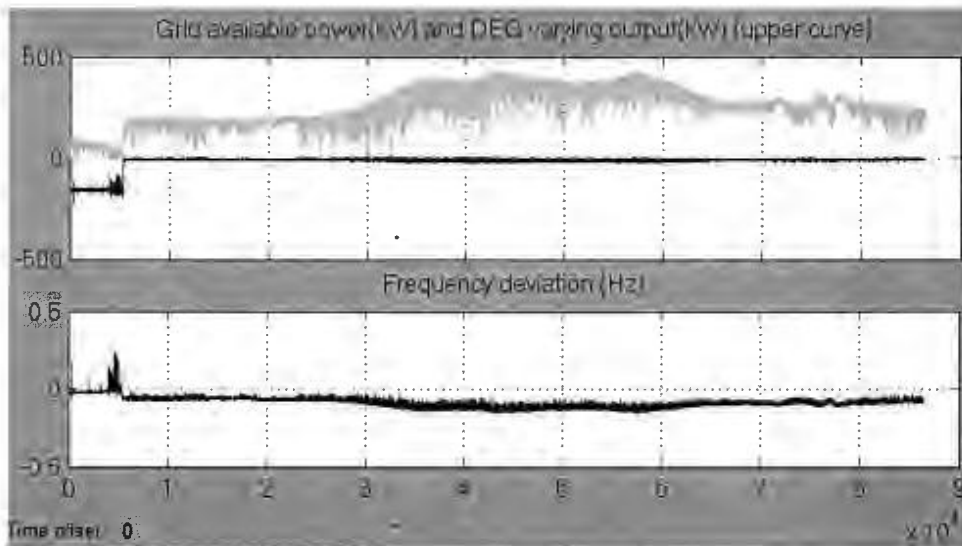


**Figure 5.12.** In the top part, grid available power (kW) and DEG output (kW) are shown and in the lower part the resultant frequency deviation (Hz) are shown for the continuous control of DEG in

**Mode 2**

### 5.4.3 Mode 3: DEG is operating with 10 minutes time constraint

In this mode DEG can operate independently for the whole time but it will remain in its present operating state for at least 10 minutes after any recent switch over. Simulations results of mode 3 are shown From Figure 5.13 to Figure 5.16. It can be observed that DEG is remaining in its last state for 10 minutes. Total fuel consumption in this mode using same wind and load data is 2110L and maximum frequency dip is found -10Hz. That may be acceptable. In Table 5.1 all diesel consumption results are summarized.

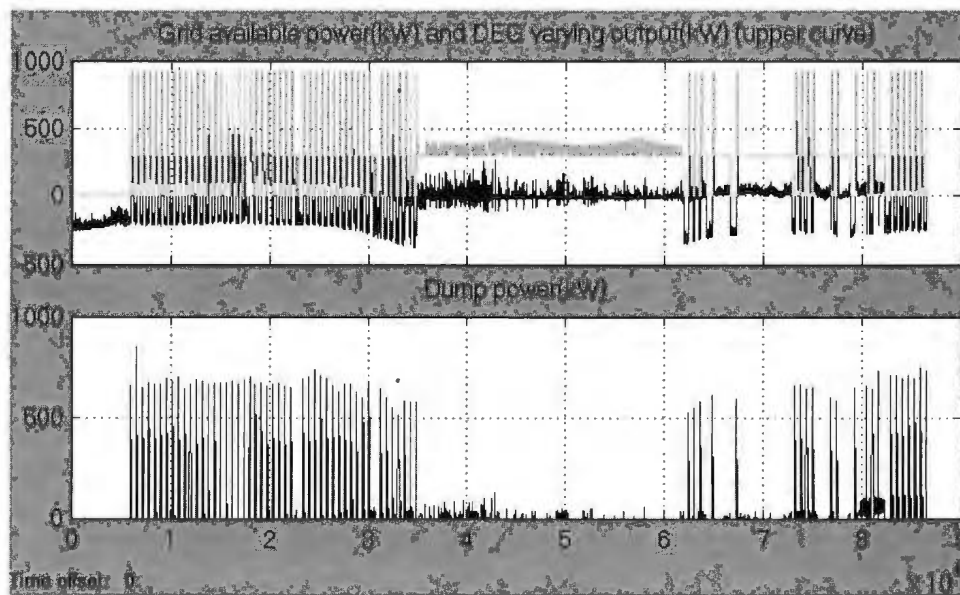


Figure 5.13. In the top part, grid available power (kW) and DEG output (kW) (with flat 300kW value) are shown and in the lower part dump power (kW) is shown for the mode 3

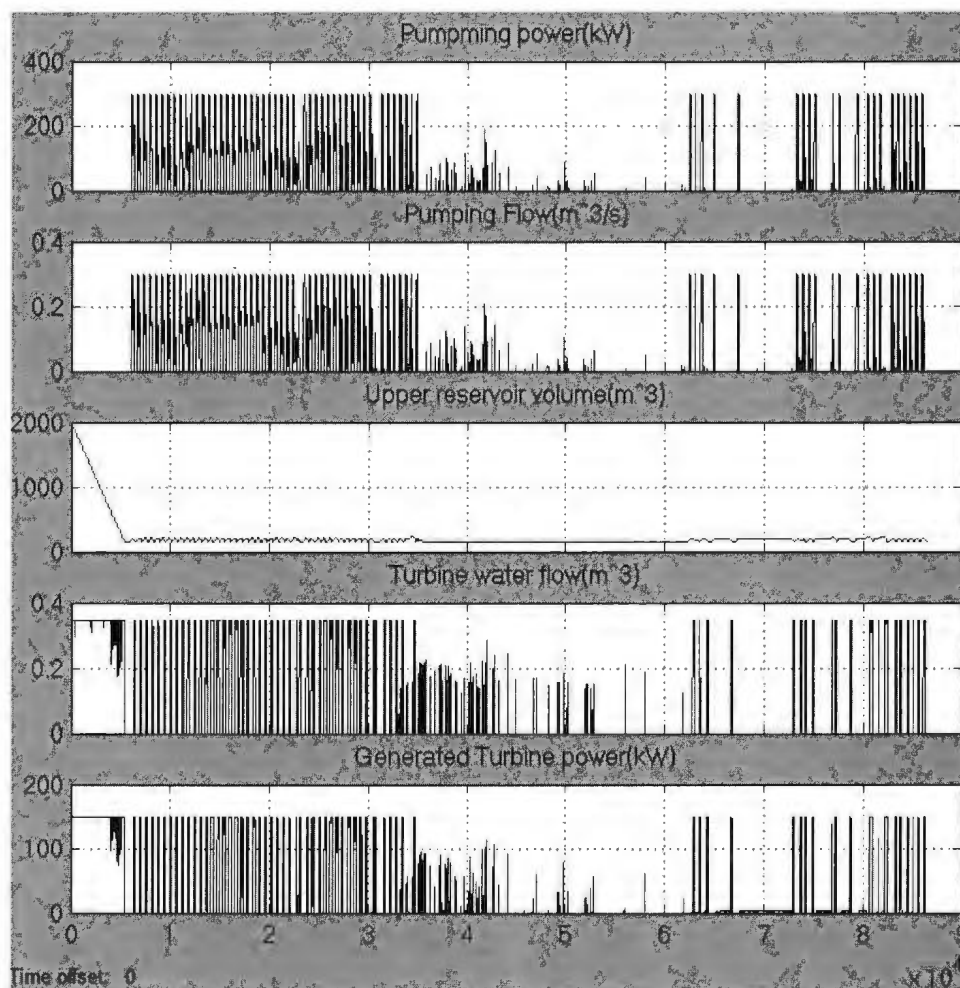


Figure 5.14. Pumping power (kW), pumping water flow rate (m<sup>3</sup>/s), upper reservoir water volume (m<sup>3</sup>), turbine water flow (m<sup>3</sup>/s) and turbine generated power (kW) for the mode 3

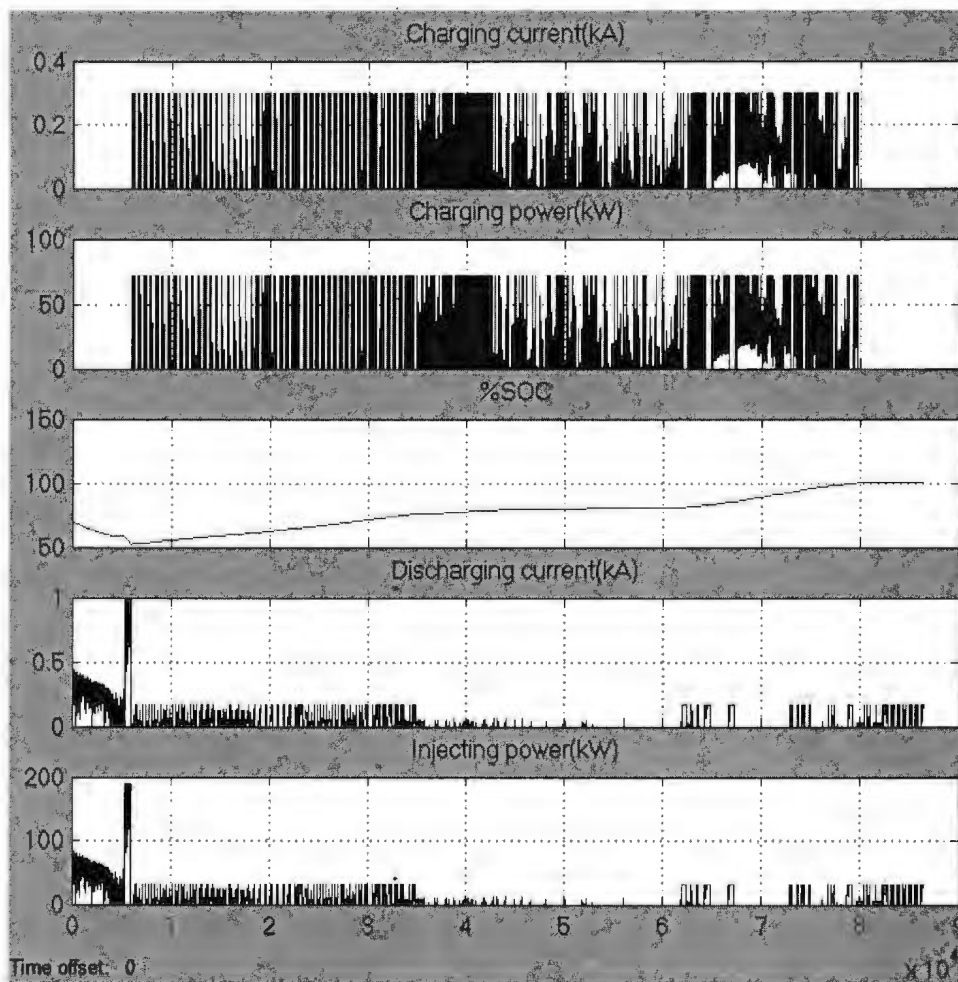


Figure 5.15. BB charging current (kA), charging power (kW), percentage of state of charge, discharging current (kA) and the power injected to the grid (kW) due to the discharging of the battery are shown above for the mode 3

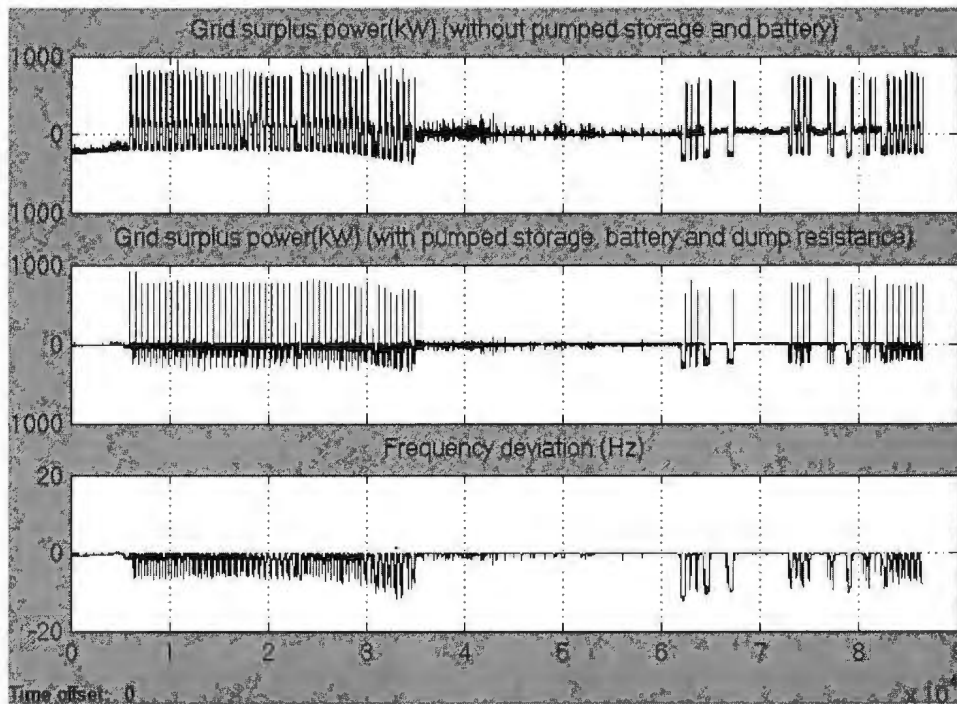


Figure 5.16. Grid surplus power (kW) with and without pumped storage, battery and dump load and the resultant frequency deviation are shown above for the mode 3

Table 5.1. Study of Diesel consumption for different modes

MODES	DEG operation mode	Diesel Intake (Liter)	Maximum Frequency deviation (Hz)	No. of Switching
Mode 1	Always ON	2323	-1.5	0
Mode 2	ON/OFF	1866	-7	Many
	Continuous control	2039	-0.15	0
Mode 3	Minimum 10 min after last switching over	2110	-10	Less

## 5.5 Conclusion

Dynamic simulation and supervisory control of a remote hybrid power system with pumped hydro and battery storage system has been presented in this paper. Simulation

results indicate that the continuous control is giving the best solution in terms of fuel consumption and frequency stability. Incorporating an inverter type DEG with the proposed pumped hydro system, battery bank and dump load can maximize the wind energy penetration in Ramea hybrid system and reduce the diesel consumption and stabilize the system frequency.

## **5.6 Acknowledgment**

The authors gratefully acknowledge the contributions of Newfoundland and Labrador Hydro for their assistance to provide necessary information and data of Ramea hybrid power system.

## **5.7 References**

- [1] The "Ramea Island," [Online]. Available: <http://www.ramea.ca/>. [Accessed 30 03 2013].
- [2] CANMET Energy, "Natural Resource Canada," Natural Resource Canada, 07-07-2007. [Online]. Available: <http://canmetenergy.nrcan.gc.ca/renewables/wind/464>. [Accessed 30 03 2013].
- [3] M. Oprisan, "IEA Wind," IEA Wind – KWEA Joint Workshop, 01-04-2007. [Online]. Available: [http://www.ieawind.org/wnd\\_info/KWEA\\_pdf/Oprisan\\_KWEA\\_.pdf](http://www.ieawind.org/wnd_info/KWEA_pdf/Oprisan_KWEA_.pdf). [Accessed 30 03 2013].

- [4] M. T. Iqbal, "Feasibility Study of Pumped Hydro Energy Storage for Ramea Wind-Diesel HPS," The Harris Centre, MUN, St. John's, 2009.
- [5] D.-J. Lee and L. Wang, "Small-Signal Stability Analysis of an Autonomous Hybrid Renewable Energy Power Generation/Energy Storage System Part I: Time-Domain Simulations," IEEE TRANSACTIONS ON ENERGY CONVERSION, vol. 23, no. 1, pp. 311-320, 2008.
- [6] Md. Rahimul Hasan Asif and Tariq Iqbal, "A novel method to model a HPS with pumped hydro storage for Ramea, Newfoundland", IEEE, Newfoundland Electrical and Computer Engineering Conference 2012
- [7] A. G. Rodríguez, A. G. Rodríguez and M. B. Payán, "Estimating Wind Turbines Mechanical Constants," in International Conference On Renewable Energies And Power Quality (ICREPQ'07), Bilbao, 2007.
- [8] Windmatic, "Windmatic 15s," [Online]. Available: <http://windmatic.com/15s-brochure.pdf>. [Accessed 30 03 2013].
- [9] Northern Power Systems, "Northern Power 100," [Online]. Available: [http://www.northernpower.com/pdf/NPS100-21\\_SpecSheet\\_EU-A4\\_English\\_2012.pdf](http://www.northernpower.com/pdf/NPS100-21_SpecSheet_EU-A4_English_2012.pdf). [Accessed 30 03 2013].
- [10] Advantica Inc., "Moment of Inertia and Pump Startup/Failure," 14 03 2011. [Online]. Available: [http://my.advanticagroup.com/support/allsecure/watersecure/releases\\_advisories/KBA\\_pump\\_moment\\_of\\_inertia.pdf](http://my.advanticagroup.com/support/allsecure/watersecure/releases_advisories/KBA_pump_moment_of_inertia.pdf). [Accessed 30 03 2013].

- [11] "The Engineering Toolbox," [Online]. Available: [http://www.engineeringtoolbox.com/minor-loss-coefficients-pipes-d\\_626.html](http://www.engineeringtoolbox.com/minor-loss-coefficients-pipes-d_626.html). [Accessed 30 01 2013].
- [12] G. Brown, "Henry Darcy and His Law," 22 06 2000. [Online]. Available: <http://biosystems.okstate.edu/darcy/index.htm>. [Accessed 30 03 2013].
- [13] Renewables First, "Pelton & Turgo Turbines," Renewables First, [Online]. Available: <http://www.renewablesfirst.co.uk/pelton-and-turgo-turbines.html>. [Accessed 30 03 2013].
- [14] Chen, H., Cong, T., Yang, W., Tan, C., Li, Y., and Ding, Y., Progress in electrical energy storage system: a critical review. Progress in Natural Science 19 (2008), 291–312.

## 5.8 Biographies

M. R. H. Asif achieved Bachelor degree in Electrical and Electronics Engineering from Bangladesh University of Engineering and Technology, Dhaka, Bangladesh. His employment experience included the Robi Axiata Limited as a Specialist in Radio Network Optimization.

Currently he is a Masters candidate in Electrical Engineering department at Memorial University of Newfoundland. He is an IEEE Student member since September 2012.

His research interest includes renewable energy, hybrid power systems and power electronics.

M. T. Iqbal received the B.Sc. (EE) degree from the University of Engineering and Technology, Lahore in 1986, the M. Sc. Nuclear Engineering degree from the Quaid-e-Azam University, Islamabad in 1988 and the Ph.D. degree in Electrical Engineering from the Imperial College London in 1994. Since 2001 he is working at Faculty of Engineering and Applied Science, Memorial University of Newfoundland. Presently he is a full Professor.

His teaching activities cover a range of electrical engineering topics including renewable energy systems and power electronics. Currently, his research focuses on modeling and control of hybrid energy systems.

## 6 Conclusion, Contribution and Future Work

### 6.1 Conclusion

The main conclusions of this research are:

#### 6.1.1 **Faster simulation with simpler but detailed dynamic model and intelligent supervisory controller is possible**

This study shows a new way to model a hybrid power system with a detailed dynamic simulation model along with a supervisory controller. Giving priority to the simplicity, simulation time and accuracy; dynamic model for all components of Ramea hybrid power system with a proposed pumped hydro system and battery bank have been done. Simulation time is significantly reduced due to the simplicity of the technique used here. A computer with Intel Core2Duo 2.1GHz processor, 4GB RAM and simulation time step of 0.01s, one day (86400 seconds) simulation for any case takes only 30 minutes. Modeling with Simulink built in blocks has been tried before moving with this modeling technique which led to prolongs simulation time and most of the time simulation did not converge at all. 1<sup>st</sup> order transfer functions giving almost same dynamic characteristics depending on the sizing of the corresponding components and their functions blocks have been modeled with real world characteristics curves, losses and necessary nonlinear efficiencies.

### 6.1.2 Analyses for all extreme cases could be done

Comprehensive case studies of Ramea hybrid power system along with output results have been presented in this research. It can be concluded from the simulation results of six possible extreme cases that, higher penetration of wind energy results in low diesel consumption. It can be obtained if a 925kW DEG is operated in a minimum of 300kW settings and results indicate that it maintains a fairly stable system frequency for the whole operation time.

**Table 6.1. Maximum system frequency deviation for all six cases**

<b>Case</b>	<b>Load</b>	<b>Wind speed</b>	<b>Maximum frequency deviation</b>
<b>1</b>	Low (200kW to 330kW)	Low (0m/s to 9m/s)	1.3Hz
<b>2</b>	Low (200kW to 330kW)	High (10m/s to 20m/s)	~0Hz
<b>3</b>	High (590kW to 990kW)	Low (0m/s to 9m/s)	0.9Hz
<b>4</b>	High (590kW to 990kW)	High (10m/s to 20m/s)	0.4Hz
<b>5</b>	Abrupt load change (500kW to 700kW at 200s and vice versa at 700s)	Steady in midrange (5m/s)	0.2Hz
<b>6</b>	Steady in midrange (500kW)	Abrupt wind speed change (8m/s to 11m/s at 200s and vice versa at 700s)	1.1Hz

In Table 6.1 above it has been shown that maximum system frequency deviations are quite reasonable and only occur for a short duration. Besides, proposed dump load can prevent system frequency spikes in high wind or low load and battery bank is working as a buffer between turning on and off of the mechanical devices e.g. pump, turbine or even DEG. In consequence, altogether system operation is much easier and less frequency deviations is observed even for most extreme condition of the wind speed and load demand. Overall response found in the study is quite satisfactory for a remote location such as Ramea Island.

### **6.1.3 Modified control of DEG is required for high penetration of wind energy**

In the later part of this research, in Chapter 5 diesel consumptions for various operating mode of diesel engine generator have been studied and simulation results indicate that the continuous control of DEG delivering the best result in terms of fuel consumption and frequency stability. Reduced fuel consumption leads to lower cost of energy, less greenhouse gas emissions and smaller diesel reserve requirement. Three operational modes have been studied i.e. Mode 1: DEG always ON, Mode 2: DEG ON-OFF without any time delay, modified Mode 2: DEG Continuous control and Mode 3: DEG ON-OFF with 10min time delay. An inverter type continuous controlled DEG would consume 2039 liter which is around 300 liter less than always ON mode and results in a maximum of 0.15Hz frequency dip. The wind energy penetration in Ramea HPS can be maximized by incorporating an inverter type DEG with the proposed PHS system and dual storage facilities; BB and DL.

## **6.2 Contribution**

Some major contributions of this research to the field of renewable energy are:

### **6.2.1 Novel method for dynamic modeling**

Modeling method used here is novel. Use of Simulink customizable function block instead of built-in subsystem blocks provides a lot of flexibility to modify and design according to the original devices. In most of the Simulink pre-built blocks, all parameters cannot be modified as needed or an additional parameter cannot be incorporated. For higher order complex design, or in a complicated design such as this HPS, simulation does not converge. This novel modeling method gives an endless opportunity to have complete control over the modeling and simulation. Another important aspect of this technique is, built-in Simulink blocks still can be used in this model and MATLAB codes inside the function block can be modified too.

### **6.2.2 Compatibility and flexibility**

This model can be used to study system stability and be modified easily for potential future modification to the remote HPS. Any type of dynamic controller e.g. fuzzy, neural network can be implemented here too. For any change of the existing system components only system characteristics parameters and transfer function need to be modified. By this process this model can be used to justify feasibility of a PHS system in a HPS for a different location. Different wind data and load data of any day can be fed into this model to determine the system expected response. If enough time is given, this model will be

able to simulate few months of operations and study any desired parameters e.g. fuel consumption as well. Such kind of flexibility is not possible to find in any commercially available software.

### **6.2.3 Supervisory controller design and simulation**

Designed supervisory controller has a real time control algorithm which dynamically monitors available surplus or missing power in the grid and operates pumps or generator as required and also controls charging and discharging of the battery bank. The proposed supervisory controller controls two energy storage systems and flattens the total generation curve and follows the fluctuating demand curve to reduce the system transients. Supervisory controller developed in this research typically keeps the DEG always ON in the range of 30% to 100% of the rated power operation of DEG. For high penetration HPS supervisory controller has been introduced for different operational mode of DEG e.g. continuous control, DEG ON-OFF operation etc. High penetration diesel OFF operation of HPS needs complicated control over all of the system components hence an intelligent supervisory controller. Load following strategy has been used in this study. That means DEG has not been used to charge the BB. But cycle charging or any other customized strategy can be developed easily if needed.

### 6.3 Future Work

- This model can be developed further by integrating higher order models in the blocks of system components but simulation time will increase considerably. More complicated models may give better performance of the system and provide opportunity to analyze higher order transient responses.
- AC voltage and reactive power analysis of the system can be done to observe AC transient behavior e.g. phase angle, reactive power measurements. Integration of synchronous condenser or variable capacitors into the existing system can be done using higher order dynamic models. Controls of such system will be more complicated.
- Other types of dynamic controllers e.g. fuzzy logic, neural network can be used here as a future work to study possible improvement to the transient behavior of this model.
- This model can be experimented for other remote hybrid power systems with different ratings and configurations by changing the block parameters as needed.
- A detailed environmental impact analysis and economic analysis can also be done.

## Appendix A

Power Curve WM 15 S USA

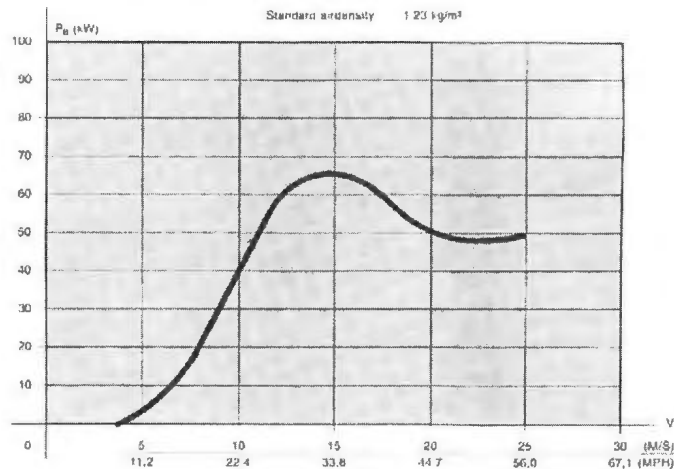


Figure A.1. Power curve for Windmatic 15s wind turbine

## Technical specifications WM 15 S

<b>CONNECTION TO MAINS</b>		<b>AERODYNAMIC BRAKES</b>		<b>Small generator</b>	
Voltage	480 V	Type	spoilers	Rated electrical power	13 kW
Frequency	60 Hz	Releasing	centrifugally	Rated RPM	1230 RPM
<b>PERFORMANCE</b>		<b>NACELLE</b>		<b>Large generator</b>	
Cut-in wind speed	3.5 m/s	Cover material	aluminum	Rated electrical power	66 kW
Wind speed for max power	15 m/s	Chassis material	hot dip galvanized steel	Rated RPM	1212 RPM
Cut-out wind speed	25 m/s	<b>Dimensions (length x width x height)</b>		<b>CONNECTION BETWEEN LARGE AND SMALL GENERATOR</b>	
Design wind speed	30 m/s	2690 x 1325 x 1320 mm		Type	V-belt transmission
Max electrical power	66 kW	Mass (excl. turbine)	3990 kg	Gear ratio	1:1.42
<b>TURBINE</b>		<b>MAIN BEARINGS</b>		<b>YAWING SYSTEM</b>	
Type	3 blades, stall regulated up wind turbine	Type	spherical roller bearings	Type	yaw gear wheel with external teeth and oilon bearings
Diameter	15.5 m	Number	2	Operation	on/off electrical control of yawing motor from wind vane signals
Direction of rotation	counterclockwise	<b>OPERATION BRAKE</b>		Yawing period	0.8°/sec
RPM	40.4/57.58 RPM	Type	disc brake	<b>CONTROL SYSTEM</b>	
Tilt angle	5°	Location	turbine shaft	Type	electrical, based on micro-processors
Cone angle	0°	Operation	hydraulic	Function	control, supervising connection of generators b.m.c. thyristors
Mass (incl. hub)	1180 kg	<b>GEARBOX</b>			
<b>BLADES</b>		Type	oil lubricated hollow shaft		
Blade suspension	self-supported	Number of stages	3		
Beam material	reinforced fiber-glass Polyester with steel root	Gear ratio	1:20.83		
Shell material	reinforced fiber-glass Polyester	Rated power	130 kW (DIN)		
Aeroflex	NACA 63-200	<b>COUPLING</b>			
Pitch	fixed	Type	flexible rubber coupling		
Length	7.45 m	<b>GENERATORS</b>			
		Type	asynchronous with squirrel cage		

Figure A.2. Technical specification of Windmatic 15s wind turbine

Power Curve (1-Motor Rotor) Standard Air Density (1.225 kg/m<sup>3</sup>)

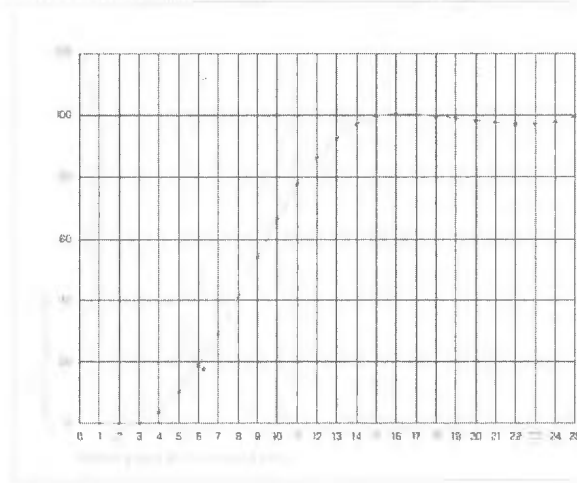


Figure A.3. Power curve of Northern Power 100 wind turbine

GENERAL CONFIGURATION	DESCRIPTION
Model	Northern Power® 100-21
Design Class	IEC IIA (air density 1.225 kg/m <sup>3</sup> , average annual wind below 8.6 m/s, 50-yr peak gust below 59.5 m/s)
Design Life	20 years
Hub Height	37 m (121 ft) / 30 m (98 ft)
Tower Type	Tubular steel monopole
Orientation	Upwind
Rotor Diameter	71 m (233 ft)
Power Regulation	Variable speed, stall control
Certifications	UL1741, UL1004-4, CSA C22.2 No. 107.1-D1, CSA C22.2 No. 100.04, IEC CE compliant
PERFORMANCE	DESCRIPTION
Rated Electrical Power	100 kW, 3 Phase, 480 VAC, 60/50 Hz
Rated Wind Speed	4.5 m/s (10.2 mph)
Maximum Rotation Speed	15 rpm
Cut-In Wind Speed	3.5 m/s (7.8 mph)
Cut-Out Wind Speed	25 m/s (56 mph)
Extreme Wind Speed	59.5 m/s (133 mph)
WEIGHT	DESCRIPTION
Rotor (21-meter) & Nacelle (standard)	7,200 kg (16,100 lbs)
Tower (37-meter)	13,800 kg (30,000 lbs)
DRIVE TRAIN	DESCRIPTION
Gearbox Type	No gearbox (direct drive)
Generator Type	Permanent magnet, passively cooled
BRAKE SYSTEM	DESCRIPTION
Service Brake Type	Two motor-controlled calipers
Normal Shutdown Brake	Generator dynamic brake and two motor-controlled calipers
Emergency Shutdown Brake	Generator dynamic brake and two spring-applied calipers
YAW SYSTEM	DESCRIPTION
Control	Active, electromechanically driven with wind direction/speed sensors and automatic cable unwind

Figure A.4. Technical specification of Northern Power 100 wind turbine

## DIESEL GENERATOR SET



Image shown may not reflect actual package.

### STANDBY 1000 ekW 1250 kVA 60 Hz 1800 rpm 480 Volts

Caterpillar is leading the power generation marketplace with Power Solutions engineered to deliver unmatched flexibility, expandability, reliability, and cost-effectiveness.

### TECHNICAL DATA

Open Generator Set - - 1800 rpm/60 Hz/480 Volts	DM9939	
Low Fuel Consumption		
<b>Generator Set Package Performance</b>		
Genset Power rating @ 0.8 pf	1250 kVA	
Genset Power rating with fan	1000 ekW	
<b>Fuel Consumption</b>		
100% load with fan	262.7 L/hr	69.4 Gal/hr
75% load with fan	195.9 L/hr	51.8 Gal/hr
50% load with fan	135.9 L/hr	35.9 Gal/hr
<b>Cooling System<sup>1</sup></b>		
Air flow restriction (system)	0.12 kPa	0.48 in. water
Engine coolant capacity	55.0 L	14.5 gal
<b>Inlet Air</b>		
Combustion air inlet flow rate	82.6 m <sup>3</sup> /min	2917.0 cfm
<b>Exhaust System</b>		
Exhaust stack gas temperature	473.4 °C	884.1 °F
Exhaust gas flow rate	214.7 m <sup>3</sup> /min	7582.1 cfm
Exhaust flange size (internal diameter)	203 mm	8 in
Exhaust system backpressure (maximum allowable)	10.0 kPa	40.2 in. water
<b>Heat Rejection</b>		
Heat rejection to coolant (total)	359 kW	20416 Btu/min
Heat rejection to exhaust (total)	965 kW	54879 Btu/min
Heat rejection to aftercooler	249 kW	14161 Btu/min
Heat rejection to atmosphere from engine	127 kW	7222 Btu/min
Heat rejection to atmosphere from generator	62.7 kW	3565.7 Btu/min
<b>Alternator<sup>2</sup></b>		
Motor starting capability @ 30% voltage dip	2734 skVA	
Frame	1402	
Temperature Rise	125 °C	225 °F
<b>Lube System</b>		
Sump refill with filter	99.0 L	26.2 gal
<b>Emissions (Nominal)<sup>3</sup></b>		
NO <sub>x</sub> g/hp-hr	6.1 g/hp-hr	
CO g/hp-hr	.18 g/hp-hr	
HC g/hp-hr	.01 g/hp-hr	
PM g/hp-hr	.02 g/hp-hr	

Figure A.5. Datasheet of 1000kW Diesel Engine Generator, fuel consumption data has been taken

from here



**THREE PHASE SYNCHRONOUS GENERATOR**  
**MJH 400 LB4**

CONTINUOUS DUTY

**4 poles**  
**50 Hz - 1500 rpm**

AMBIENT TEMPERATURE		40°C	Number of leads		6
INSULATION CLASS		F	WINDING DATA		Winding pitch: 5/8
POWER FACTOR		0.8			
TEMPERATURE RISE			105/40 cl.F	80/40 cl.B	
VOLTAGE		Star	V	3000	
RATING		kVA	1020	890	
		kW	816	712	
EFFICIENCY [%] @ 0.8 p.f.		4/4	94.9	94.8	
		3/4	94.9	94.8	
		2/4	94.5	94.3	
EFFICIENCY [%] @ 1 p.f.		4/4	98.0	95.9	
		3/4	96.0	95.9	
		2/4	95.7	95.5	
SHORT CIRCUIT RATIO		SCR	0.56	0.64	
REACTANCES [%]					
Direct axis synchronous		X <sub>d</sub>	225	196	
Quadrature axis synchronous		X <sub>q</sub>	122	106	
Direct axis transient		X <sub>d'</sub>	20.0	17.5	
Direct axis subtransient		X <sub>d''</sub>	9.0	7.9	
Quadrature axis subtransient		X <sub>q'</sub>	10.0	8.7	
Negative sequence		X <sub>2</sub>	9.0	7.9	
Zero sequence		X <sub>0</sub>	2.4	2.1	
TIME CONSTANTS [s]					
Open circuit		T <sub>d0</sub>		2.43	
Transient		T <sub>d</sub>		0.19	
Subtransient		T <sub>d'</sub>		0.016	
Armature		T <sub>a</sub>		0.025	
<b>MECHANICAL CHARACTERISTICS</b>					
D-end bearing/Lubrication		6324 C3 / With grease nipple			
N-end bearing/Lubrication		6318 Z C3 / Prelubricated			
Overspeed [r.p.m.]		2250			
Inertia (J) [kgm <sup>2</sup> ]		Refer to B34 construction	20		
Weight [kg]		Refer to B34 construction	3000		
Method of cooling		IC01			
Cooling air required [m <sup>3</sup> /s]		1.30			
Degree of protection		IP23			
Types of construction available		B2 (SAE) - IM B34 - IM B20			
Direction of rotation (Standard)		CW			
<b>OTHER DATA</b>					
Overloads		10% for 1 hour every 12 hours			
3-phase short circuit sustained current		≥ 300 % (3 In) with VARICOMP device			
Voltage regulation accuracy		± 1% in steady state condition			
Radio interference		EN 55011 - Class B Group 1			
Wave form THF		< 5%			
Total harmonic content		< 3% - At no load			
<b>STANDARDS</b>					
IEC 60034-1 CEI 2-3 BS 4999-5000 VDE 0530 NF 51-100 111 OVE M-10 NEMA MG 1-22					

Figure A.6. Datasheet of 816kW Diesel Engine Generator, inertia data has been taken from here

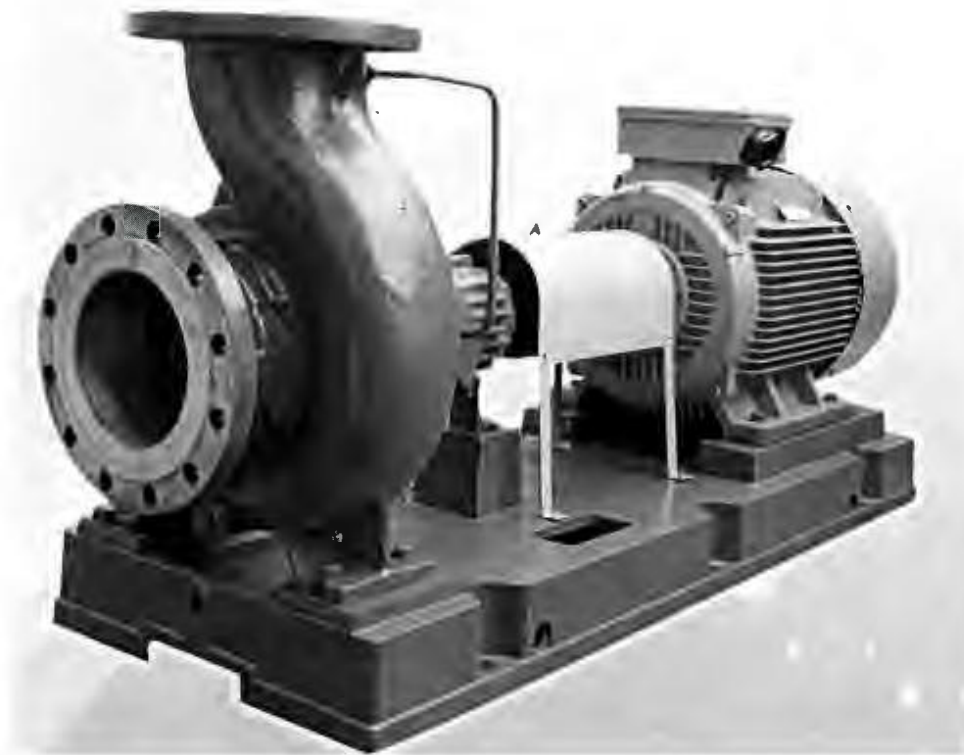


**Figure A.7. Centrifugal pump with induction motor coupled**



**Figure A.8. Multi-jet Pelton wheel turbine**

## Appendix B

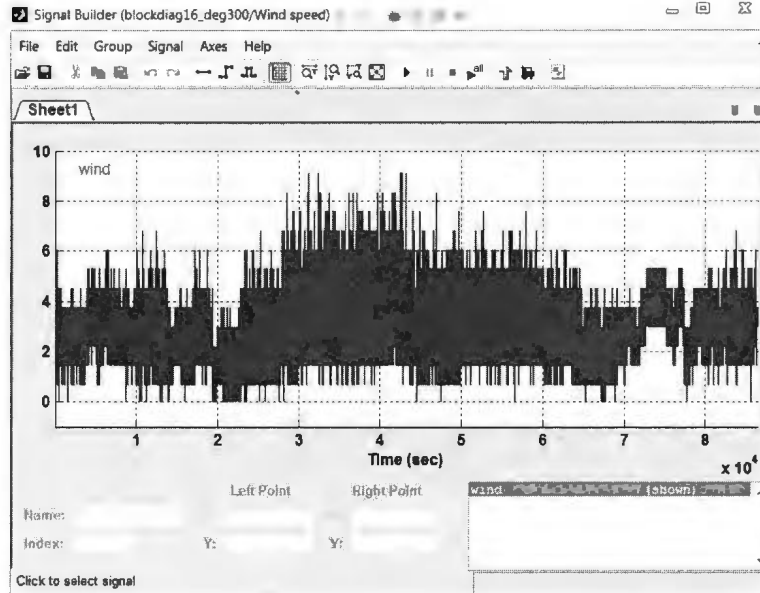


Figure B.1. Wind data input window

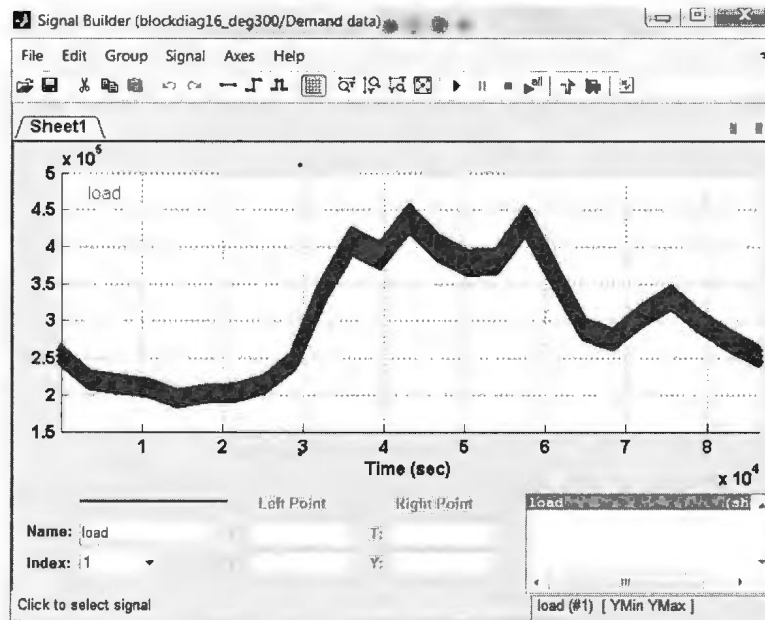


Figure B.2. Load data input window

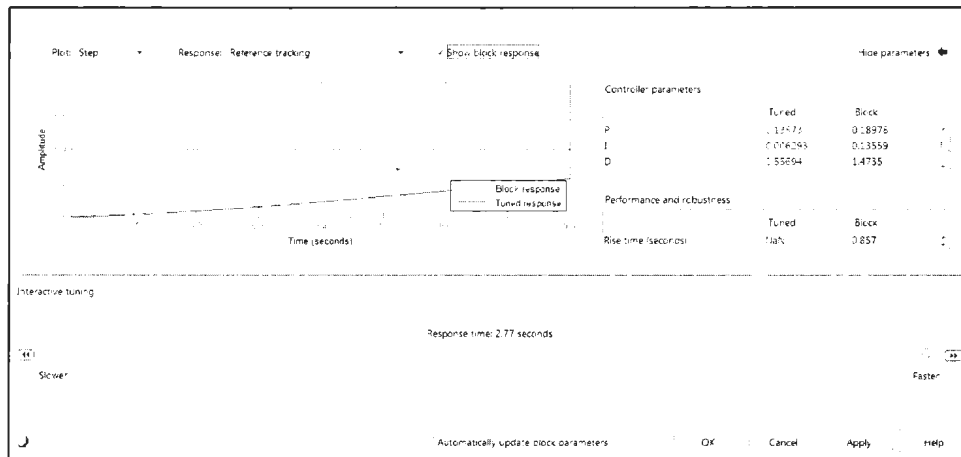


Figure B.3. Simulink built in interactive PID tuner

```
function p = f2p(df)
%#codegen

pu = (62 - (df + 60))/2;      %per unit power requirement
dpu = 1 - pu;               %delta per unit power
p = dpu * 6250000;          %delta power injection
```

Figure B.4. Simulink function block for diesel engine frequency droop

```
function d = diesel(x)
%#codegen

d = 0;

if x ~= 0
    d = 2E-14*x^2 + 5E-08*x + 0.0101;
end

if x == 0;
    d = 0;
end
```

Figure B.5. Simulink function block for measurement of diesel consumption

```

function [vres,qres_out] = reservoir(qres_in,turbctrl,vres_prev,ts)
%reservoir

hres = 63;
dens = 1000;
g = 9.81;
turbeff = 0.7;

qres_out = 0;
vres = vres_prev;

if qres_in > 0 && turbctrl == 0
    qres_out=0;
    vres = vres_prev + qres_in * ts;
end

if qres_in == 0 && turbctrl > 0
    qres_out = turbctrl/(hres*dens*g*turbeff);
    vres = vres_prev - qres_out * ts;
end

```

Figure B.6. Simulink function block for upper water reservoir

```

function Hloss = pipeloss(qres)
%pipeloss

%parameters:
Lpipe=70;           %pipe length
Dpipe=0.30;        %pipe diameter
Apipe=pi*(Dpipe/2)^2; %pipe area

g=9.81;
%dens=1000;        %water density
%mu=0.0102;       %viscosity at 20C
klossco=7;        %minor loss coefficient for water meter

|
Velowaterpump = qres/Apipe;           %water velocity in pipe
%Re=(Velowaterpump*Lpipe*dens)/mu;   %Reynolds number
Re = 2000;

flam=64/Re;                          %Darcy Friction Factor for laminar flow

%pipefric=flam*Lpipe/Lpipe*(Velowaterpump^2/(2*g));
%Darcy-Weisbach equation for head loss due to friction

%pipefric = (8*flam*Lpipe*qres^2)/(g*3.1416^2*Dpipe^5);
%lossmeter = klossco*(Velowaterpump^2)/(2*g);

Hloss = %pipefric + %lossmeter;       %head loss for the pump

```

Figure B.7. Simulink function block for dynamic losses inside the pipe

```

function [ibat_discharg,soc] = batterybank(ibat_charg,soc_prev,discharctrl,ts)
%#codegen

%ind_cap = 200;          %individual capacity in Ahr
%nbat_ser = 20;         %
%v_bat = 12*nbat_ser;   %battery voltage
%in_bat = 320;          %number of battery
%in_para = n_bat nbat_ser;

multiplier = 1;
%tot_cap = ind_cap*n_bat*3600;    %total capacity in coulomb

ibat_discharg = 0;
soc = soc_prev;

if ibat_charg > 0 && discharctrl == 0
    ibat_discharg = 0;
    soc = soc_prev + ibat_charg * ts;
end

if ibat_charg == 0 && discharctrl > 0
    ibat_discharg = discharctrl;

    if ibat_discharg > 150          %Peukert's law
        multiplier = 1/((10^0.2)^((ibat_discharg/15)^(-0.2)));
    end
    soc = soc_prev - ibat_discharg * multiplier * ts;
end
end

```

Figure B.8. Simulink function block for battery bank

```

% reservoir volume checking TURBINE ON
if vres > 150

    %grid power deficit is higher than 150kw TURBINE ON
    if -pgrid > 150000
        deg_f = 0;
        deg_p = 0;
        turbine_p = 150000;
    end

    %grid power in 50kw to 150kw range TURBINE ON
    if -pgrid >= 50000 && -pgrid <= 150000
        deg_f = del_f;
        deg_p = 300000;
        turbine_p = -pgrid;
    end

    %grid power deficit is less than 50kw TURBINE OFF
    if -pgrid < 50000
        deg_f = del_f;
        deg_p = 300000;
        turbine_p = 0;
    end

    %clipping negative values
    if turbine_p < 0
        turbine_p = 0;
    end
end
end

```

Figure B.9. Part of the code in supervisory controller







